

Closed-loop optimization of general conditions for heteroaryl Suzuki coupling

Nicholas H. Angello, Vandana Rathore, Wiktor Beker, Edward R. Jira, Agnieszka Wołos, Rafał Roszak, Alán Aspuru-Guzik, Charles M. Schroeder, Bartosz A. Grzybowski, Martin D. Burke

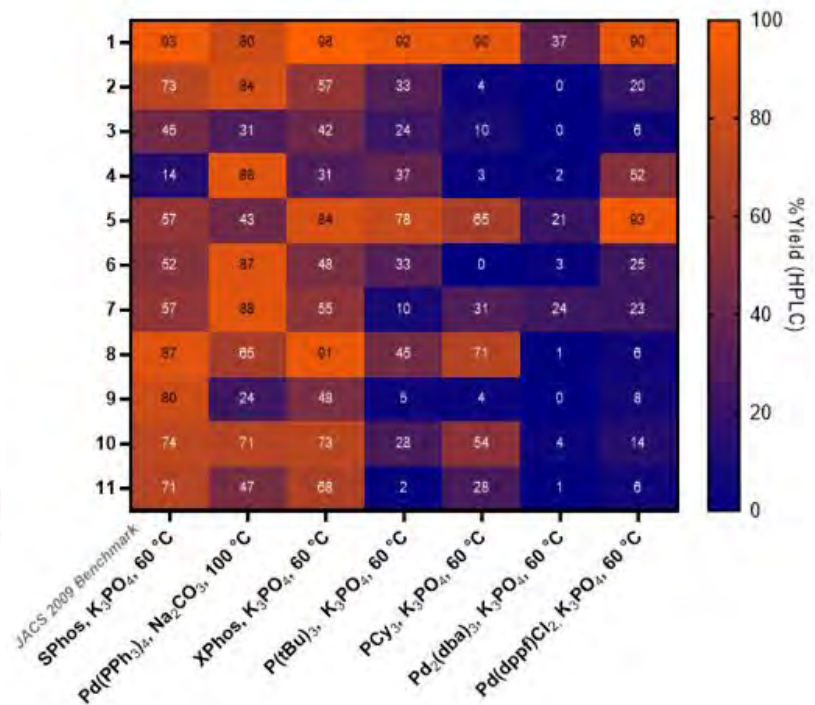
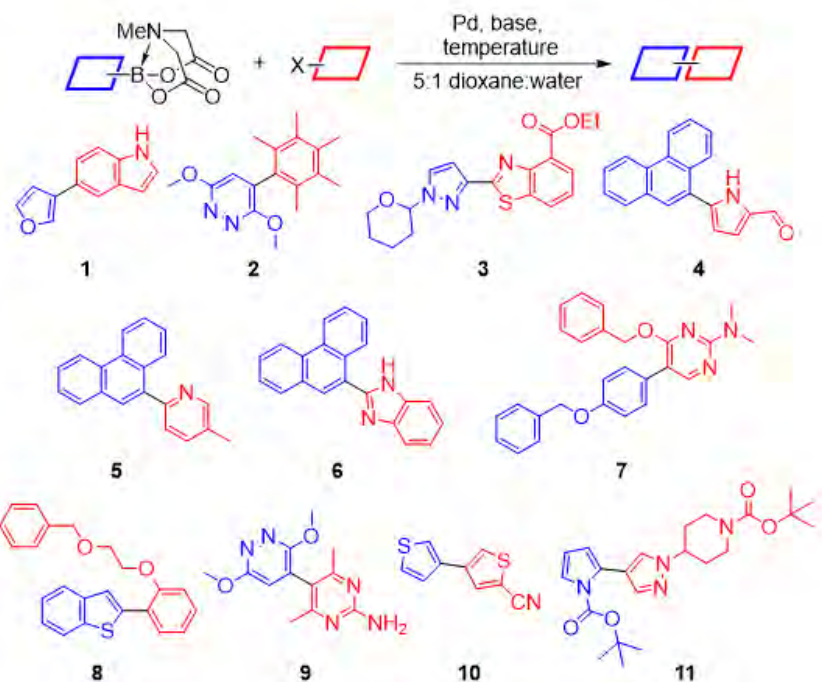


Research Questions

- Using AI and automated synthesis, can we discover reaction conditions optimized for generality?

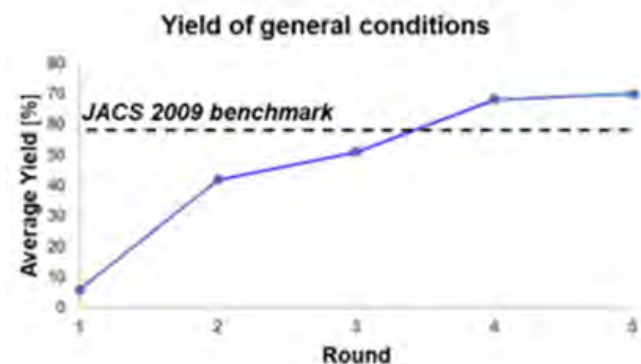
Methods and Results

Computationally selected diverse starter set (chosen from all commercial building blocks) → Robotically generated training set data, duplicates, $\pm 2\%$ yield → Closed-loop optimization



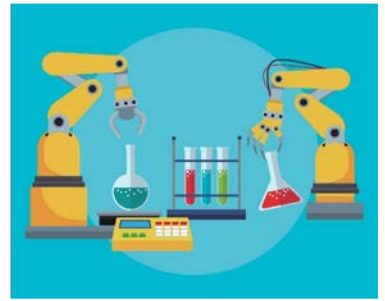
Conclusion

After 5 rounds of closed-loop optimization (>400 automated reactions including duplicates), AI discovered more general reaction conditions than known previously. We estimate this result is 2-3 times faster than random sampling.



Automated integration of experiment, theory, and data to accelerate graphene synthesis

E. M. Campo, Department of Materials Science and Engineering, University of Maryland at College Park, USA
W. Y. Rojas, Institute of Physics, Czech Academy of Sciences of the Czech Republic, Prague, CR

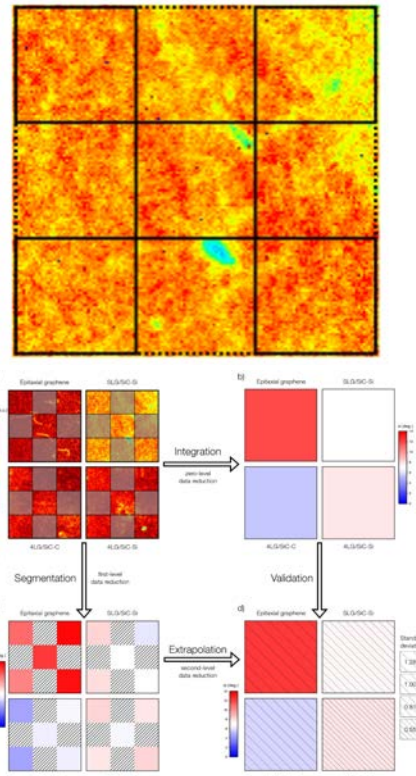
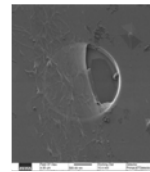


Research Questions

- Can industrial fabrication of graphene benefit from ML/AI technologies?
- Can defects be characterized with atomic sensitivity at wafer scale?
- What advanced characterization techniques can be exploited to accelerated fabrication?

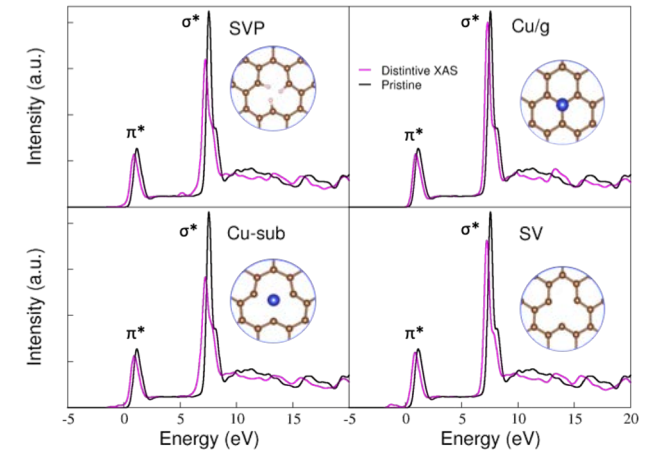
Methods and Results

- Electron/ion microscopies to benchmark superficial defects.
- Experimental Near Edge X-ray Absorption Fine Spectroscopy(NEXAFS) Imaging reduction describes corrugation and strain distribution at wafer levels.
- Approximately 7000 spectra of likely defects have calculated and will be openly available @dat.NIST.gov
- Exploit experimental hyperspectral NEXAFS imaging through a theoretical defect library.



Conclusion

Metrology and ML/AI algorithms along with defects fingerprinting are needed for automated characterization of graphene.



Enabling Automation of Chemical Reaction Optimization with Rxn Rover, a User-Friendly, Modular Software

Zachery Crandall, Kevin Basemann, Austin Thompson, Long Qi, Theresa L. Windus



Introduction

Laboratory automation can increase research efficiency, improve laboratory safety, and increase the reproducibility of results. Chemical reaction optimization is a prime candidate for automation, since it usually requires many, repetitive experiments to search the reaction space and converge on an optimal result. Commercial automated reactors have revolutionized spaces like the pharmaceutical industry for over a decade, but these systems tend to be expensive and require special expertise to maintain.

A more cost-effective solution would be to use existing laboratory equipment to build the automated reactor. However, creating a customized, automated reactor can be difficult, since many reactor components and analysis instrumentation have different communication protocols and programming experience is required.

Rxn Rover

Rxn Rover (pronounced “Reaction Rover”) is introduced as a flexible, free, open-source reactor automation software to allow the user to create custom, automated reactors using various plugins for reactor components, analysis instrumentation, and optimization algorithms. Rxn Rover aims to remove prerequisite programming experience, eliminate the challenge of different hardware communication protocols, and lower the barrier of entry into reaction automation to increase the accessibility, availability, and adoption of laboratory automation for reaction optimization in chemistry.

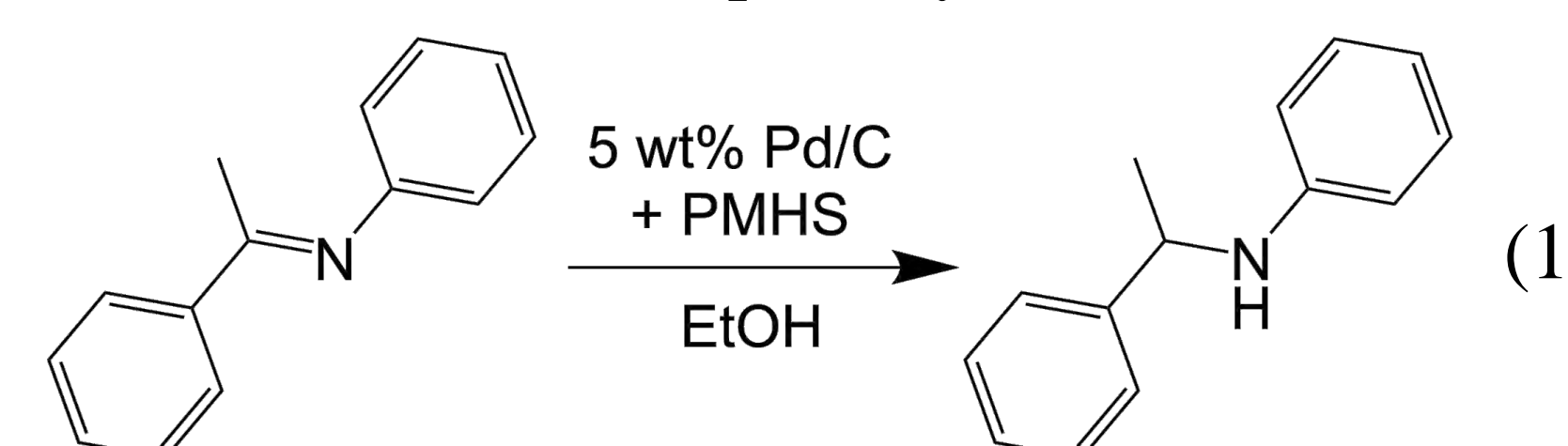
Designed to be easy to use with little to no programming experience, Rxn Rover is intended to be interacted with through its user interface (Figure 1). Plugins for various reactor components, analysis instrumentation, and optimization algorithms can be downloaded and used to enable custom reactor designs to be automated with a suitable optimization algorithm. If a plugin does not exist for the desired component, a plugin template is provided to minimize the required time and programming to incorporate the new component. Rxn Rover is programmed in LabVIEW to improve accessibility to those with little to no programming experience. However, Rxn Rover is also documented and designed to enable programmers to contribute to and expand it.

Acknowledgements

This work was primarily supported by Ames Laboratory Directed Research & Development program. T.L.W., K.B., and Z.C. were also supported by the U.S. Department of Energy (U.S. DOE), Office of Science, Basic Energy Sciences, Division of Chemical Sciences, Geosciences, and Biosciences through the Ames Laboratory Chemical Physics program. L.Q. and the reactor system was in part supported by the U.S. DOE, Office of Basic Energy Sciences, Division of Chemical Sciences, Geosciences, and Biosciences through the Ames Laboratory Catalysis program. The Ames Laboratory is operated for the U.S. DOE by Iowa State University under Contract No. DE-AC02-07CH11358. The United States Government retains and the publisher, by accepting the article for publication, acknowledges that the United States Government retains a non-exclusive, paid-up, irrevocable, world-wide license to publish or reproduce the published form of this manuscript, or allow others to do so, for United States Government purposes. We also acknowledge the useful conversations with Waters Corporation regarding the setup of the chromatography system.

Trials and Results

Three, multi-day trials are presented to demonstrate the stability of Rxn Rover while optimizing a reaction. SQSnobFit², a Python implementation of the SNOBFIT³ global, black-box optimization algorithm, was used to optimize a flow reactor performing heterogeneously catalyzed imine reduction relevant to energy conversion (Scheme 1). Various pump models from ChromTech (P-MXT, Series III, and P-M110B) were used, along with an OMEGA temperature controller. A WatersTM PATROLTM ultra-performance liquid chromatograph with a photo-diode array detector was used to analyze the results of each trial and quantify the results.



Optimization was successful in each trial with optimal yields of >70% reached after 21 hours, 41 hours, and 56 hours. Time to optimal yield increased as the concentration of the catalyst doubled in each subsequent trial, broadening the search space. However, algorithm performance was secondary to ensuring that Rxn Rover could robustly perform the optimization for a long period of time over many reaction iterations. Rxn Rover was able to perform these trials for 62 hours (68 reactions), 88 hours (108 reactions), and 103 hours (111 reactions) (Figure 2).

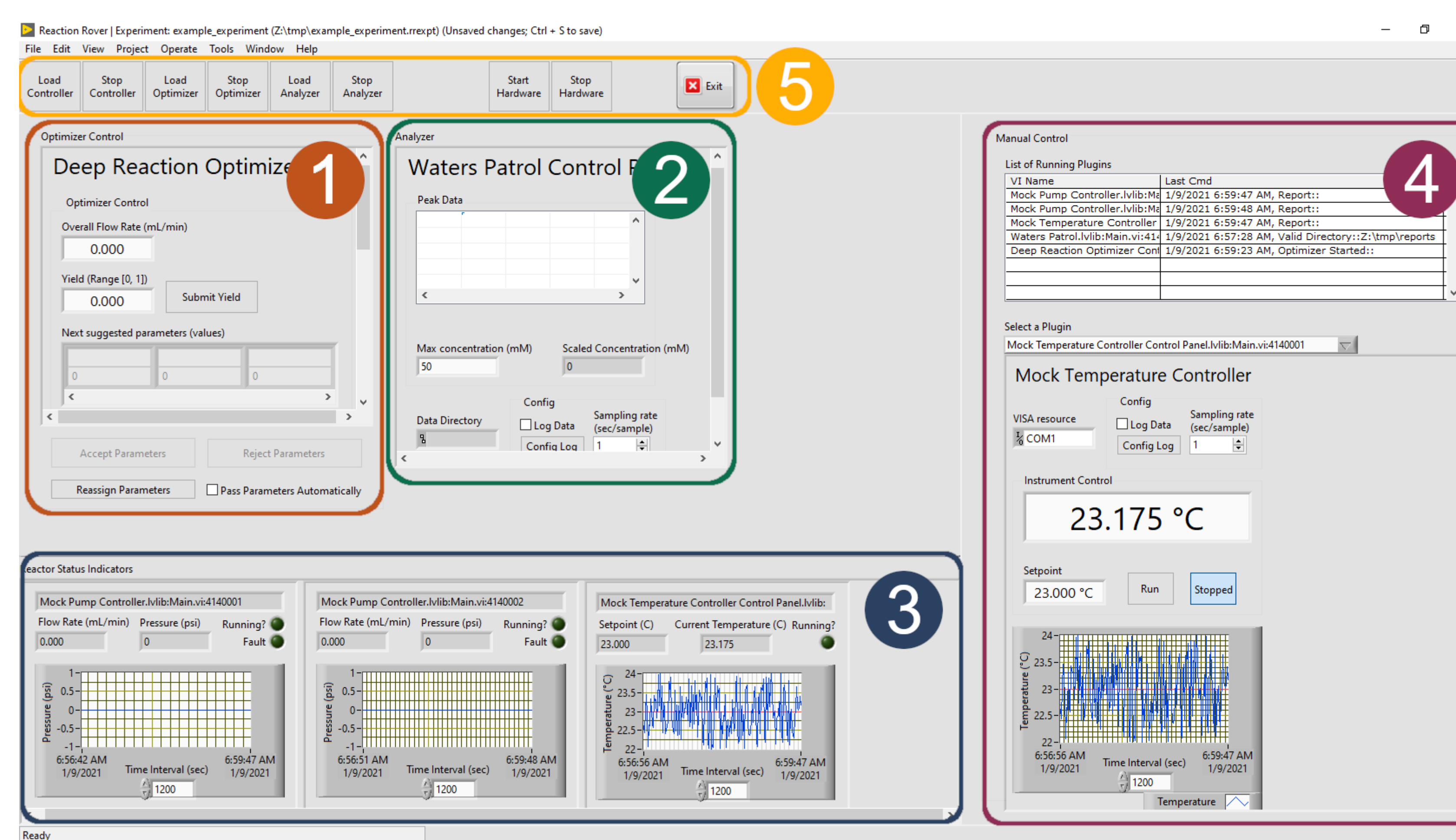


Figure 1. Rxn Rover user interface showing the areas where plugins are loaded for the optimizer (#1; orange), analyzer (#2; green), and reactor components (#3; blue), along with manual control of individual reactor components (#4; purple) and overall reactor controls (#5; yellow).¹

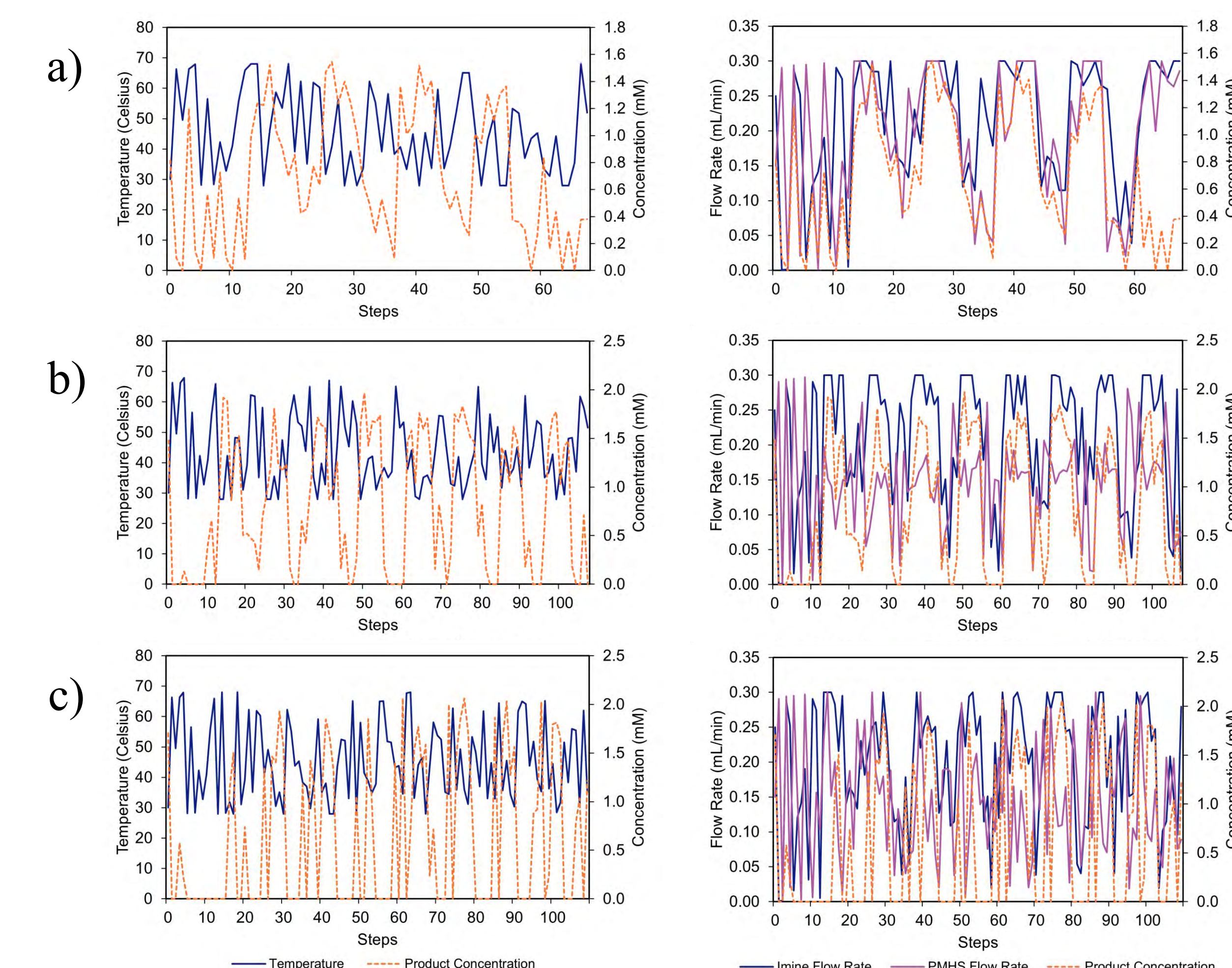


Figure 2. Parameter search during optimization trials with temperature and product concentration per iteration (left column) and flow rates and product concentration per iteration (right column). Trial 1 (a), trial 2 (b), and trial 3 (c) are listed from top to bottom.

Conclusions

Through chemical reaction automation, Rxn Rover can maximize efficacy of research and development with non-stop reaction discovery, improve the safety and consistency of reactions by minimizing human interaction with the optimization process, and increase reproducibility through detailed logging of reaction conditions and results and by recording experimental setups for later reproduction. As a free, open-source software, Rxn Rover is also positioned to provide resource-limited institutions with more access to laboratory automation.

References

- (under review) Z. Crandall, K. Basemann, L. Qi and T. L. Windus, *Reaction Chemistry & Engineering*, 2021, **00**.
- W. Lavrijsen and scikit-quant, 2020.
- W. Huyer and A. Neumaier, *ACM Transactions on Mathematical Software*, 2008, **35**, 1-25.

Abstract

How do you make the most of limited time and resources in the laboratory? The single-word answer is automation. The oxidation laboratories at bp, were early adopters of automation principles, and this has paid dividends in the team's continued expansion of capabilities. This poster presents a breakdown of how bp uses automation to investigate lubricants safely over long periods of time.

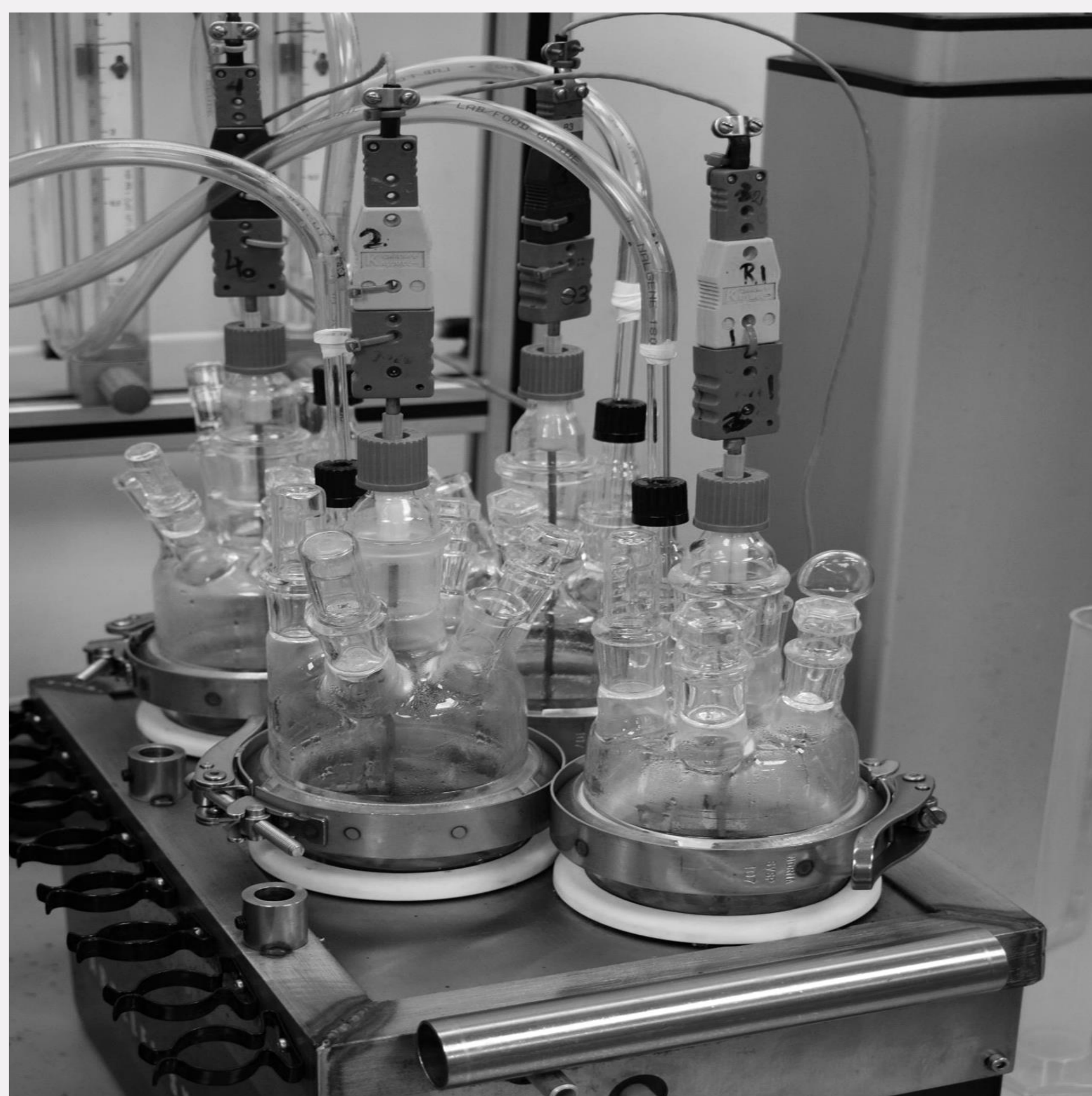


Figure 1. Automated parallel system used in the bp lab.

Introduction

Lubricants are substances used to ease the relative motion of solids bodies by reducing friction and wear between surfaces [1].

Degradation of lubricants by oxidative mechanism is a very serious challenge. New formulated lubricants may have desirable properties, however; oxidation could lead to considerable loss of performance such as [2]:

- Corrosion by organic acids.
- Formation of polymers.
- Viscosity changes.
- Loss of electrical resistivity.

The oxidation laboratories at bp perform a variety of stability tests to measure resistance to oxidation under different conditions.



Figure 2. Automated parallel system used in the bp lab.

Results

One of the most important tests bp perform on lubricant samples is observing changes in a properties, and thus performance, over time. bp undertakes this test over long periods of times with the aid of automation and parallel chemistry.

The total acid number (TAN) is a measure of acidity that is determined by the amount of potassium hydroxide in milligrams that is needed to neutralize the acids in one gram of the sample [3].

In this test (shown in Figure 3), Sample 1 was used in reactor 1 and 2, while Sample 2 was used in reactor 3 and 4. It could be seen that:

- Sample 1 is significantly more stable over time.
- Consistency between experiments by comparing similar samples in different reactors.

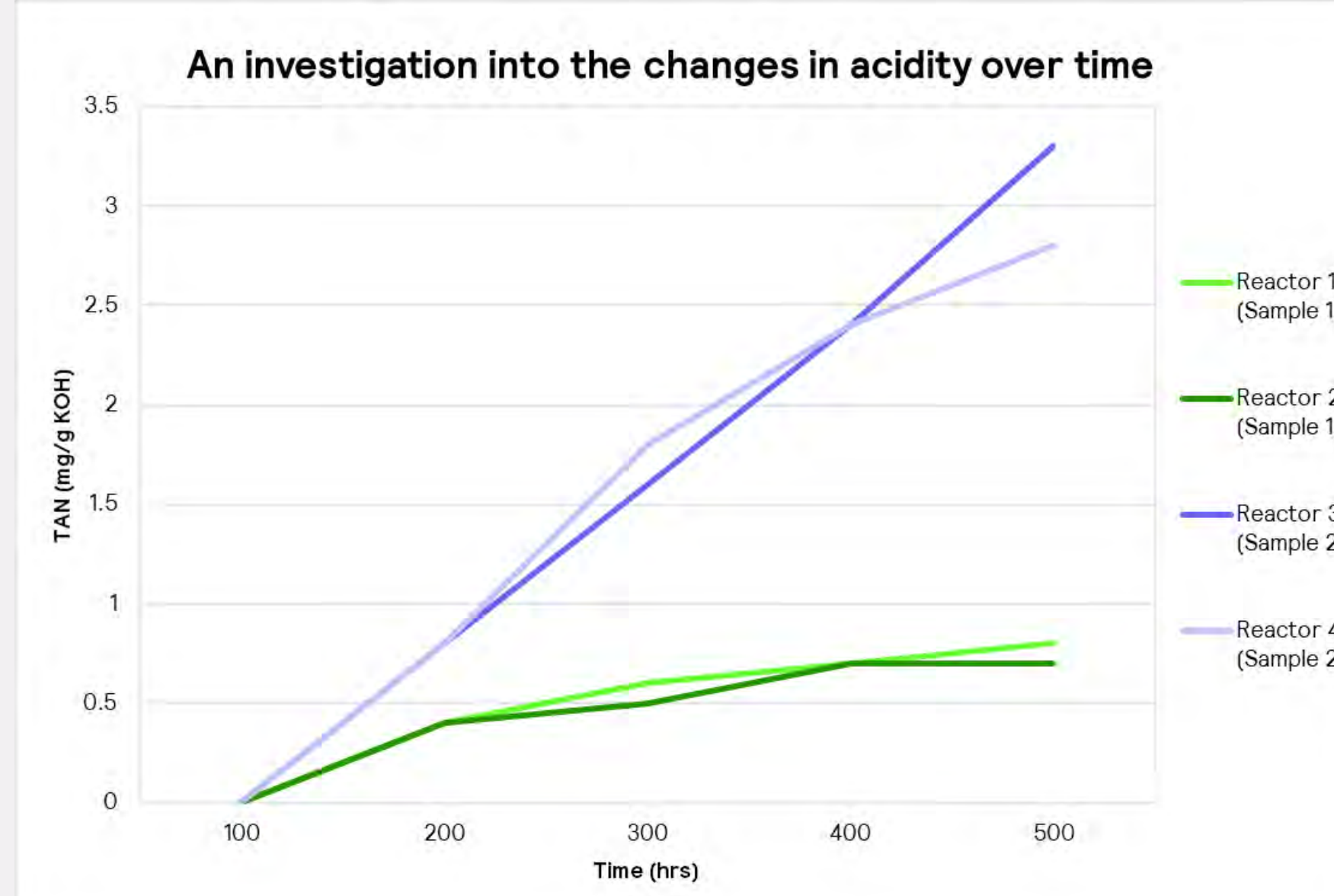


Figure 3. Variation in the total acid number over time.

To investigate the viscosity changes over time, bp takes samples and measures kinematic viscosity at 100 °C, referred to as KV₁₀₀ [4].

The time-dependent variation in kinematic viscosities of Sample 1 and 2 are shown in Figure 4. It could be seen that:

- The increase in viscosity of Sample 1 with time is considerably lower than that of Sample 2.
- There is consistency between experiments by comparing similar samples in different reactors.

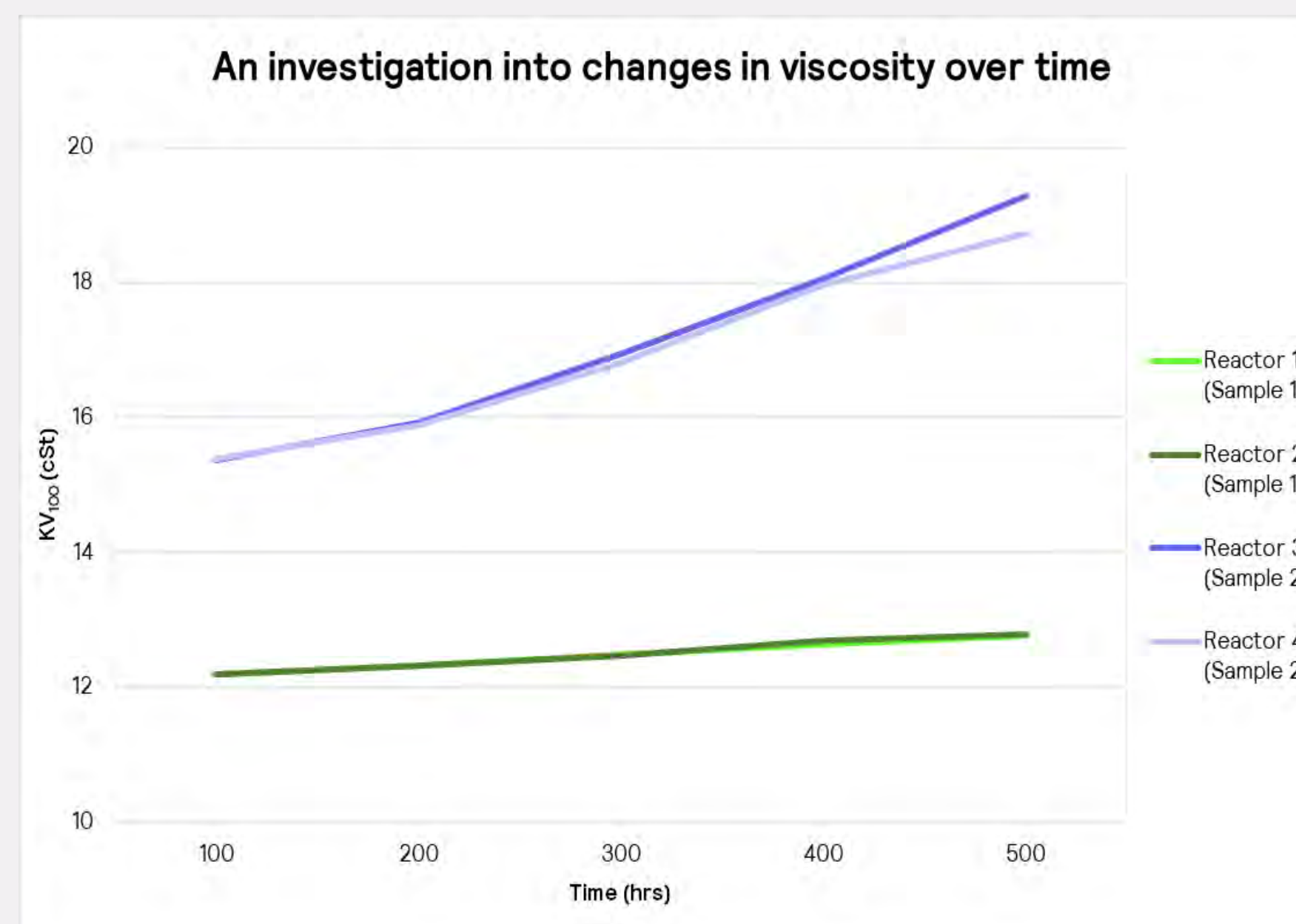


Figure 4. Variation in viscosity as a function of experiment time.



Figure 5. Automated parallel system used in the bp lab.

Discussion

Stability is one of the most important factors in lubricants characterization. Automation and parallel chemistry has helped bp to perform various stability tests on their lubricant samples to investigate degradation over long periods of time.

The results illustrate that:

- Sample 1 has a slower rate of degradation compared with Sample 2 in terms of both acidity and viscosity.
- Consistent data can be obtained by using automation and parallel chemistry.



Figure 6. Automated parallel system used in the bp lab.

Conclusions

Lab automation and parallel chemistry can be used to:

- Perform automated stability experiments on lubricants for long periods of time.
- Make comparison between different sample of lubricants.
- Achieve precise results.

Automation and parallel chemistry can readily and easily be used for other chemistries.

Contact

Sina Ehsani, PhD
H.E.L Group
Email: sinaehsani@helgroup.com
Website: helgroup.com
Phone: 410-598-1401



H.E.L Group



@hel_group



@HELLtd

References

1. Bart, Jan CJ, Emanuele Gucciardi, and Stefano Cavallaro. Biolubricants: science and technology. Elsevier, 2012.
2. Fox, Malcolm F. Chemistry and technology of lubricants. Eds. Roy M. Mortier, and Stefan T. Orszulik. Vol. 107115. New York: Springer, 2010.
3. Park, Lydia KE, et al. "Contribution of acidic components to the total acid number (TAN) of bio-oil." Fuel 200 (2017): 171-181.
4. Hawley, J. Gary, et al. "The effect of engine and transmission oil viscometrics on vehicle fuel consumption." Proceedings of the Institution of Mechanical Engineers, Part D: Journal of Automobile Engineering 224.9 (2010): 1213-1228.

Automated Solid-Phase Synthesis of Polyethylene Glycol

Dhananjani Eriyagama, Shiyue Fang

Department of Chemistry, Michigan Technological University, Houghton MI 49931

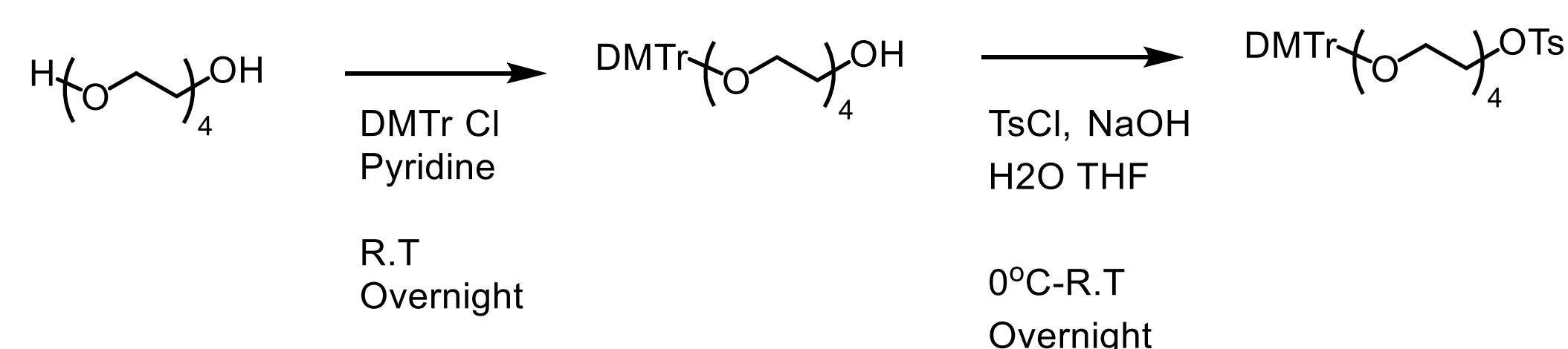
Abstract

Polyethylene glycol (PEG) and derivatives with eight, twelve, and sixteen ethylene glycol units were synthesized using automated stepwise addition of tetra ethylene glycol monomer on a solid support. One hydroxyl group of the PEG4 is protected with dimethoxy trityl group, and the other is reacted with tosyl group. The Wang resin, which contains the 4-benzyloxy benzyl alcohol function, was used as the support. The synthetic cycle consists of deprotonation, Williamson ether formation (coupling), and detritylation. Cleavage of PEGs from solid support was achieved with pure trifluoroacetic acid.

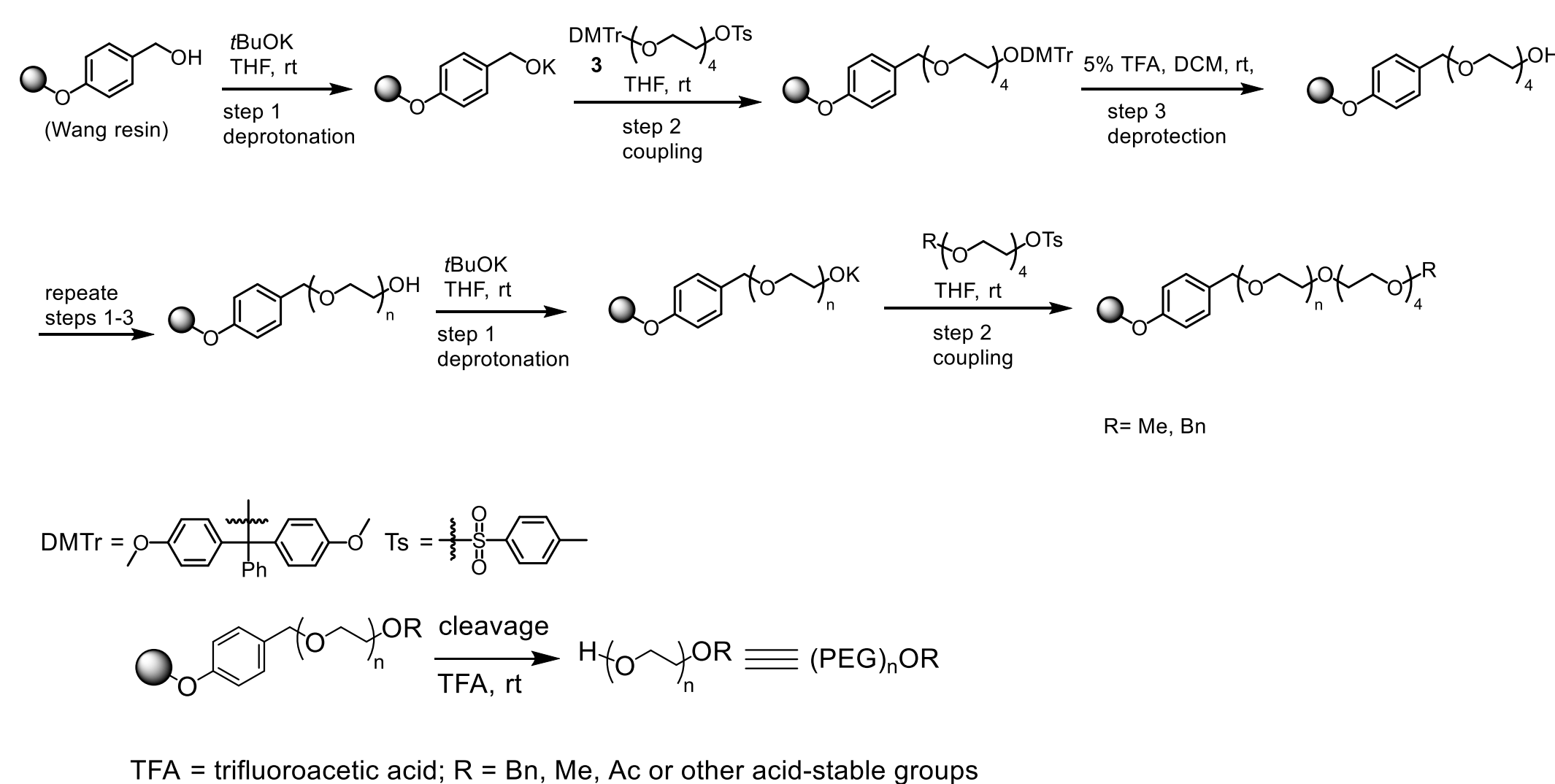
Introduction

Due to its interesting physical and chemical properties such as high solubility in water and other solvents, stable neutral and flexible structure, and biocompatibility, Polyethylene glycol (PEG) is found a variety of applications in various fields, including the pharmaceutical industry, nanomedicine, surface science, carbon nanotube functionalization, and organic-inorganic hybrid materials. PEGs are widely used in the pharmaceutical industry as an ingredient that can be attached to therapeutics, known as PEGylation. PEGs can be chemically synthesized by polymerization of ethylene oxide, which has been known for many years, and resulting PEGs have a wide range of molar masses due to the randomness of the polymerization reaction. Stepwise organic synthesis is also employed to synthesize PEGs. However, due to the harsh conditions of the reaction and the low efficiency of Williamson ether formation reaction, it is challenging to obtain longer PEGs with high purity. Even though PEGs with different lengths are used in PEGylation, they are not ideal due to several reasons such as loss of intended properties due to the heterogeneous nature of PEGs, the difficulty of achieving constant composition from batch to batch, and challenging to get FDA approval. Therefore, monodispersed PEG is preferred as a pharmaceutical ingredient. In order to obtain monodispersed PEGs, excessive purification is required. Due to the current purification methods in use, the cost of homogenous PEGs increases drastically and, as a result, increases the cost of any product that uses PEGs as an ingredient. A decrease in the efficiency of the Williamson ether formation reaction with longer PEGs is another challenge associated with more extended PEG synthesis. To overcome these problems, our research group designed a novel method called the automated solid phase stepwise synthesis of polyethylene glycol.

Design of the PEG monomer

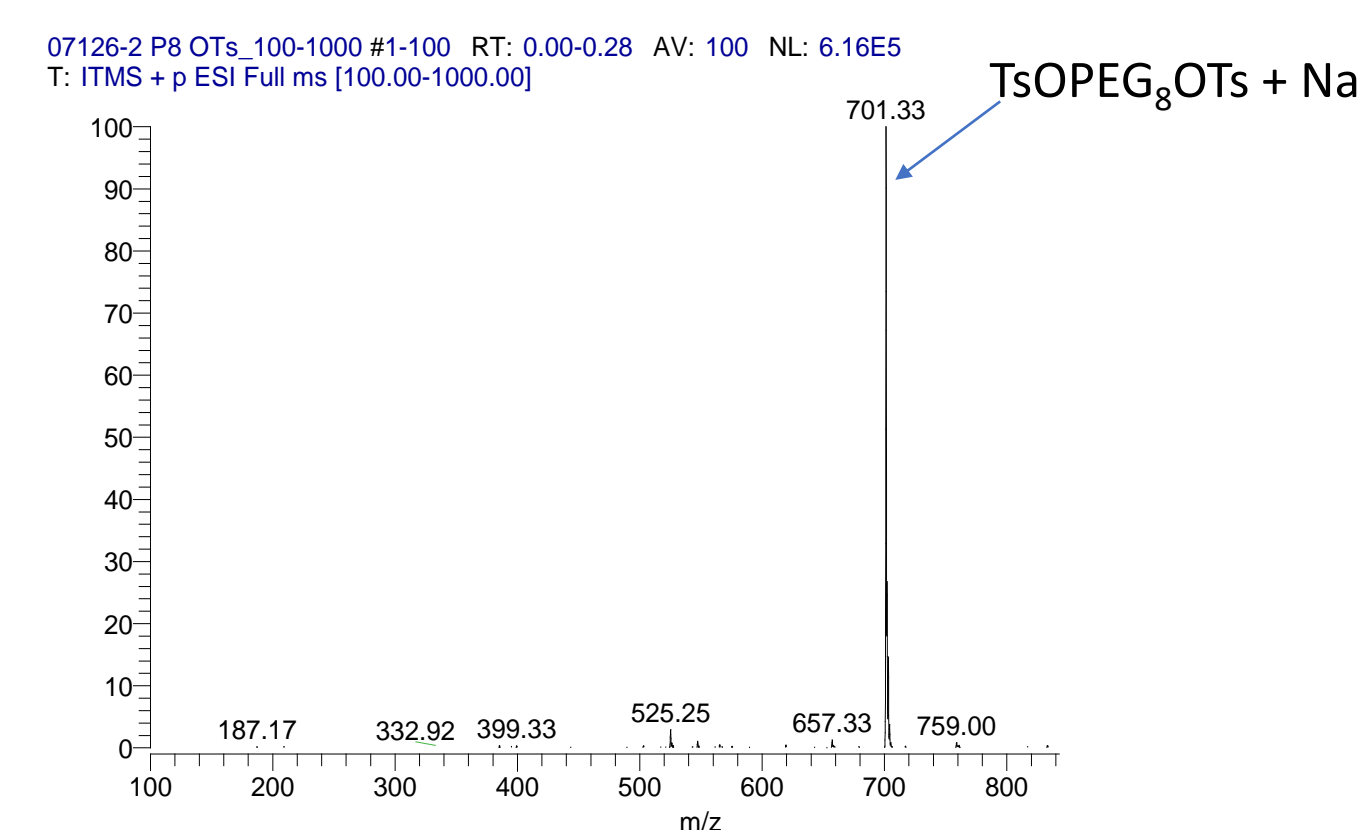


Automated PEG synthesis and cleavage

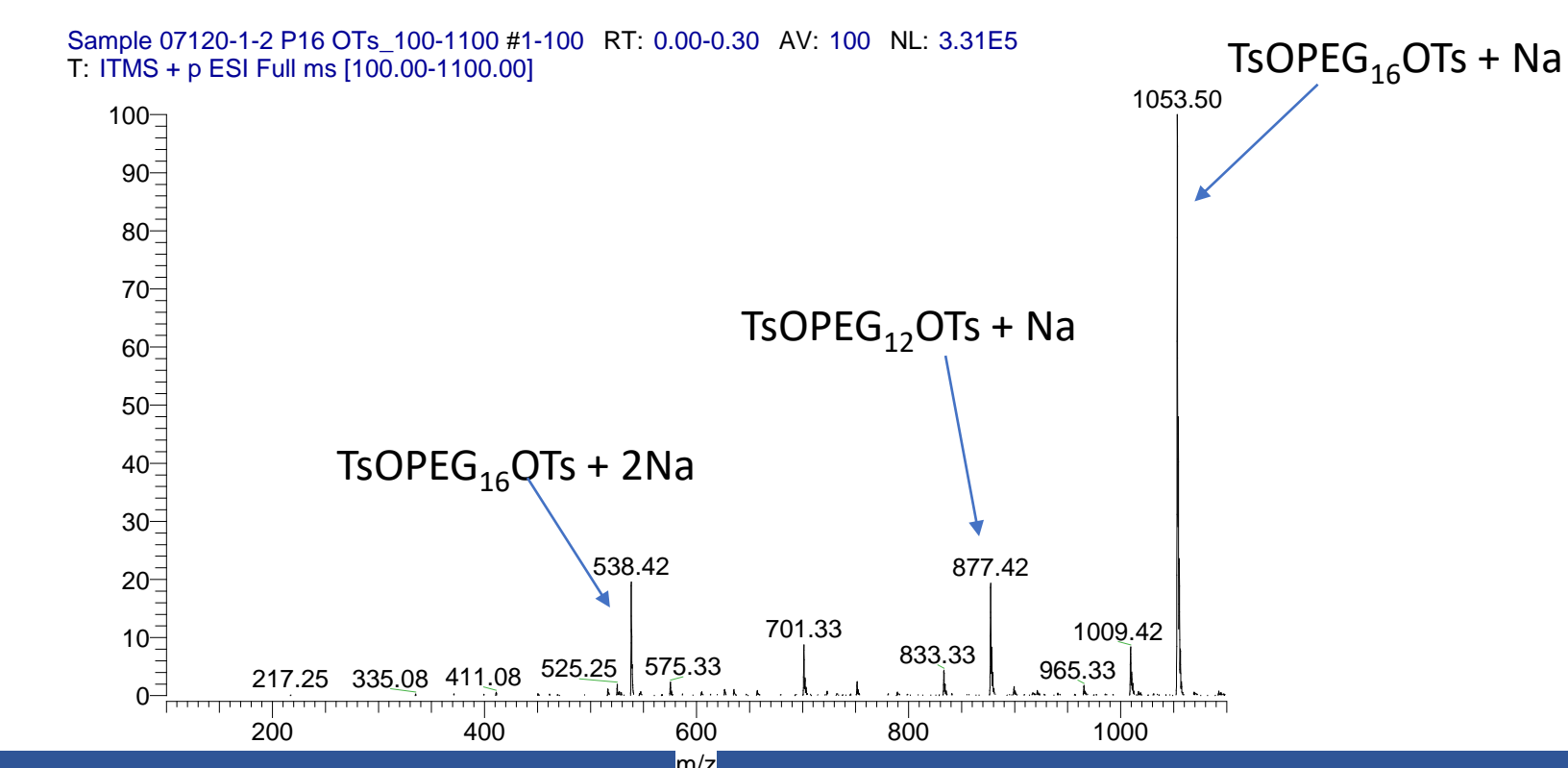


Results

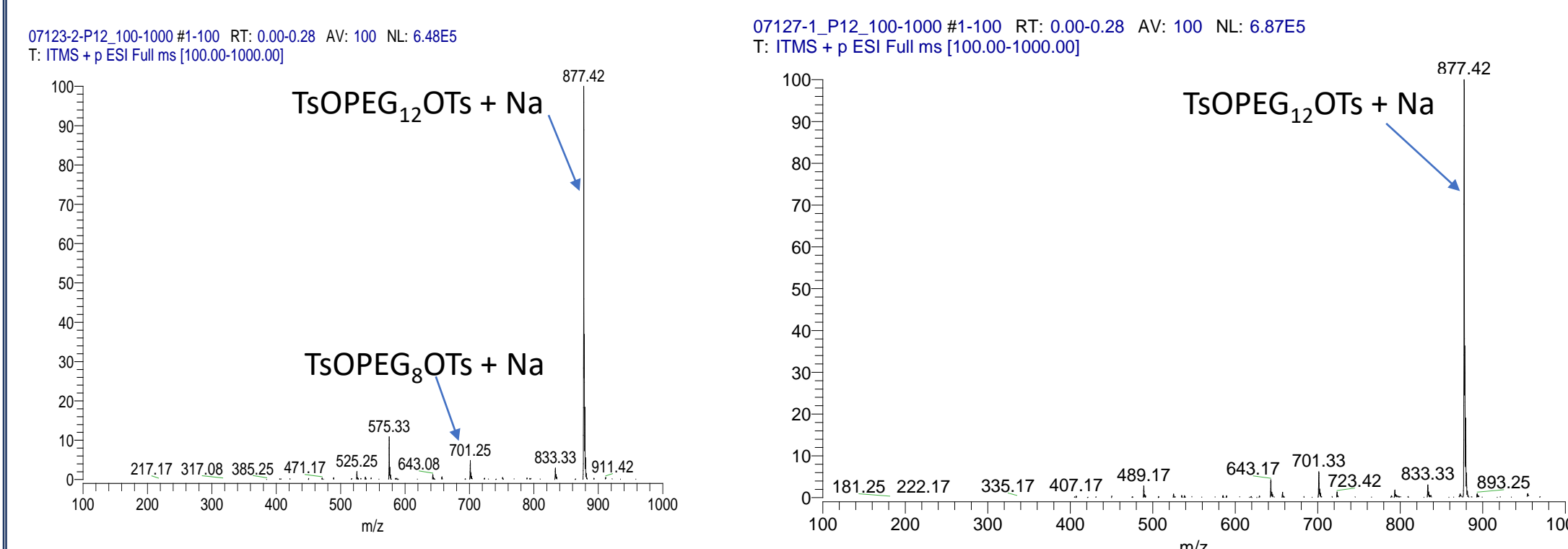
PEG 8 synthesis



PEG16 derivative synthesis



PEG 12 synthesis



Conclusion

In conclusion:
We have demonstrated that the automated stepwise solid-phase technology is suitable for the synthesis of monodisperse PEGs and their derivatives. Advantages of the method include chromatography-free synthesis, minimize human errors, reduced time and solvents required for the synthesis hence bring down the overall cost of the PEG synthesis, milder conditions for the Williamson ether formation reaction to minimize depolymerization of PEGs to increase the monodispersity of PEGs, and the overall yield. Using the technology, we successfully synthesized PEG derivatives with eight, twelve, and sixteen ethylene glycol units with close to monodispersity. We are currently tuning conditions to achieve long PEG synthesis with little purification efforts and searching for solutions to further increase the purity of PEG products.

Contact

Dhananjani Eriyagama
Michigan Technological University
Email: aeriyaga@mtu.edu
Phone: 906 231 2992

References

1. Ashok Khanal, Shiyue Fang. Solid Phase Stepwise Synthesis of Polyethylene Glycol. *Chemistry—A European Journal* **2017**, *23*, [1533-1542](#)

Acknowledgements

HRI graduate fellowship; Financial support from Grants NSF I-Corps (1754235) and NSF PFI (1918585); the assistance from D. W. Seppala (electronics), J. L. Lutz (NMR), L. R. Mazzoleni (MS), S. Schum (MS), and A. Galerneau (MS); and NSF equipment grants (CHE1048655, CHE9512455, AGS1531454); are gratefully acknowledged.

Automated Synthesis and Characterization of Metallic Nanocrystals for a Remote Physical Chemistry Lab Course

Mark P. Hendricks, *Department of Chemistry, Whitman College, Walla Walla, WA*

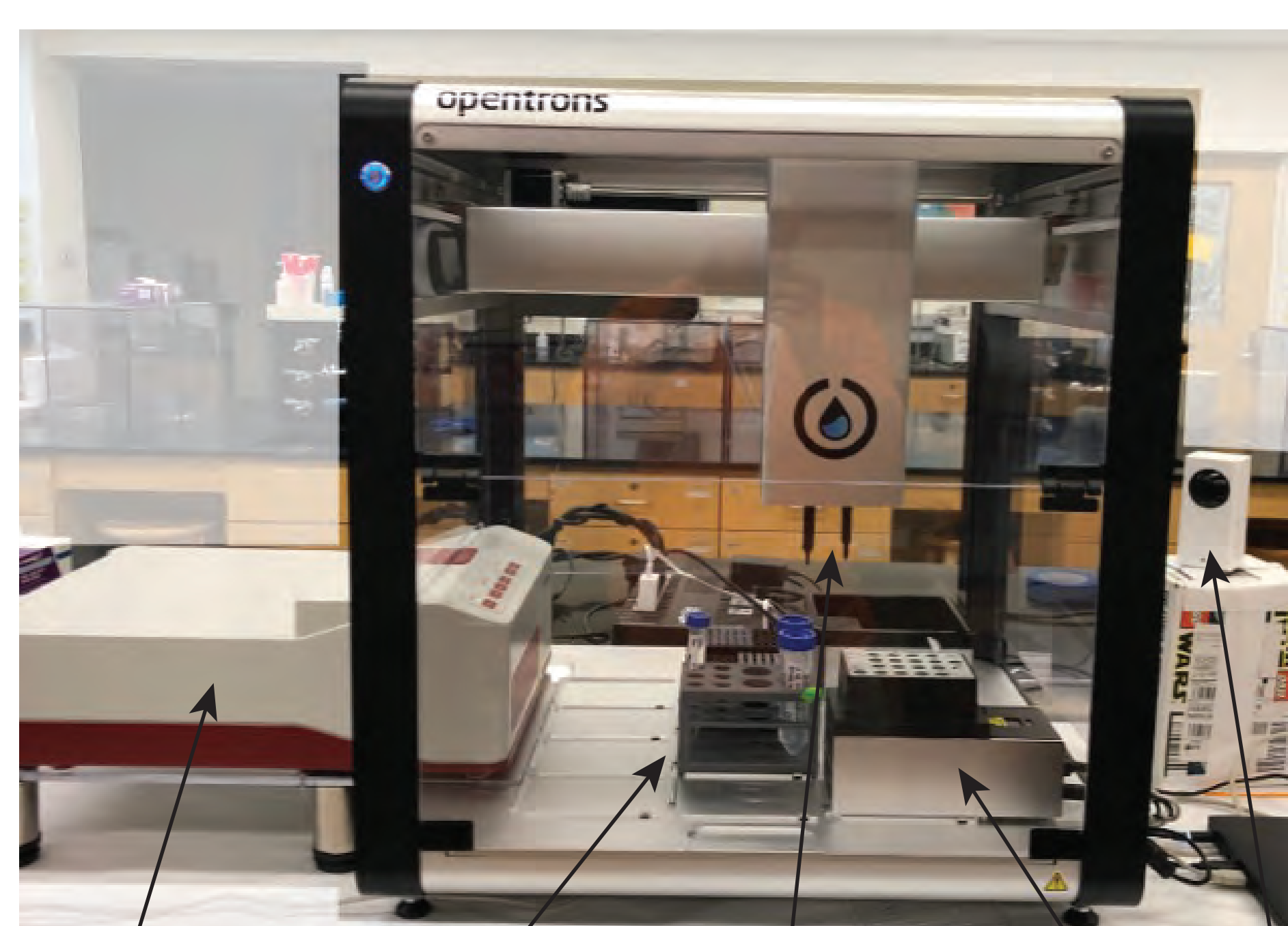
Background

In spring of 2021, Whitman College's physical chemistry laboratory course was forced online due to the covid-19 pandemic. The primary learning objectives of the course are to train students in experimental design and data analysis, so shifting to theory-based or pre-recorded labs would be challenging to satisfy these requirements. The course already included a lab automation component, which provided a unique solution: students would use lab automation tools to remotely develop a synthesis of silver nanocrystals and optimize their properties to serve as catalysts for the conversion of 4-nitrophenol to 4-aminophenol. Students were tasked with designing the synthesis and catalysis conditions themselves, but many students turned to the same literatures procedures that initially inspired the project.^{1,2}

Automated System

Our automated system consists of an Opentrons OT-2 liquid handling robot with custom-integrated BMG Labtech Spectrostar Nano UV-vis plate reader. Both silver nanocrystal synthesis and catalysis of 4-nitrophenol conversion were done in 96-well plates on the plate reader, which allows both shaking and UV-vis characterization. An Opentrons temperature control unit allowed reagents such as sodium borohydride and hydrogen peroxide to be kept cool.

During the lab period, students worked in teams to analyze the data from the prior week and then submit their reaction conditions for the upcoming week using a Google Sheet UI (below) that our control software accepts directly to execute the reactions. Reactions were run between lab periods with the instructor onsite to prepare and place reagents on the robot deck, and a camera allowed students to monitor this process in real-time if they desired.



UV-vis plate reader on deck reagents on deck 20/300 μ L pipettes camera temperature controller

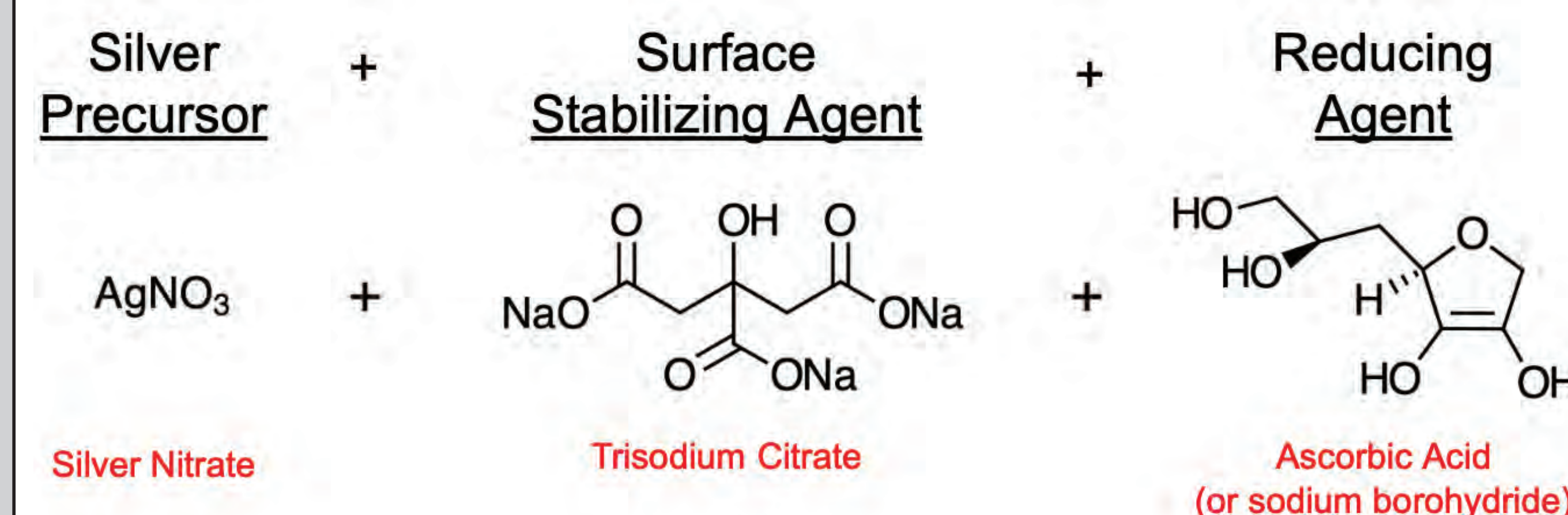
Example Input Sheet

list of reagents reactions (in unique wells) Scan for video of system in action



	A	B	C	D	E	F	G	H	I	J	K	L
1	concentration (mM)	reagent (must be unic	Pause	Mix	comments (HWM 11.1	control_1	HWM 11.2	HWM 11.3	HWM 11.4	HWM 11.5	HWM 11.6
2	Initial Destination											
3	0	water	0	0		200	0	9	12	15	18	21
4	12.5	trisodium citrate	0	0		0	27.5	20	20	20	20	20
5	0.375	silver nitrate	0	0		0	69	50	50	50	50	50
6	0.00723	potassium bromide	0	0		0	0	48	45	42	39	36
7	0.00723	potassium chloride	0	0		0	0	0	0	0	0	0
8	50	hydrogen peroxide 1	yes	0	#keep cold	0	69	48	48	48	48	48
9	50	hydrogen peroxide 2	0	0		0	0	0	0	0	0	0
10	5	sodium borohydride 1	yes	yes	#keep cold	0	34.5	25	25	25	25	25
11	50	hydrogen peroxide 3	yes	0		0	0	0	0	0	0	0
12	50	hydrogen peroxide 4	0	0		0	0	0	0	0	0	0
13	0.01	potassium bromide	0	0		0	0	0	0	0	0	0
14	1.00	potassium chloride	0	0		0	0	0	0	0	0	0
15	0.333	calcium chloride	0	0		0	0	0	0	0	0	0
16	5	sodium borohydride 2	yes	yes		0	0	0	0	0	0	0
17	0.5	silver nitrate	yes	0		0	0	0	0	0	0	0
18	16.66	sodium citrate	0	0		0	0	0	0	0	0	0
19	0.1	sodium hydroxide	0	0	new bottle (0	0	0	0	0	0	0	0
20	5	ascorbic acid	0	0	new bottle	0	0	0	0	0	0	0
21	10	ascorbic acid	0	0	new bottle	0	0	0	0	0	0	0
22	0.5	silver nitrate	0	0		0	0	0	0	0	0	0
23												

The Experiments



Example Synthesis Dataset



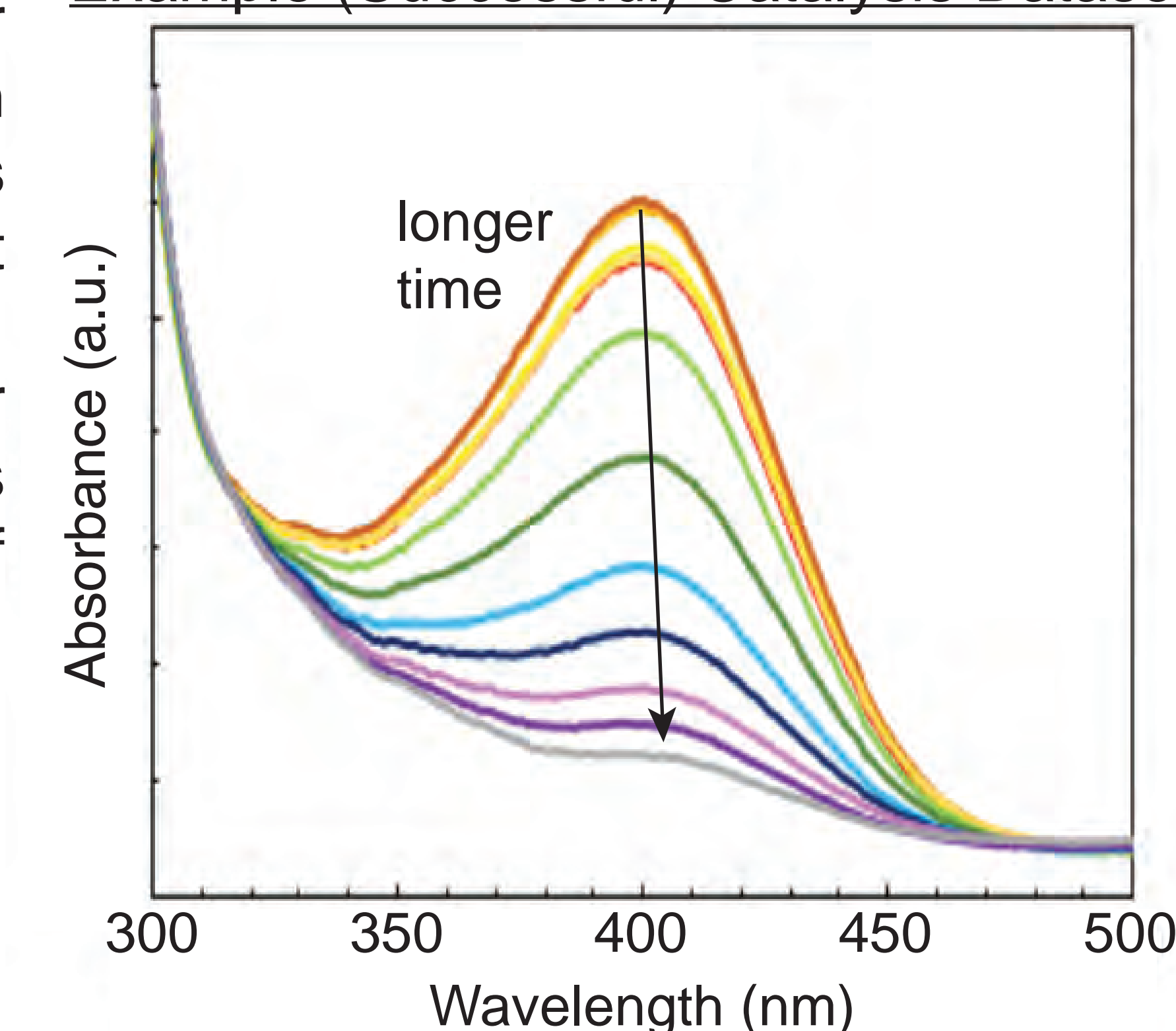
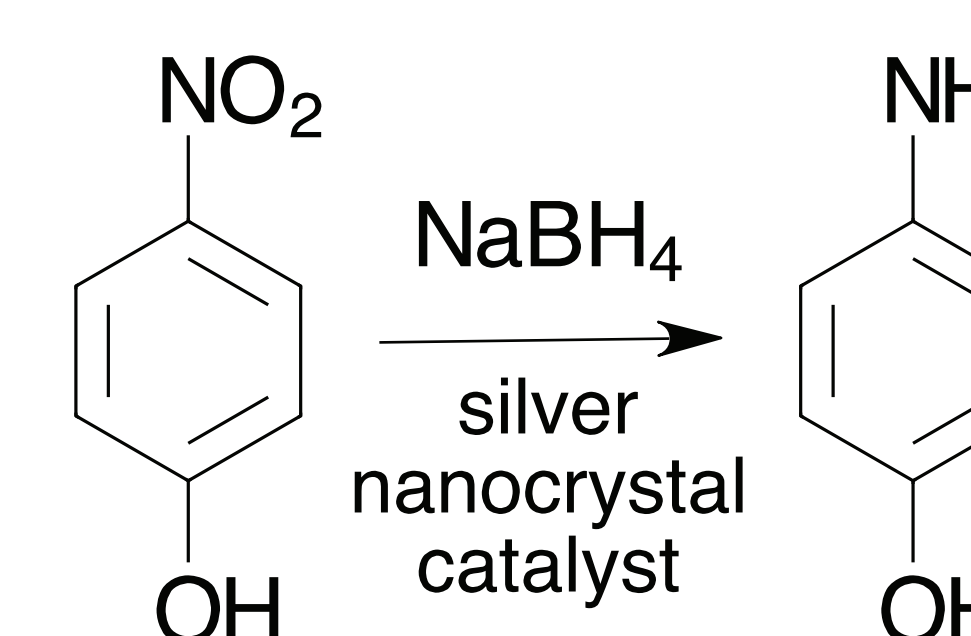
Photograph of Plate after Silver Nanocrystal Synthesis



All teams successfully produced silver nanocrystals with varying amounts of synthetic control depending on their reaction conditions.

Example (Successful) Catalysis Dataset

Most students were able to optimize their silver nanocrystals as successful catalysts for the reduction of 4-nitrophenol to 4-aminophenol, which was monitored using the absorbance of 4-nitrophenol at 400 nm (at right) using the same automated system. Students who spent longer developing their nanocrystal synthesis had less time on the catalysis section and did not always obtain clear data of conversion.



Conclusions

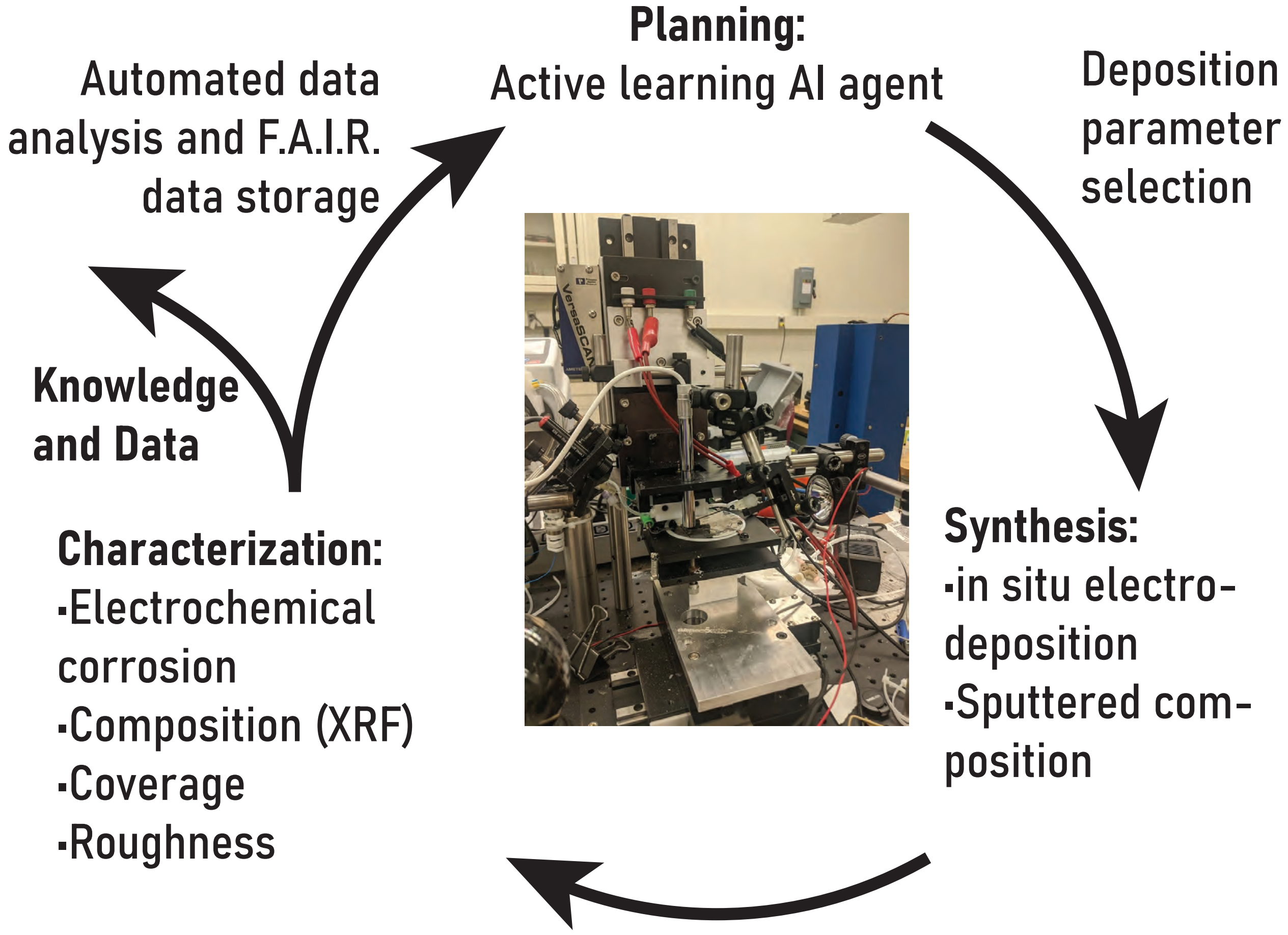
The use of a liquid-handling robot coupled with a UV-vis plate reader provided an ideal platform for a remote CURE focused on experimental design, data analysis, and concepts from physical chemistry, while also providing lessons in lab automation and data handling. Students responded positively to the experience and demonstrated learning in all areas, however they expressed some lack of engagement due to the remote and asynchronous nature of the experiments.

References

1. A. J. Frank, N. Cathcart, K. E. Maly, V. Kitaev; *J. Chem. Ed.*, 2010 87 (10), 1098-1101, DOI: 10.1021/ed100166g
2. J. Strachan, C. Barnett, T. Maschmeyer, A. F. Masters, A. Motion, A. K. L. Yuen; *J. Chem. Ed.* 2020 97 (11), 4166-4172, DOI: 10.1021/acs.jchemed.0c00499

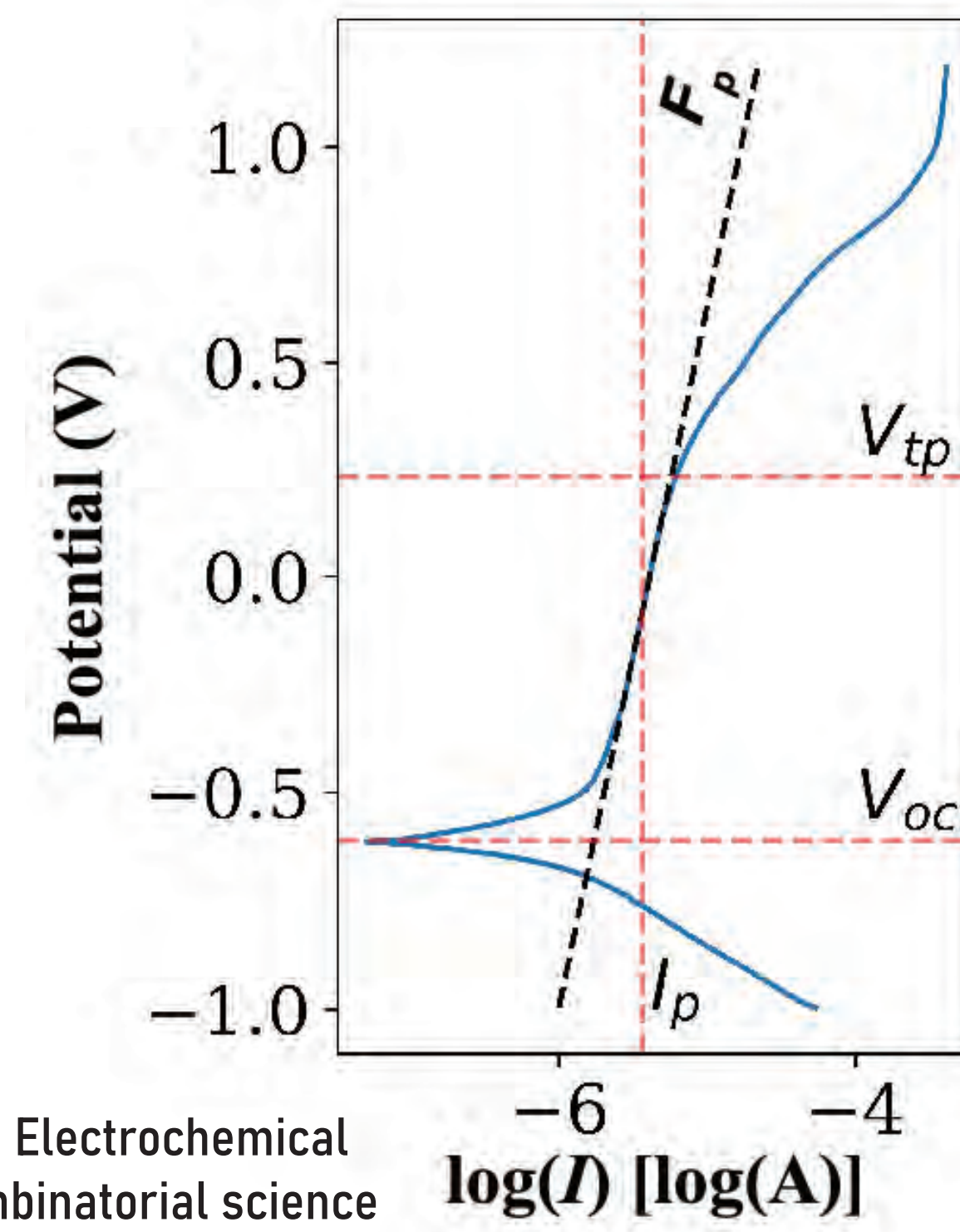
AUTONOMOUS MATERIALS DEVELOPMENT USING A SCANNING DROPLET

Goal: Closed loop autonomous materials discovery platform

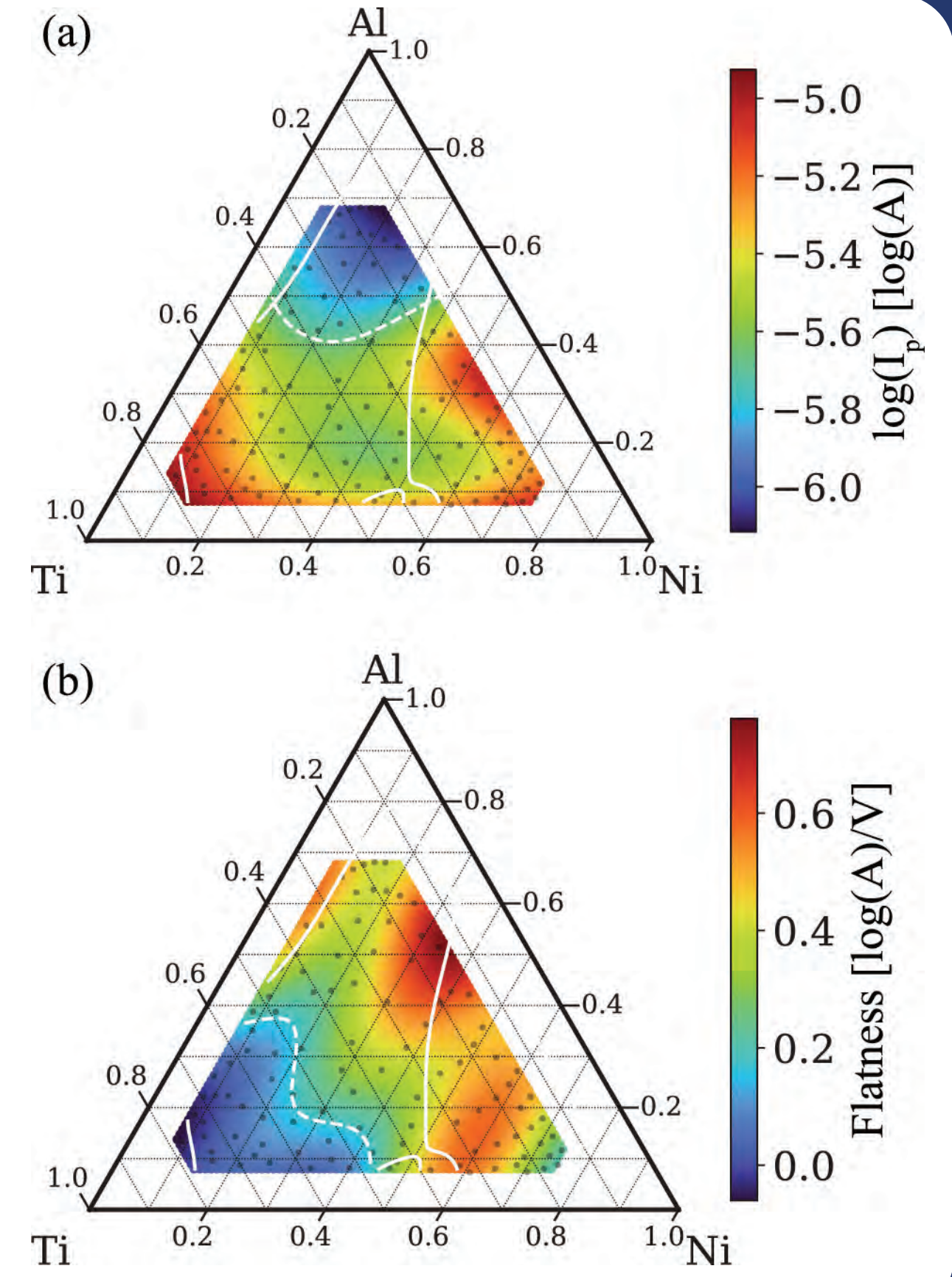


High-Throughput Corrosion Measurements: Al-Ni-Ti

- Pre-sputter deposited film with composition gradient
- Composition measured by x-ray fluorescence
- Corroded in 1 M (mol/L) NaCl
- Automated analysis of CV curves
- Highest corrosion resistance was correlated with widest x-ray diffraction features



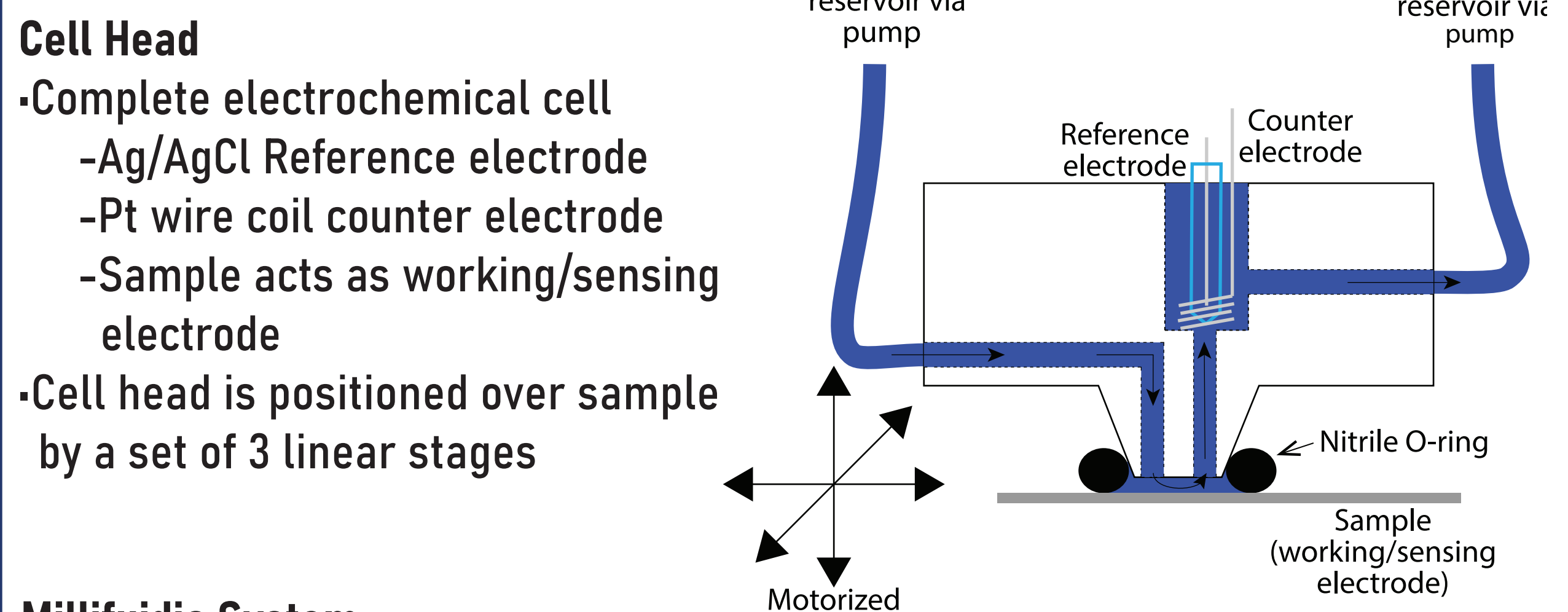
Jores, Howie, et al. "A High-Throughput Structural and Electrochemical Study of Metallic Glass Formation in Ni-Ti-AL" ACS combinatorial science 22.7 (2020): 330-338.



Hardware Implementation

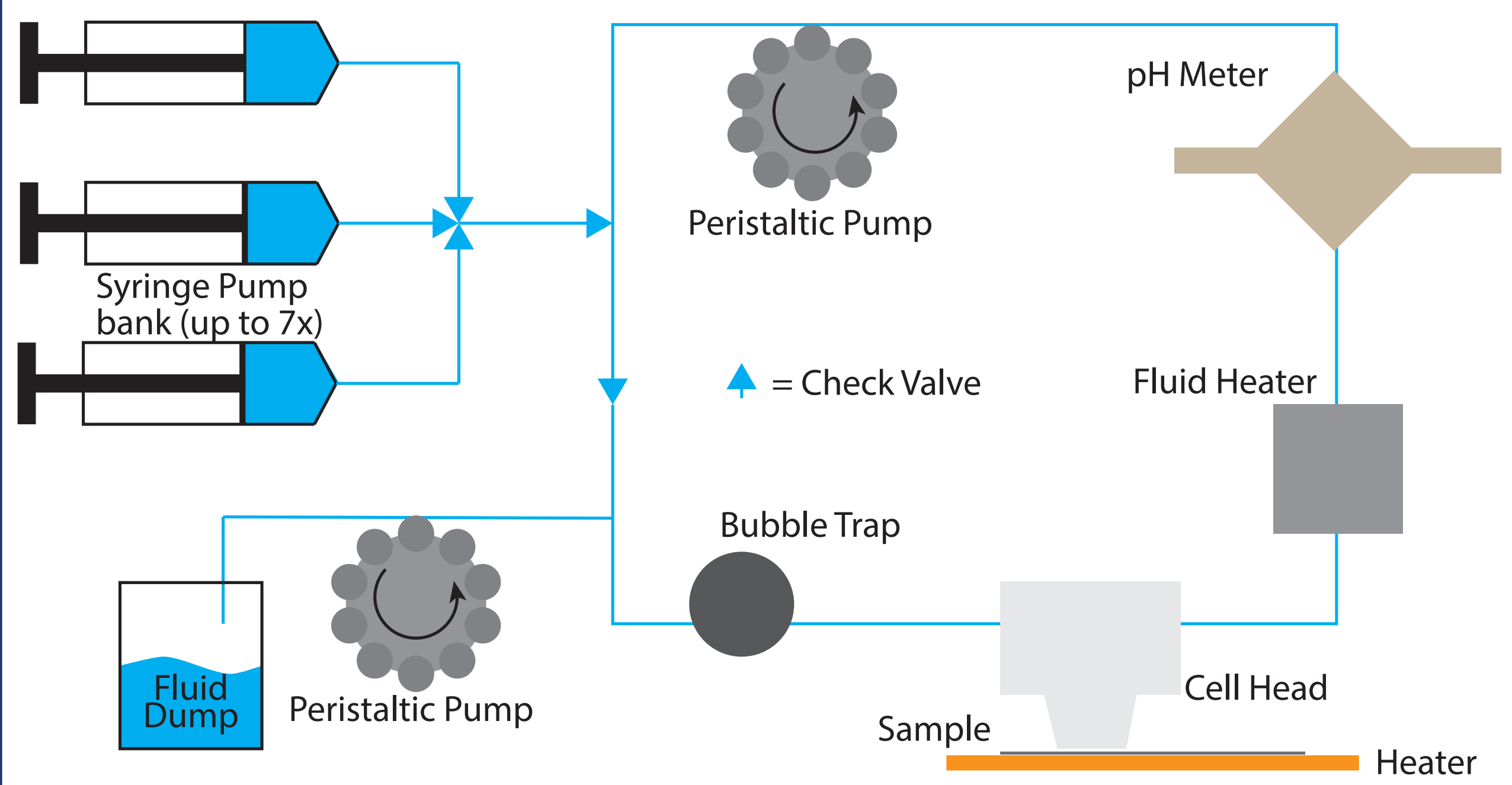
Scanning Droplet Cell
-Millifluidic System

- Compatible with any planar sample
- Minimal sample preparation
- Synthesis and Characterization capabilities



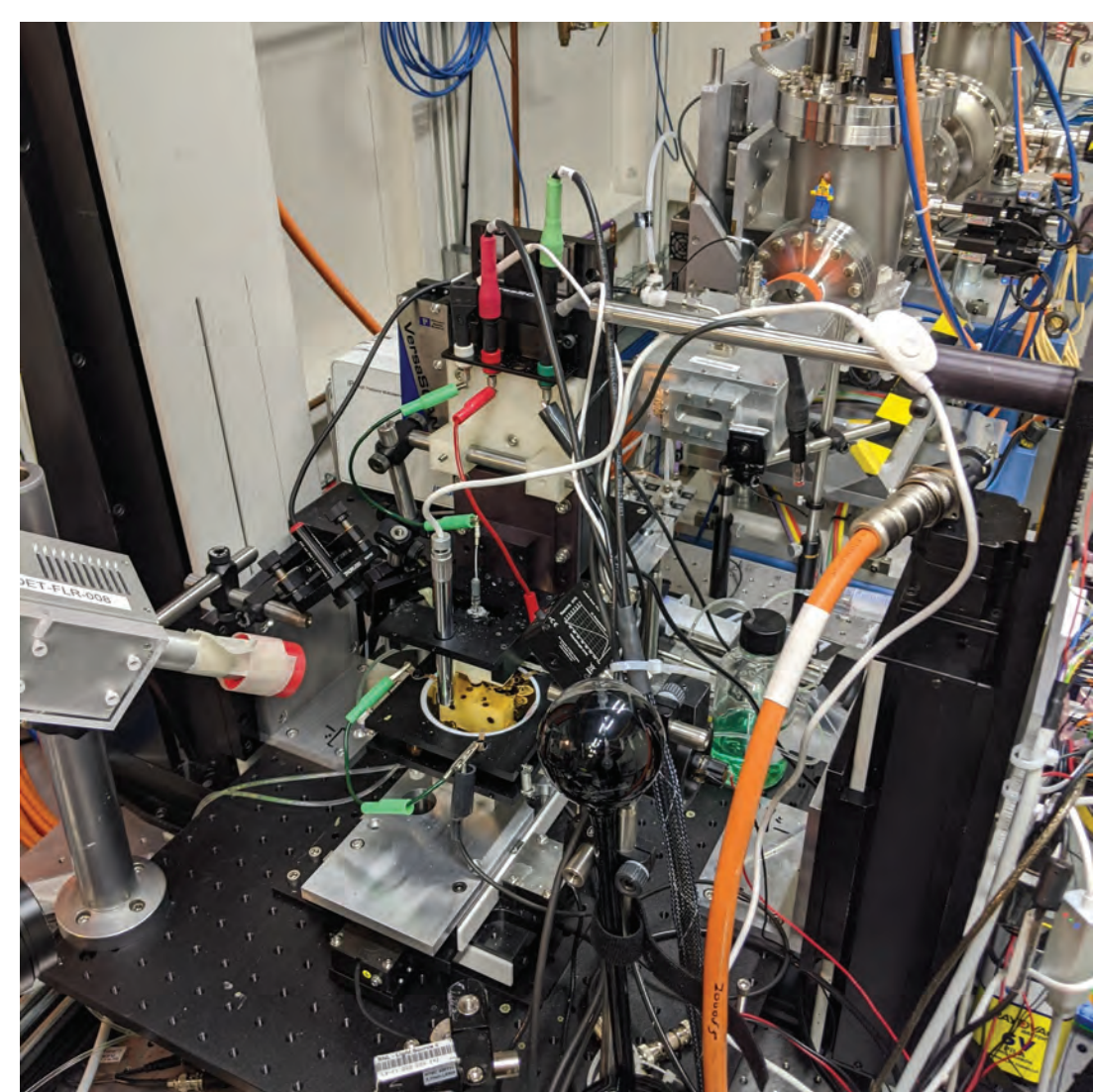
Millifluidic System

- Closed loop system to minimize fluid volume (~15 mL/experiment)
- Can vary solution concentration on the fly by differential pumping from syringe pumps



Control electronics and other components:

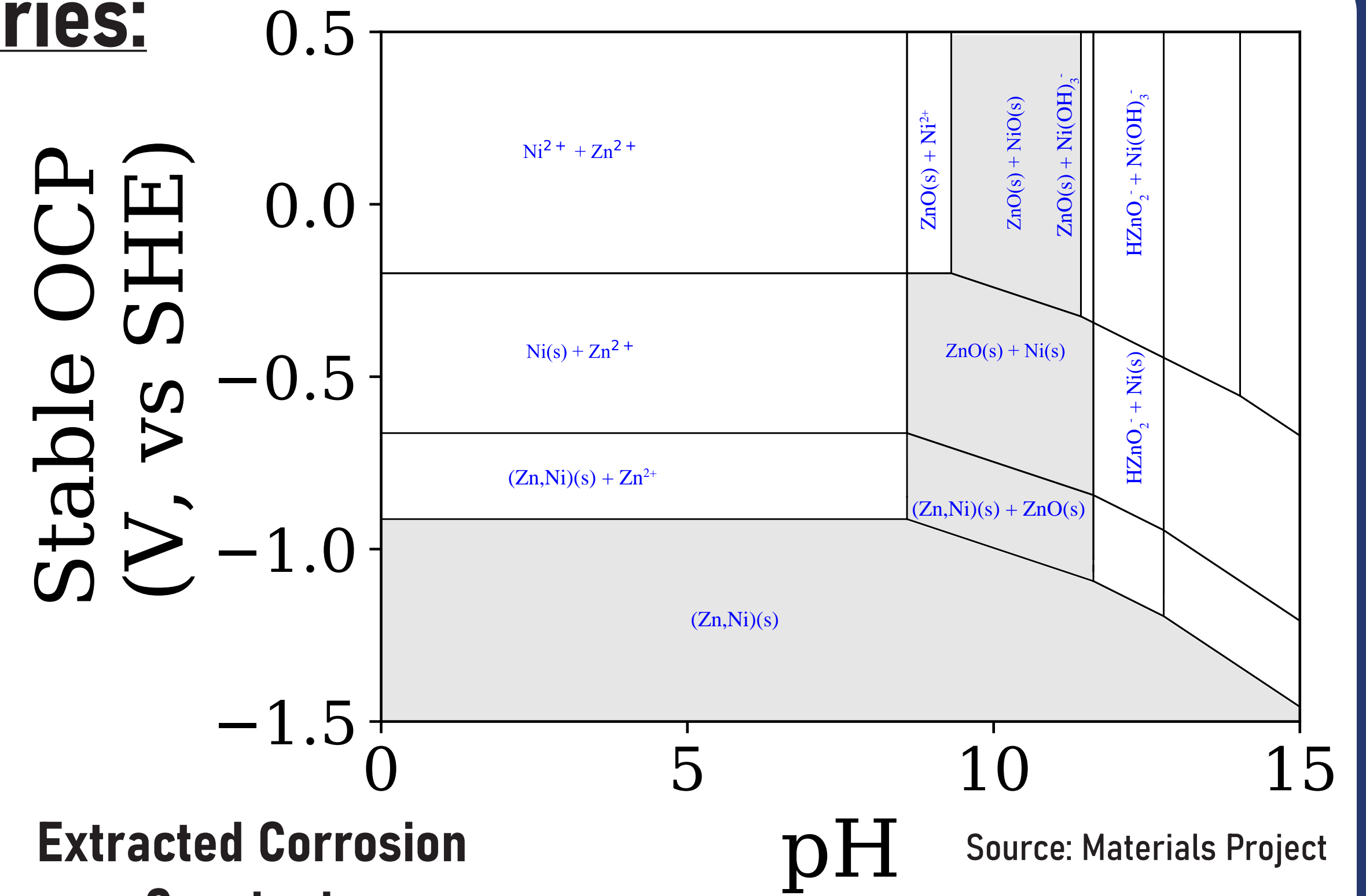
- Electrochemical reaction controlled by Ametek VersaSTAT potentiostat
- System is fully automated through a python interface
- Sites on the sample can be imaged from overhead camera
- Optical reflectance (635 nm) provides a measure of surface roughness
- Integrateable into synchrotron beamline (NLS/NIST BMM) for x-ray fluorescence and diffraction in situ



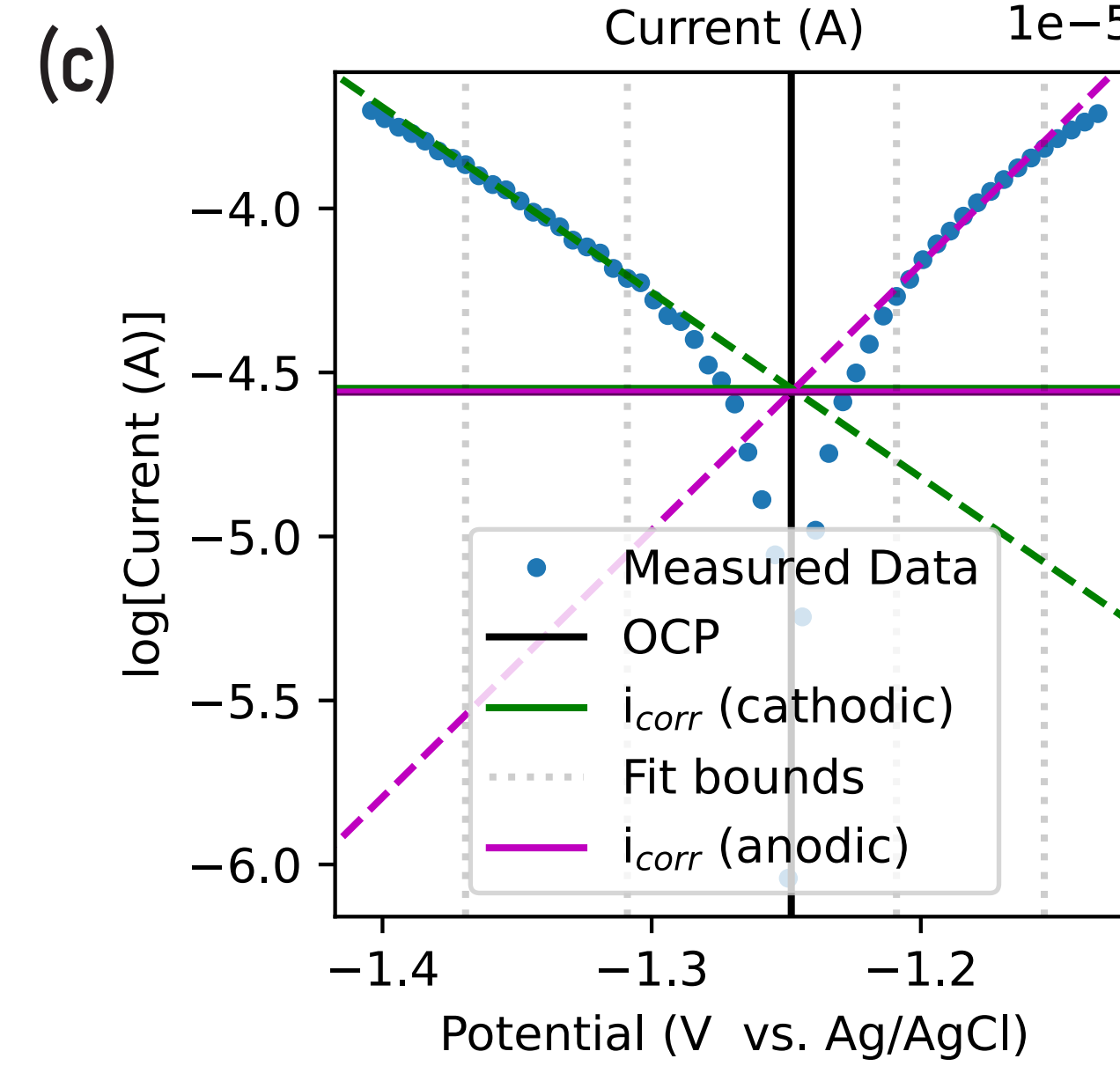
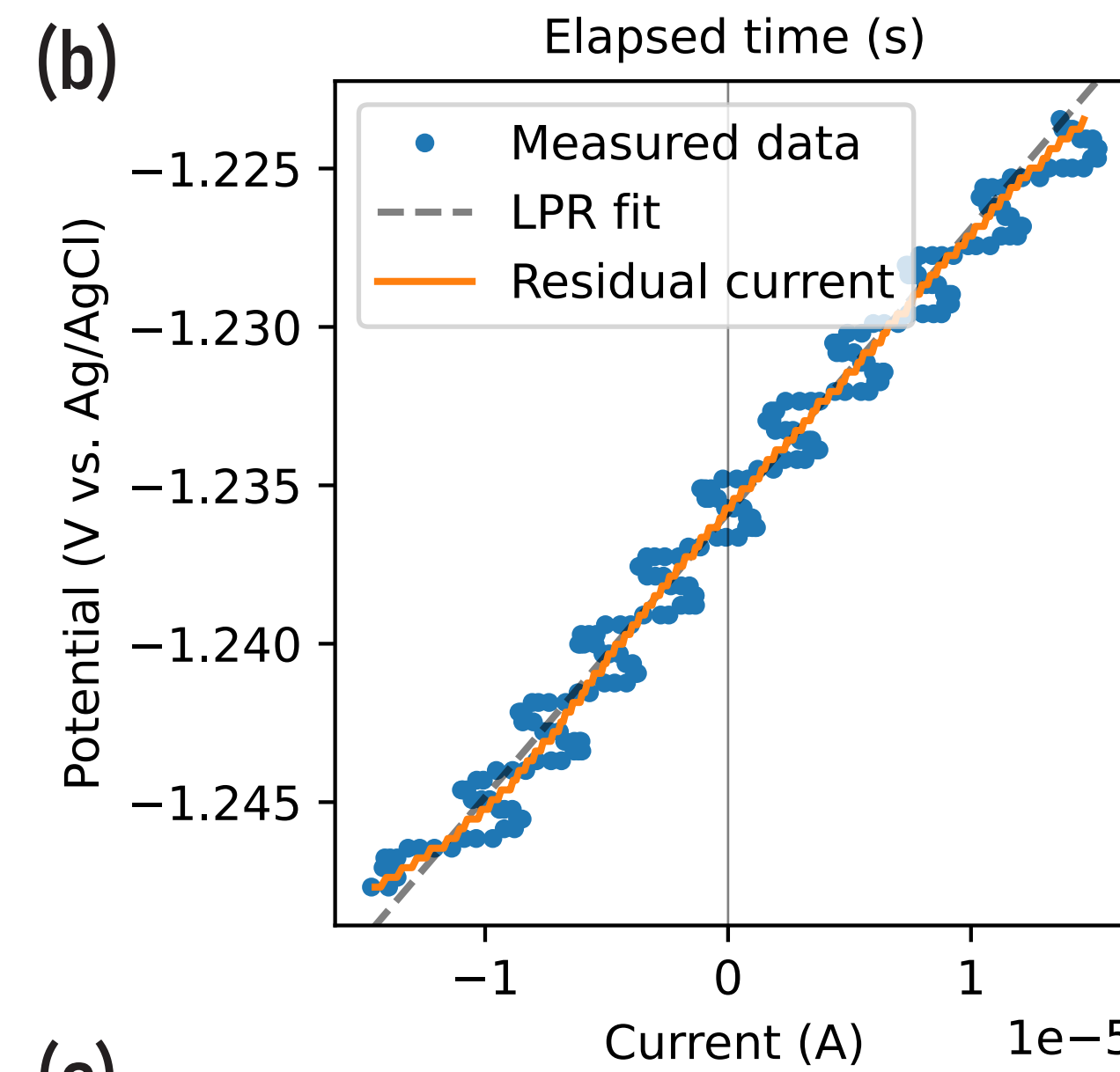
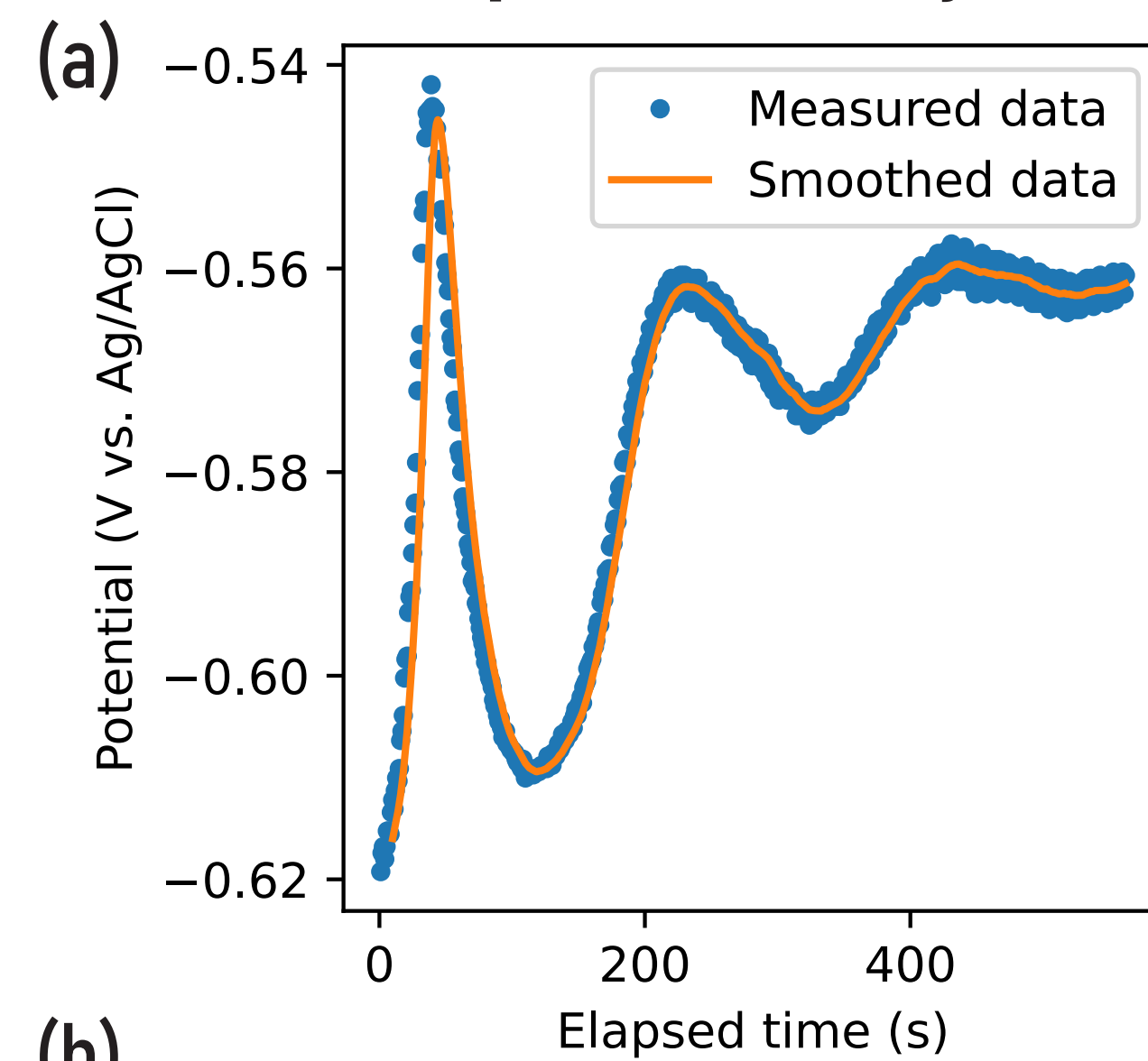
Automated pH Corrosion Series:

Zn₈₅Ni₁₅

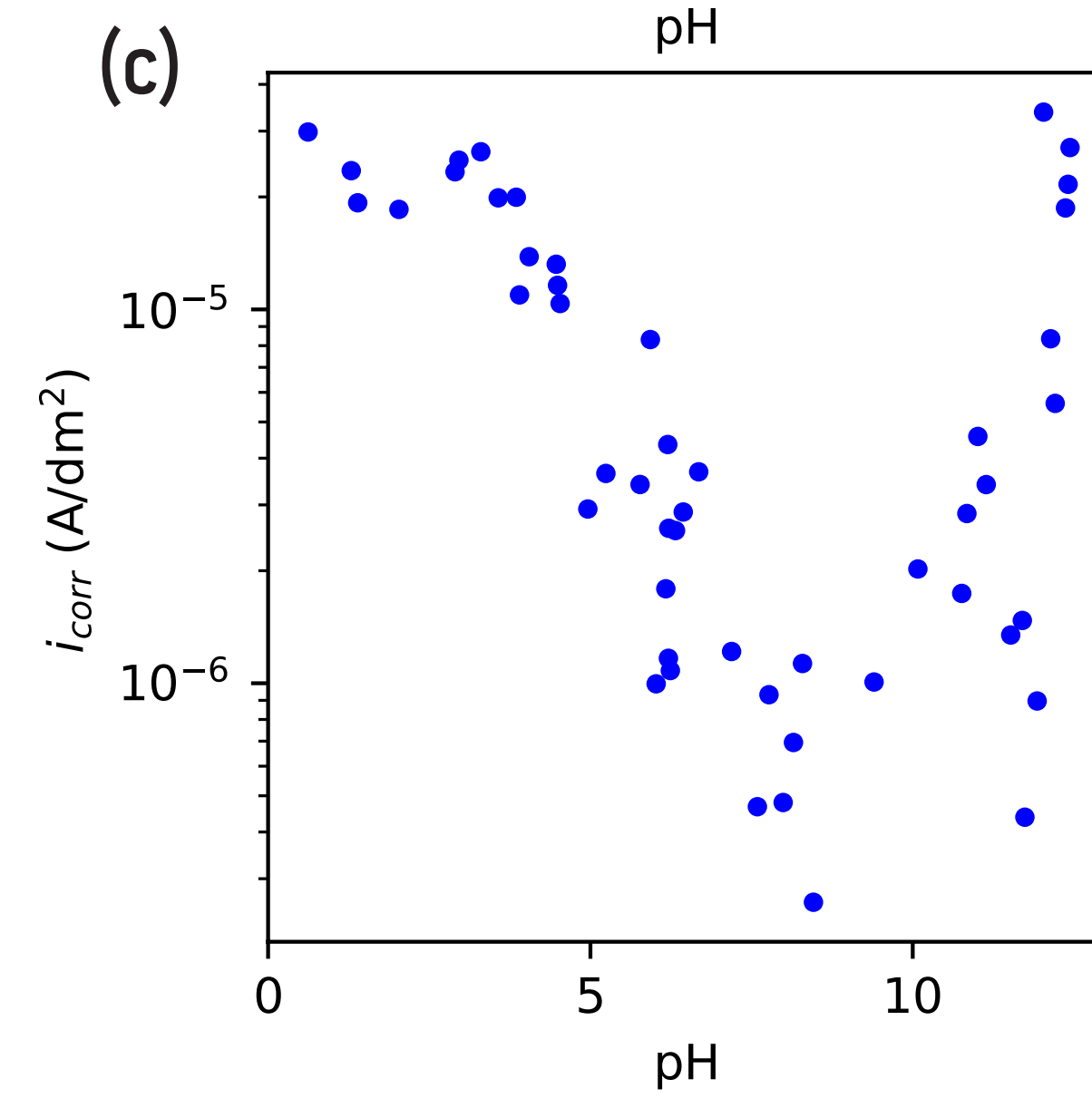
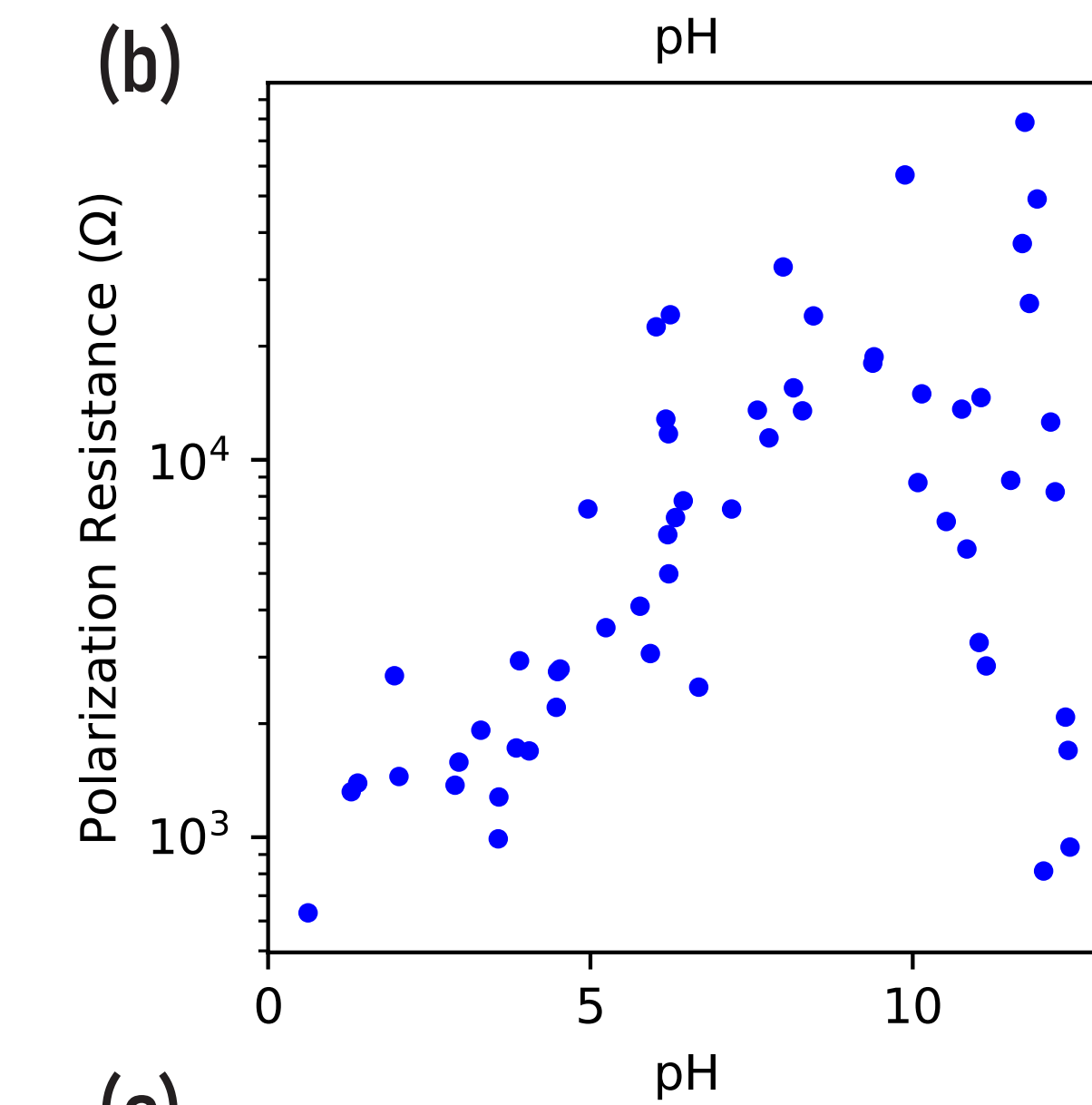
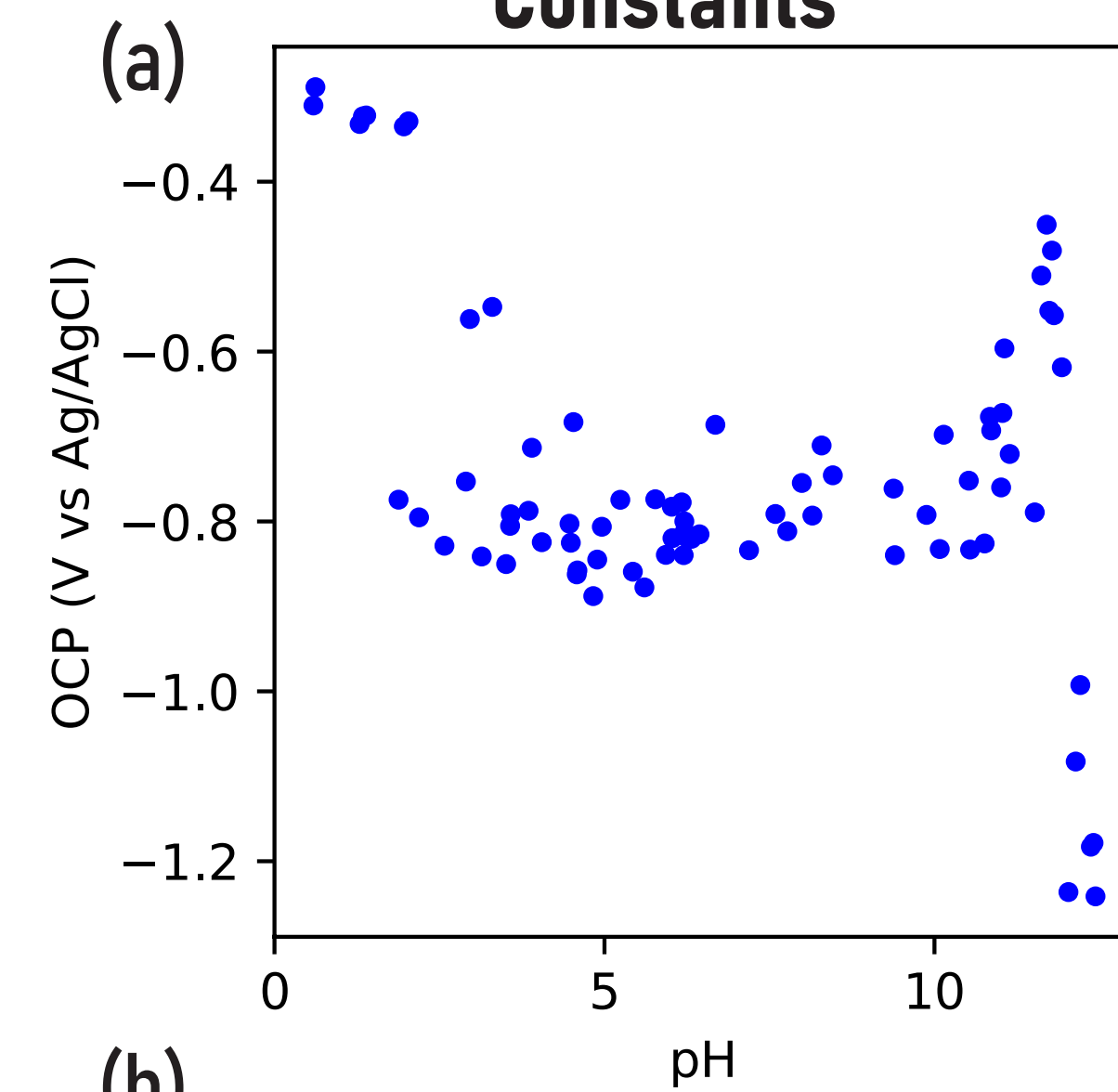
- Zn₈₅Ni₁₅ is a commercial alloy for corrosion mitigation
- Zn acts as a sacrificial anode with Ni slowing dissolution rates
- We corroded a Zn₈₅Ni₁₅ plate using over a variety of pHs using 1.0 M KOH, 0.5 M K₂SO₄, and 0.5 M H₂SO₄
- Mixing was performed on-the-fly
- Each point had (a) dynamic OCP hold, (b) 3x linear polarization resistance scans, and Tafel scan on a fresh region of sample



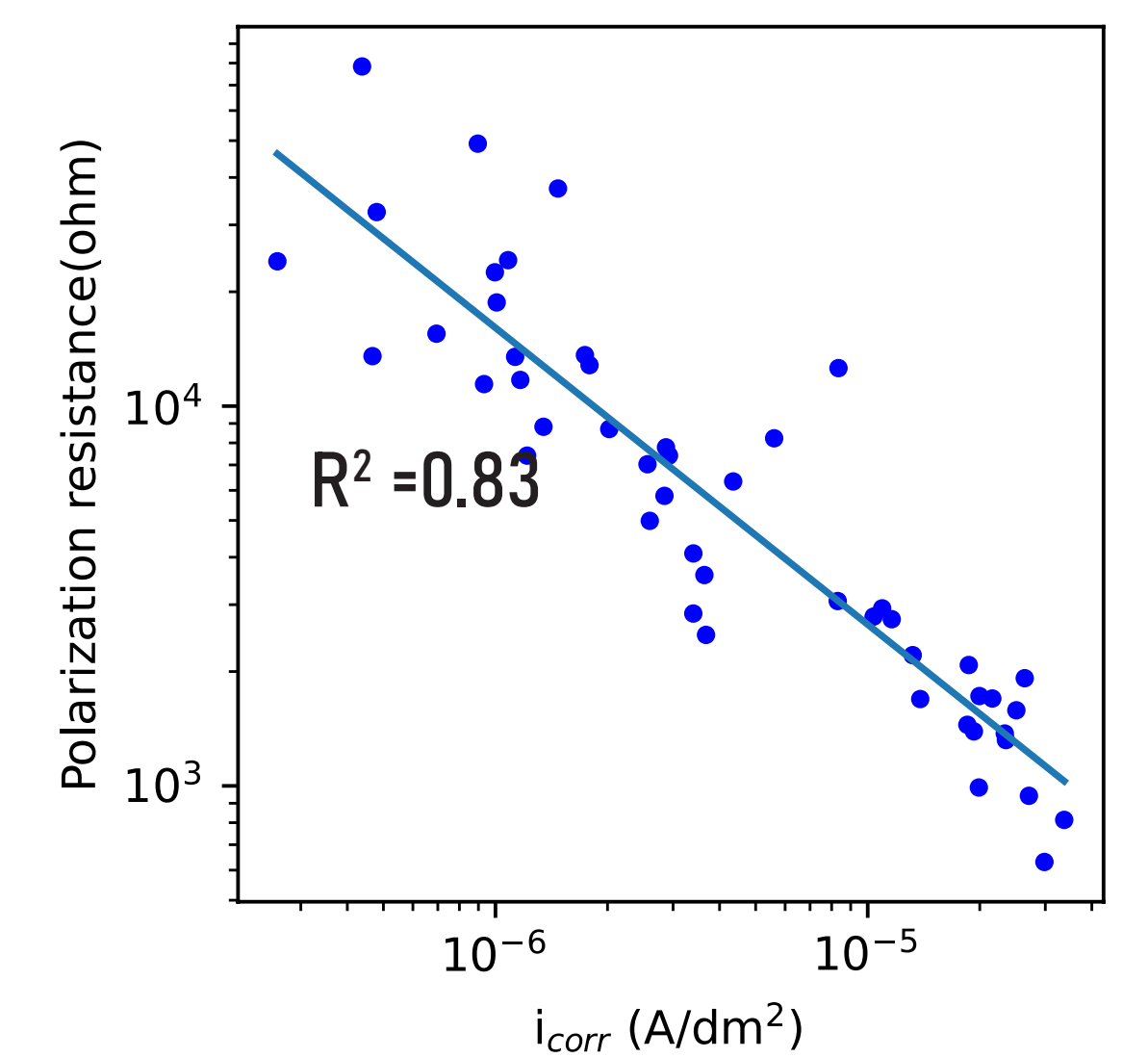
Example Data Analysis



Extracted Corrosion Constants



- Data was analyzed using automated routines
- Data is self-consistent and consistent with the literature
- OCP is consistent with expected sample surface and Pourbaix diagram
- High corrosion rates at low and high pH
- Near neutral pH the surface becomes passive and stable



Disclaimer: Certain commercial equipment, instruments, or materials are identified in this work. Such identification is not intended to imply recommendation or endorsement by NIST, nor is it intended to imply that the materials or equipment identified are necessarily the best available for the purpose.

Acknowledgments: The authors thank Atotech for providing the ZnNi sample and for useful discussion, C. Amigo (NIST) for machining, B. Ravel (NIST) for beamline work, and D. Josell (NIST) for useful discussion. This work was funded by NIST. HJ and BD acknowledge the NIST NRC postdoctoral program for funding. NH was funded under ARPA-E Award No. DE-AR0001858



Low-cost Automated Flow Chemistry and Electronic Notebooks for a Sonogashira Reaction

Mallory K. Kern, Murat Ozturk, Ashley E. DeYong, Loran O. Carlton, Laura C. Brown and Nicola L. B. Pohl

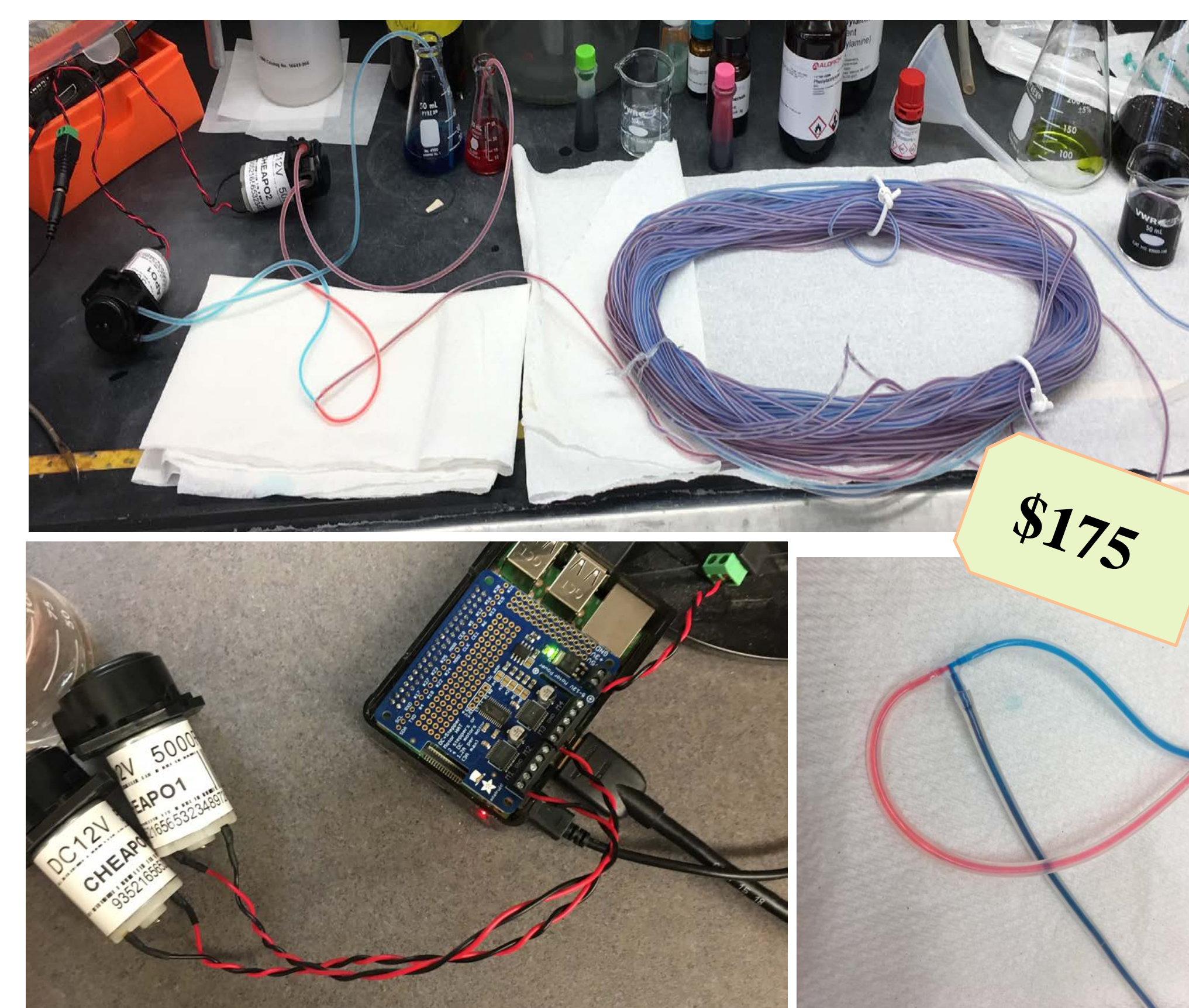
Background

The modern curriculum for undergraduate organic chemistry teaching labs is rooted in the well-established bench techniques commonly used by synthetic chemists. However, techniques and methodologies that are now common place in chemical industry are often neglected. For example, reactions are increasingly being designed and run as automated continuous flow processes. Despite the prevalence of automated chemistry, few students at the undergraduate level are exposed to automation during the course of their studies. We present here a lab that was developed for undergraduate organic chemistry students that explores the fundamentals of automated flow chemistry with a Sonogashira coupling reaction. We employ a flow apparatus that was built easily and inexpensively from commercially available peristaltic pumps, tubing, and a raspberry-pi single-board computer. Additionally, we have also developed an open source program and interface for controlling the flow apparatus. In the lab, the students run the Sonogashira coupling reaction in batch, as well as in flow, allowing them to compare the two methodologies and set-ups.

ChemSpeed Solution-Phase Automated Platform vs. Our Automated Flow System

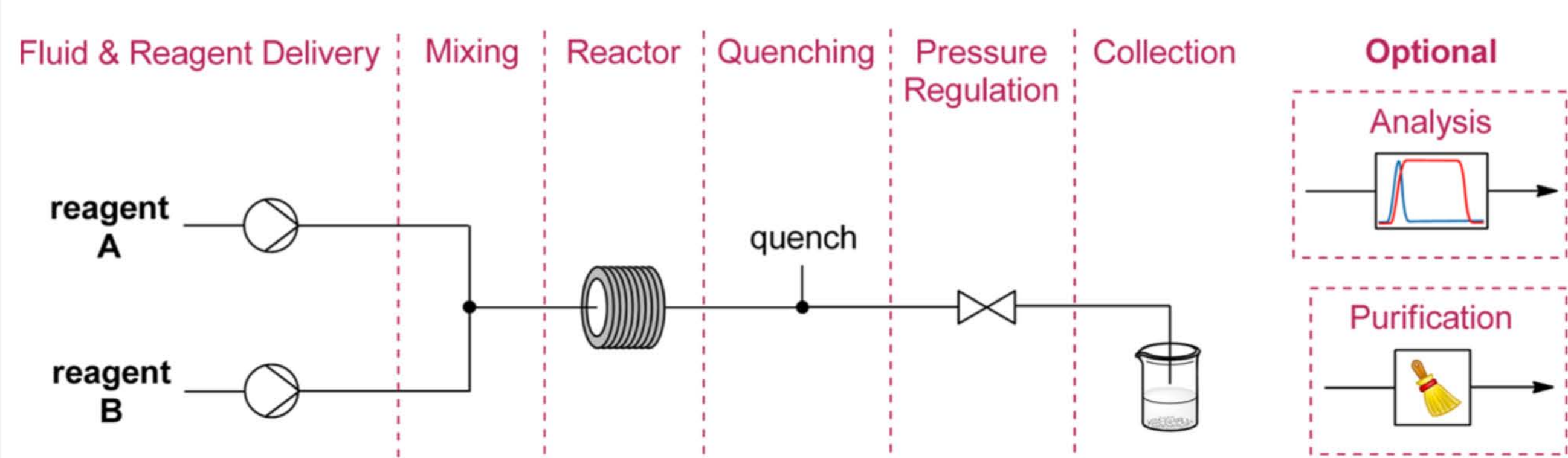


\$250,000



\$175

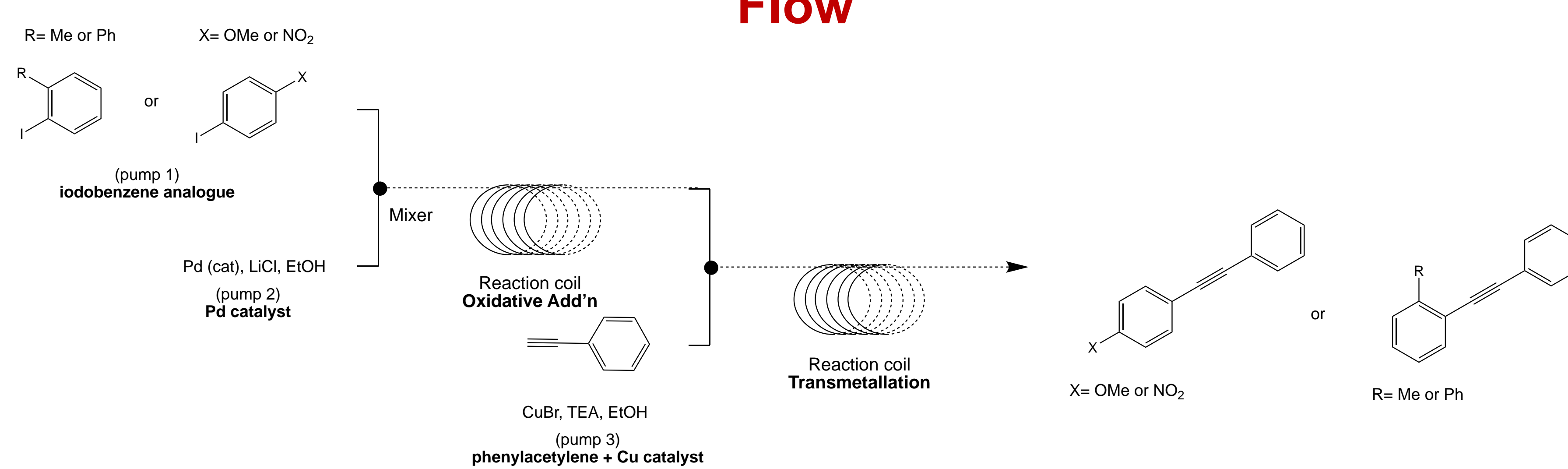
Automated Continuous Flow System



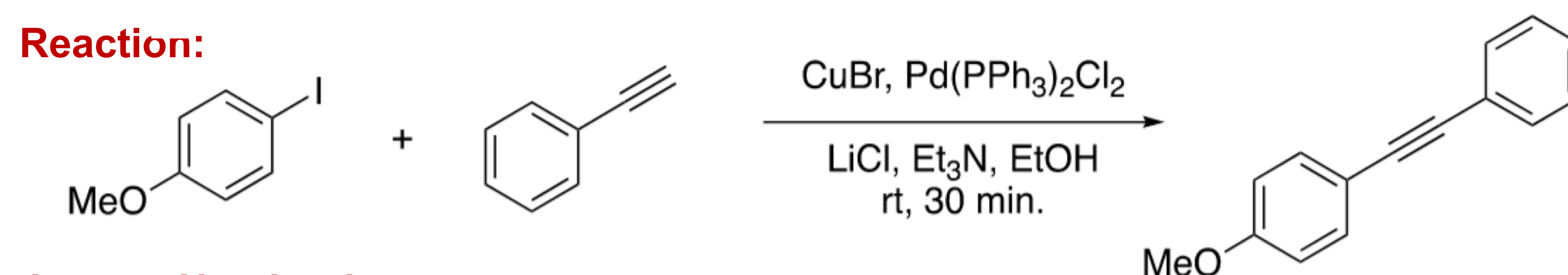
- Continuous flow system developed as a cheaper alternative to the *ChemSpeed* automation platform.
- Controlled by a raspberry pi.
- Operated using a computer program (*Mechwolf*) that can be easily accessed using a mobile device or laptop.
- Aids in reproducibility, productivity, and is highly cost-effective.



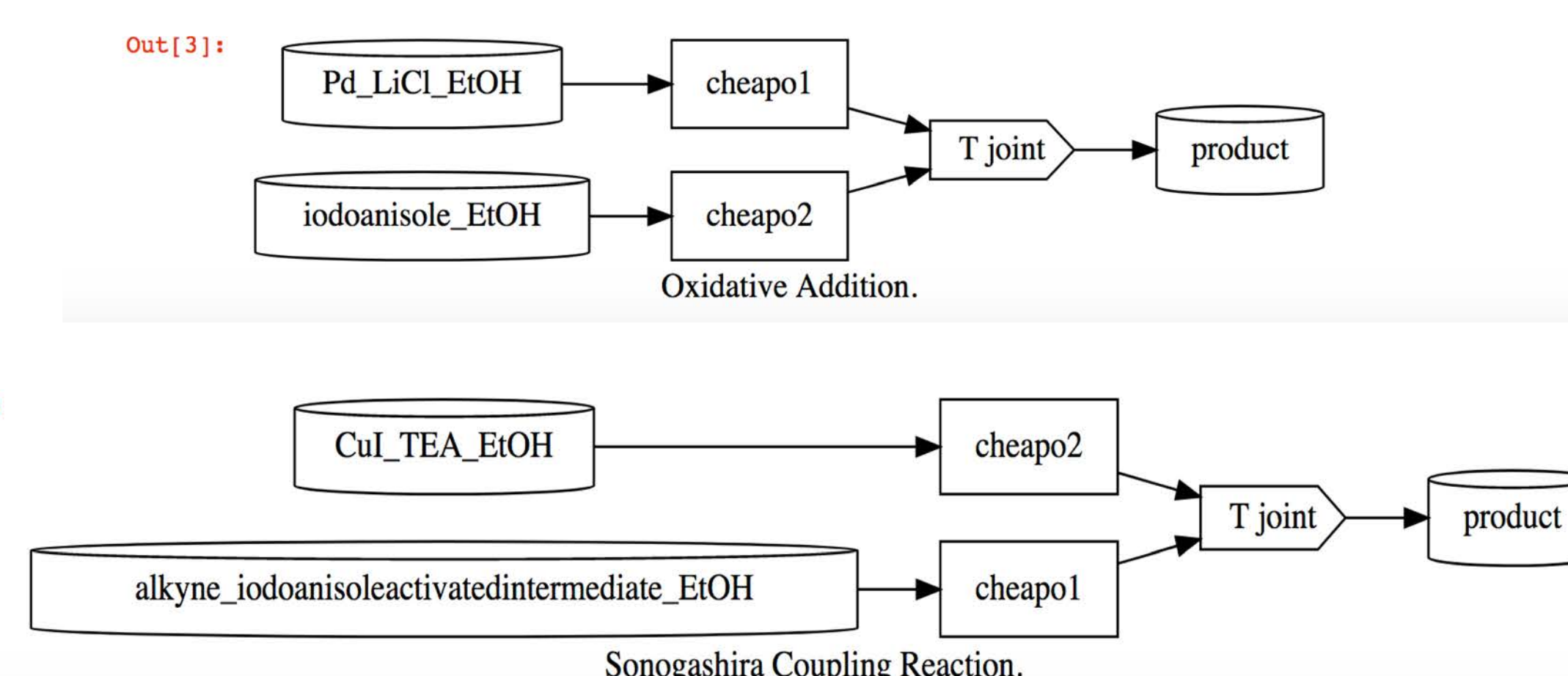
Initial Sonogashira Coupling Reaction in Automated Flow



Initial Student Data (Fall 2019)



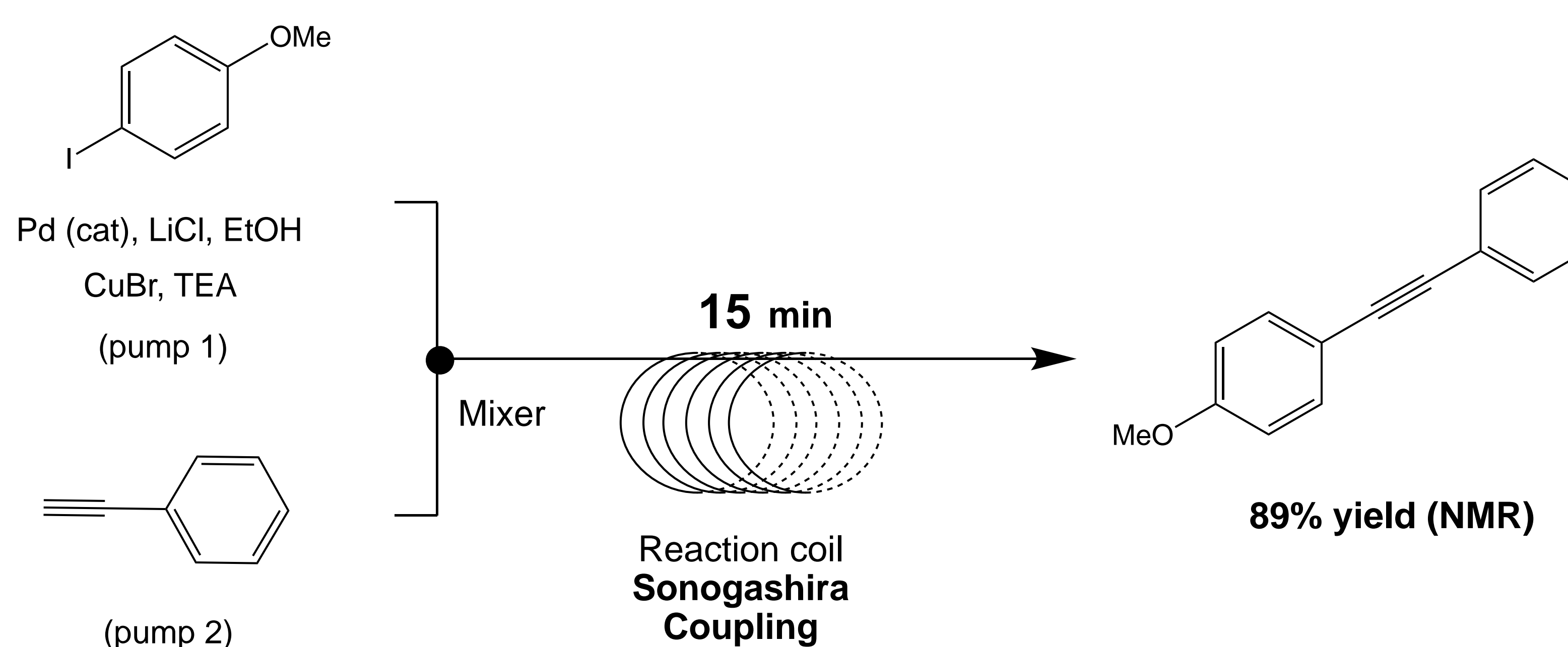
Jupyter Notebook:



Batch vs. Flow Results

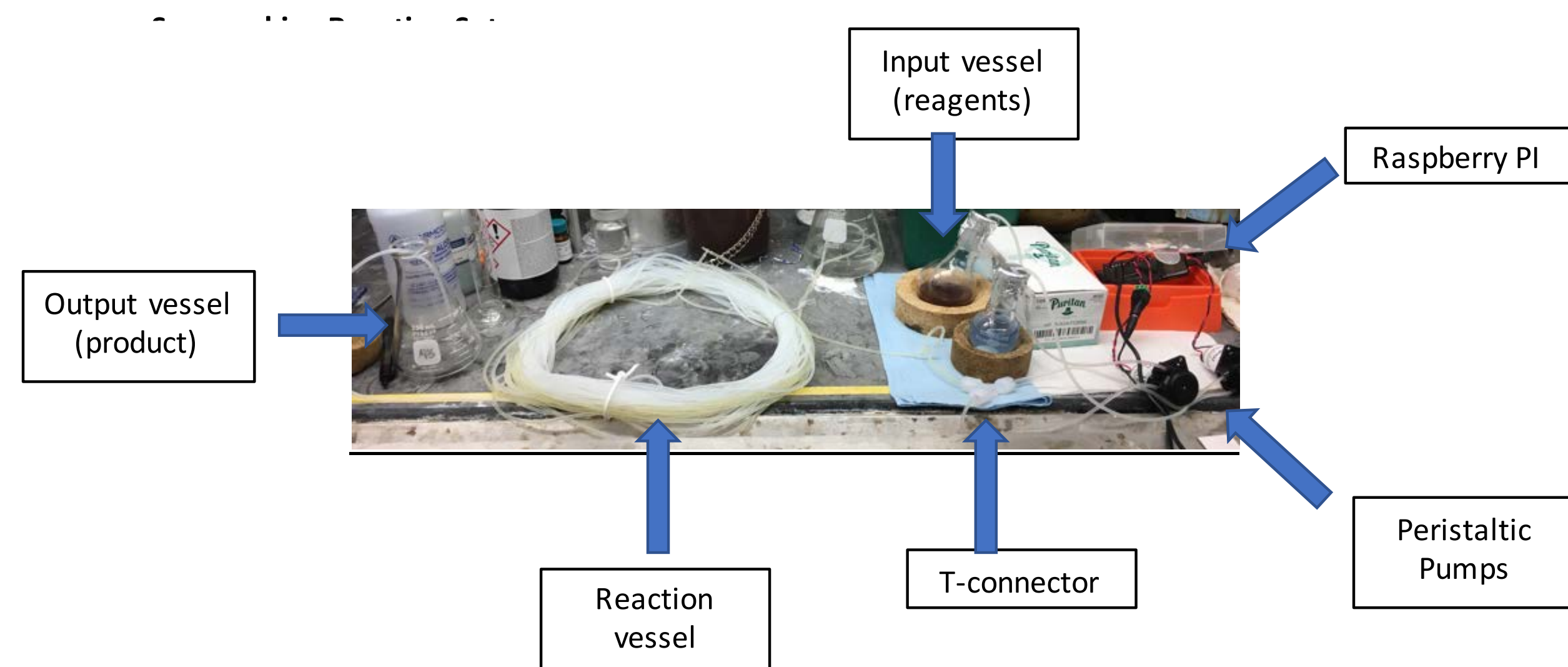
Conditions	Tuesday	Wednesday
Batch, 10 minutes	12% conv.	only sm
Batch, 30 minutes	62% conv	only sm
Flow, 10 minutes	61% conv	only sm

Current Automated Flow Conditions



Cost-Effective Automated Flow Set-Up

- Reagents pumped into silicone tubing using aquarium peristaltic pumps.
- Reaction takes place in silicone tubing "reaction vessel."
- Crude reaction flows out of the tubing, collection for further purification and data analysis.
- Peristaltic pumps controlled by raspberry pi units.



Future Work

- Run the updated lab during the fall 2021 semester.
- Obtain students pre- and post-lab questionnaires (Fall 2021) to determine their knowledge of flow chemistry and compare this with the students from Fall 2019 questionnaires.

Acknowledgements

Pohl Group

Dr. Nicola Pohl
Ashley DeYong
Gavin Stamer
Olivia Carlton

Collaborators

Dr. Laura Brown
Murat Ozturk



Applications of Parallelization in Photocatalytic Hydrogen Evolution using Homogeneous and Colloidal Cocatalysts

1. Introduction

Hydrogen is a necessary product for Haber-Bosch and as an alternative fuel source, but steam reforming to form hydrogen contributes 3% of global CO₂ emissions.¹ Our projects focus on photocatalytic water reduction and alcohol oxidation to find economical systems which reduce dependence on noble metals and carbon emitting infrastructure.^{2,3,4} Enabled by our novel 108 well parallel photoreactor, we explored over 3000 compositions of in-situ formed bimetallic nanoparticulate catalysts and over 1900 structurally diverse Iridium photosensitizers.

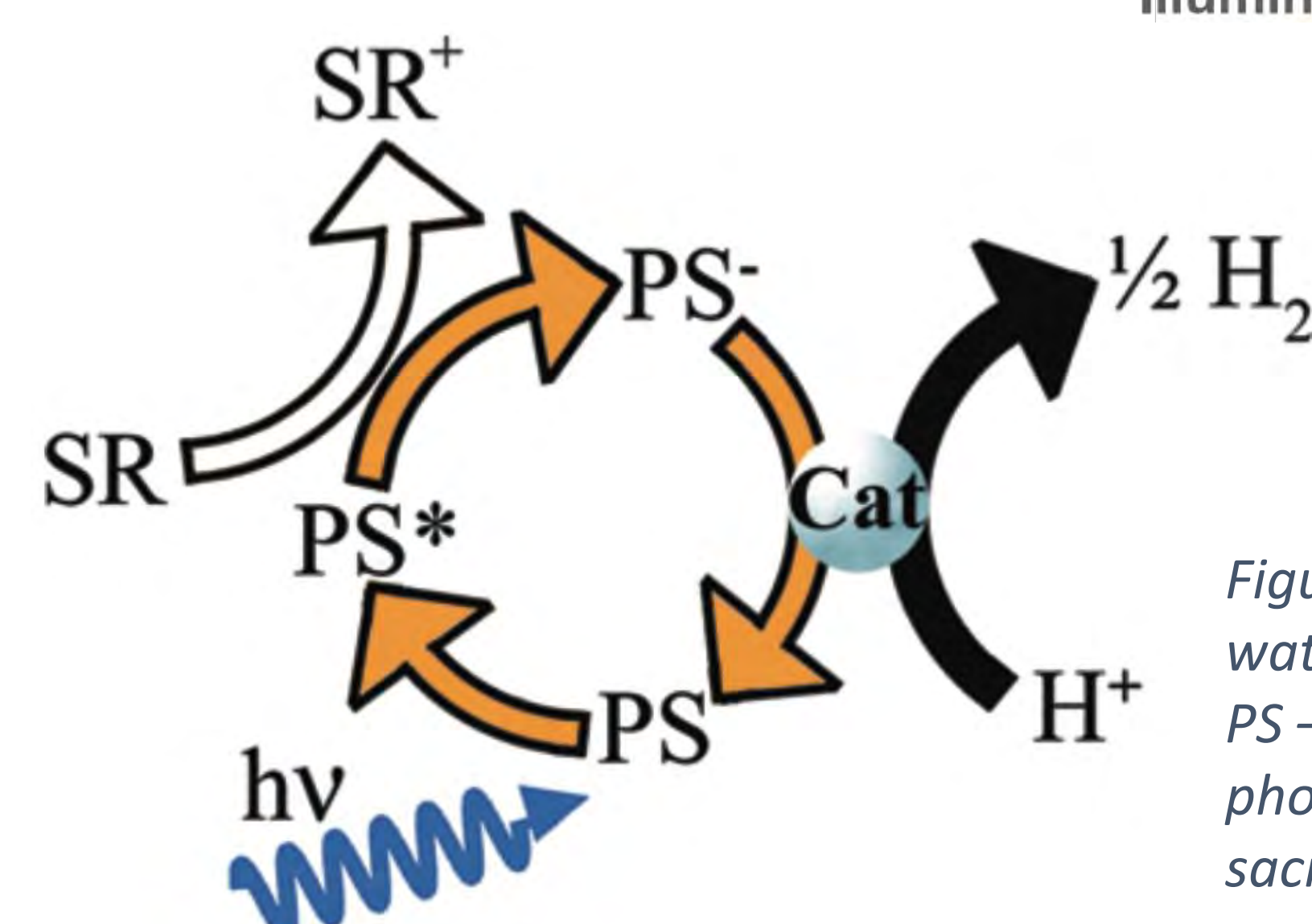


Figure 2. Photosensitized water reduction reactions, PS – iridium based photocatalyst, SR – sacrificial reductant (TEOA)

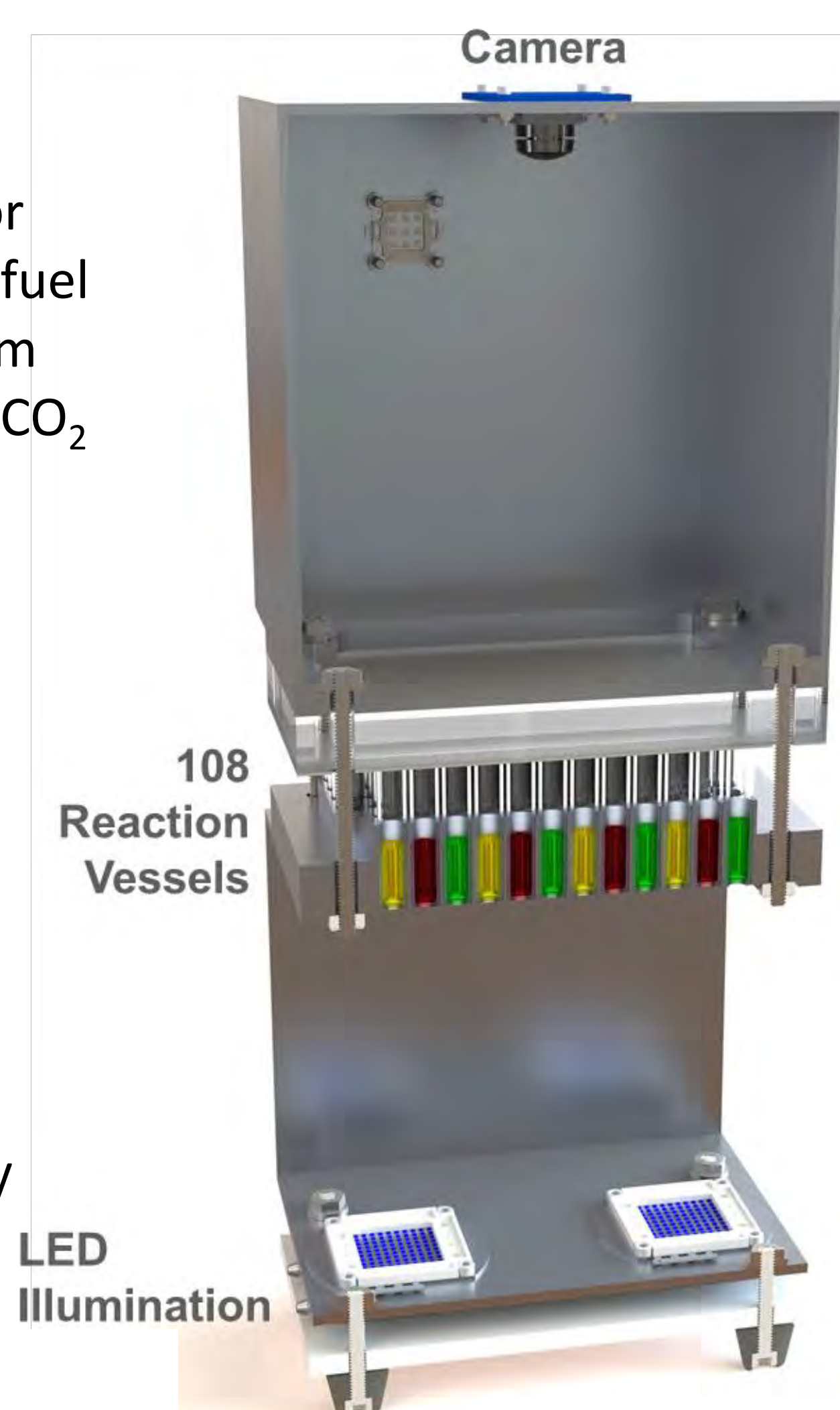


Figure 1. Mass Parallel Photoreactor Design⁵

2. Iridium Catalyst Screening

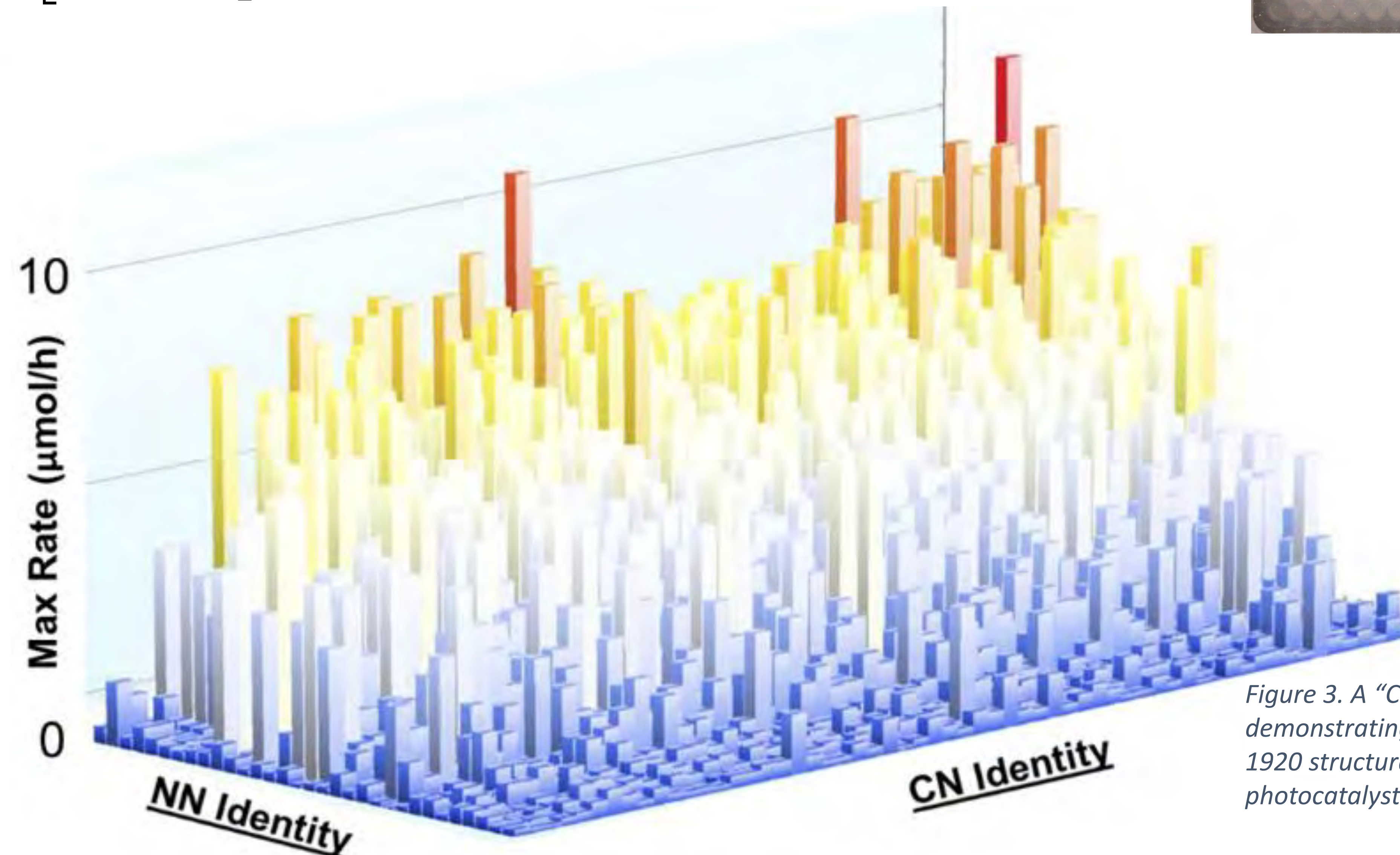
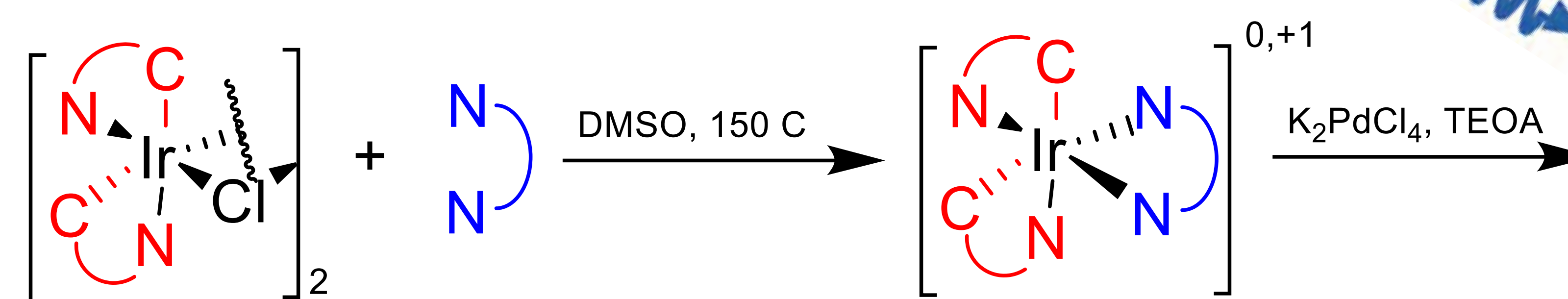


Figure 3. A “City of hydrogen” demonstrating the hydrogen yield from 1920 structurally diverse iridium photocatalysts.

Analysis of Results

- Present Structure activity relationship in ligands
- Paired with DFT calculations to provide further insight
- Greater depth investigation including ML systems is ongoing

Best C^N	Best N^N

3. Bimetallic Nanoparticle Screening

- Bimetallic combinations for limiting Pd and Pt
- Illuminated for 1000 minutes

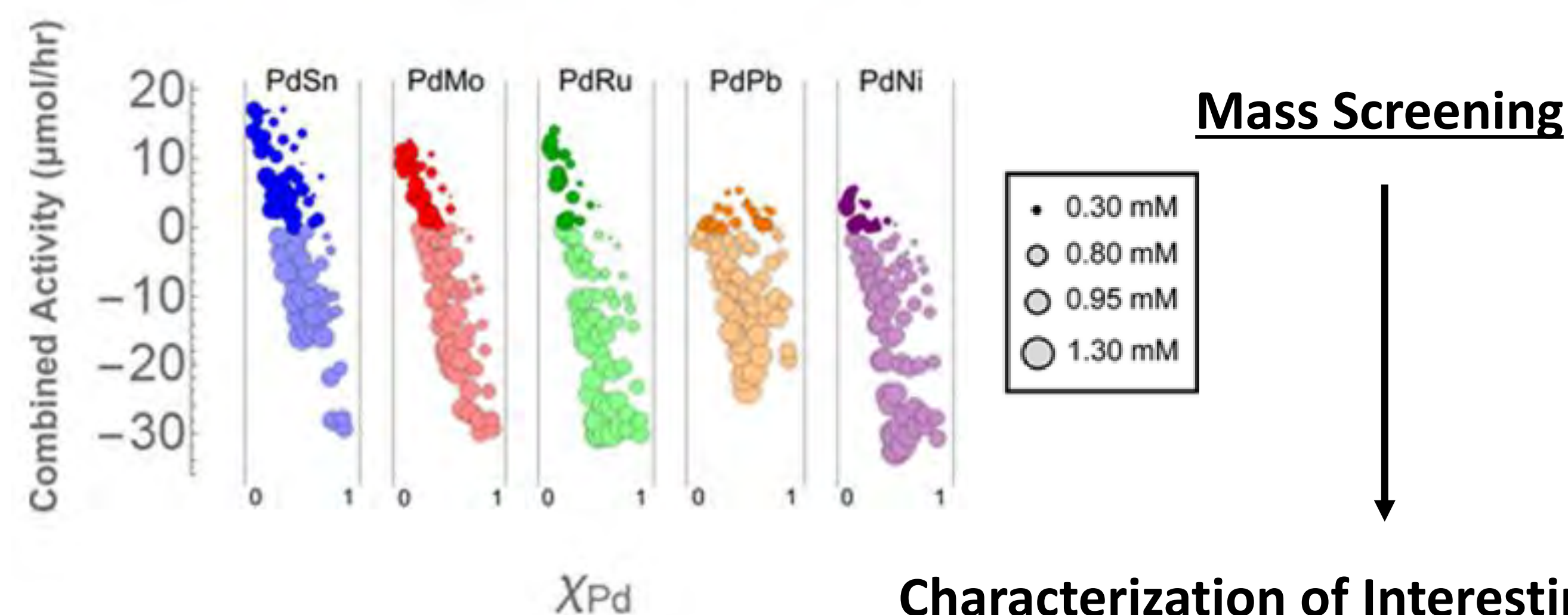
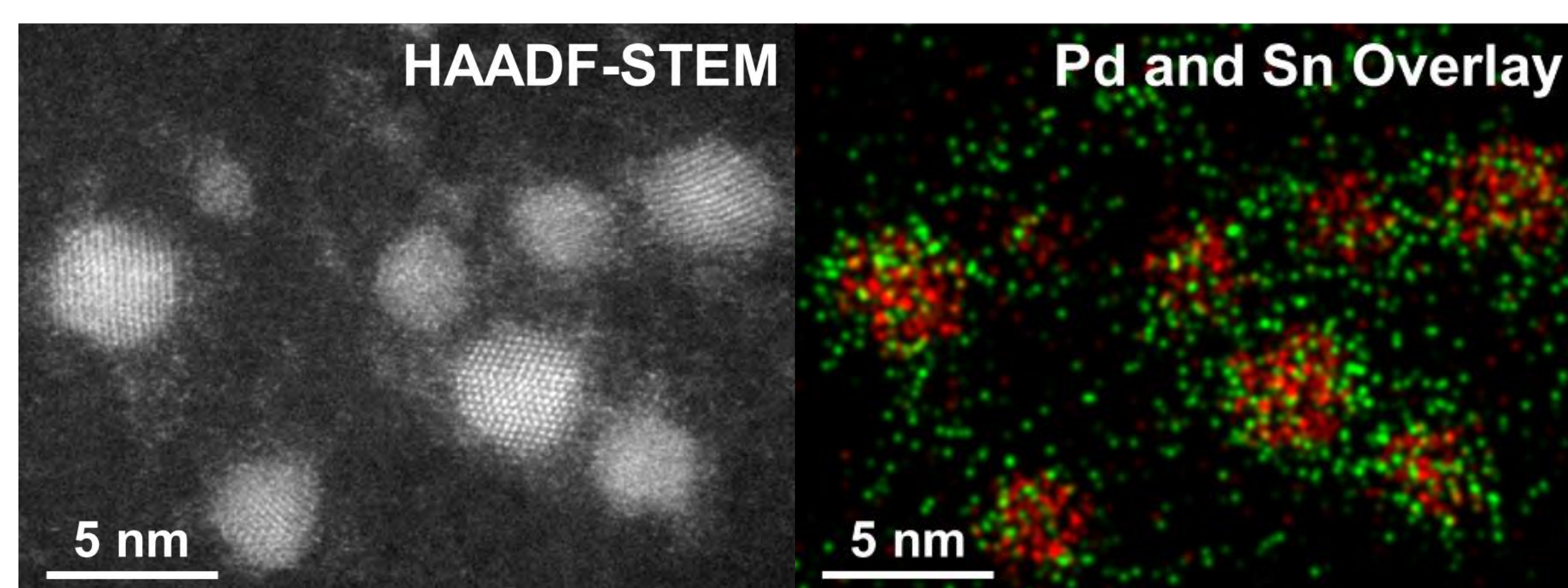
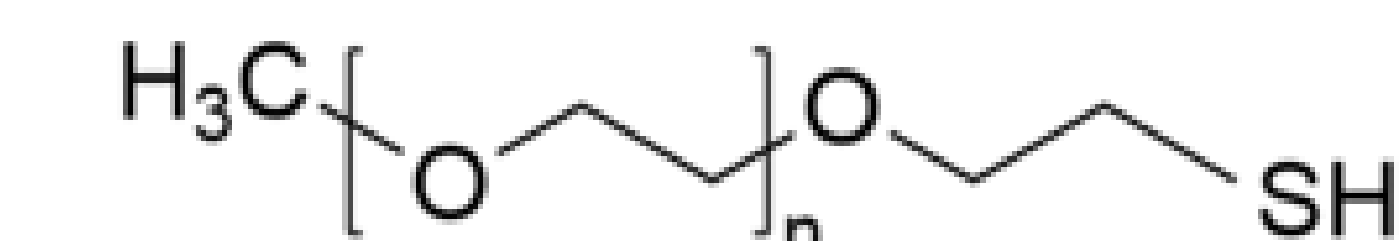


Figure 4. Plots of synergistic behavior across Pd containing compositions in bimetallic in situ nanoparticle screening.⁶

Figure 5. HAADF-STEM images depicting the size/shape of PdSn in situ synthesized nanoparticles (left) and STEM-EDS mapping of the same field (right)⁶



4. Nanoparticle Stabilization



- Addition of PEGSH increased longevity of Au based catalysts
- Comparable activity between *in situ* and *ex situ* synthesized particles

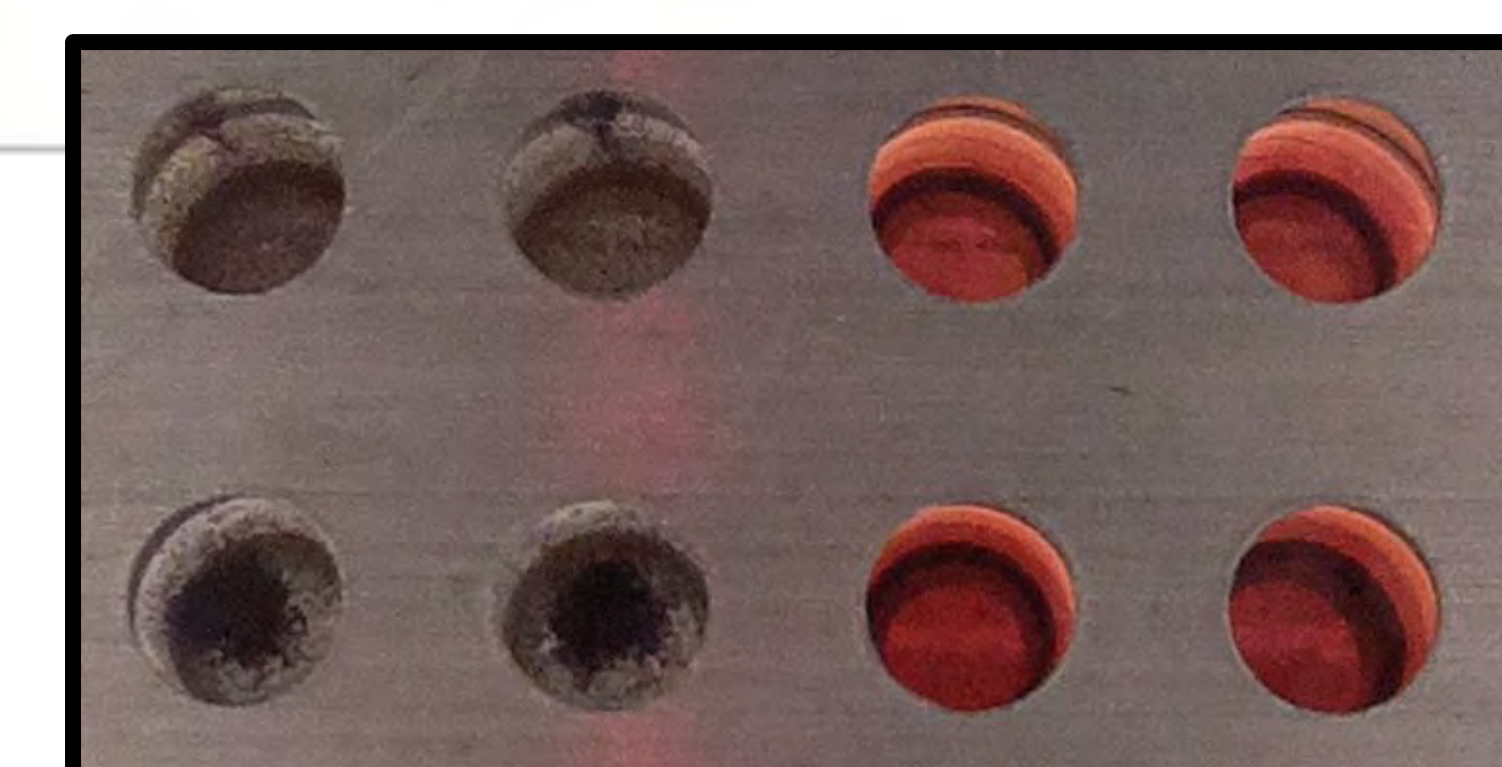


Figure 7. Images taken underneath reaction wells containing AuCu during the first round of illumination illustrating precipitation occurring when no stabilizing agent is added (left) and colloids remaining stable with PEGSH added (right)

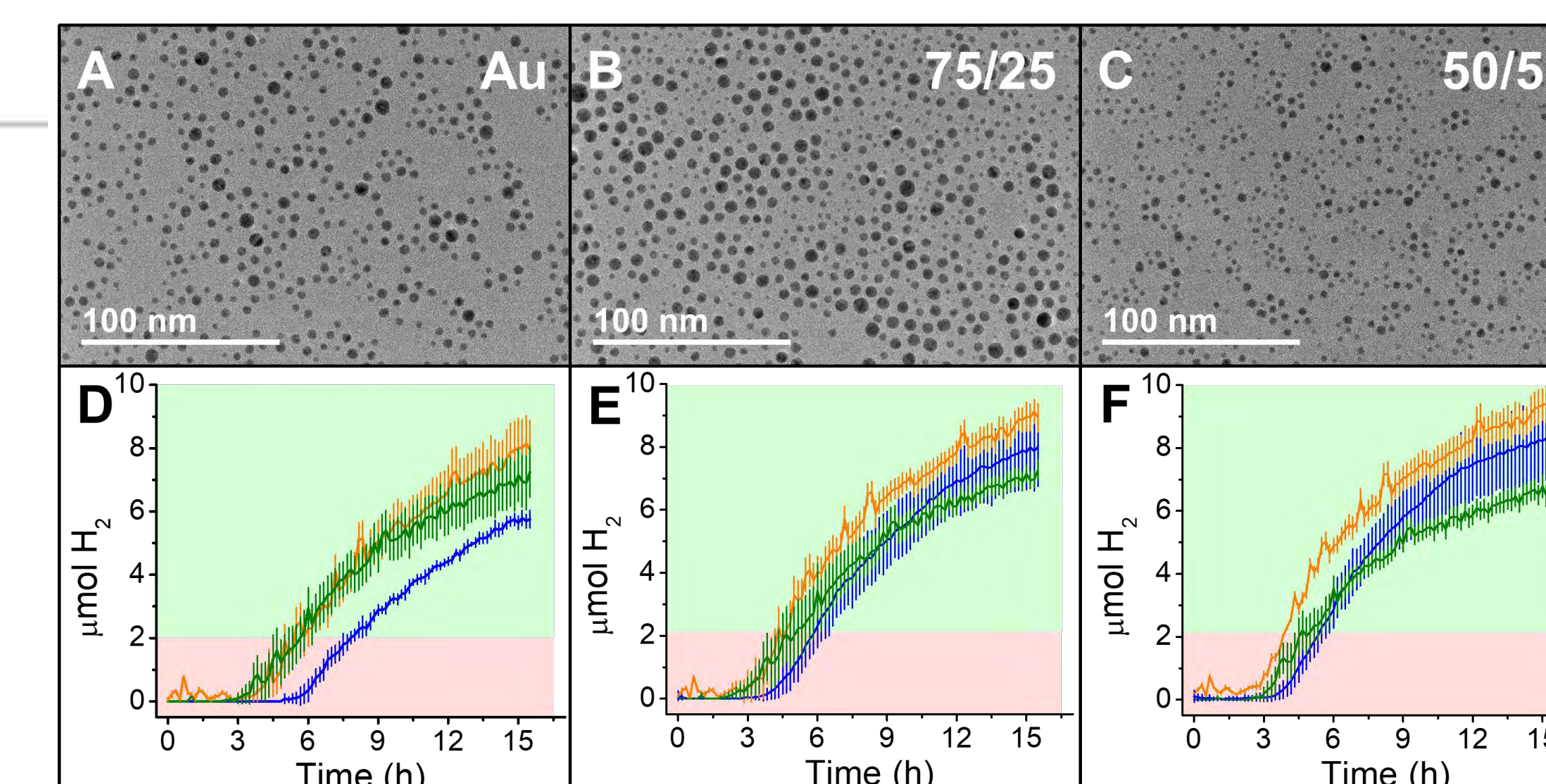


Figure 7. Hydrogen Traces (bottom) across three rounds of 15-hour illumination of in situ synthesized Au and AuCu mixtures stabilized through the addition of PEGSH 1kDa, resulting in still stable nanoparticles after 45 hours of illumination as seen in the TEM images (top).⁷

Characterization of Interesting Candidates

Computational Modeling

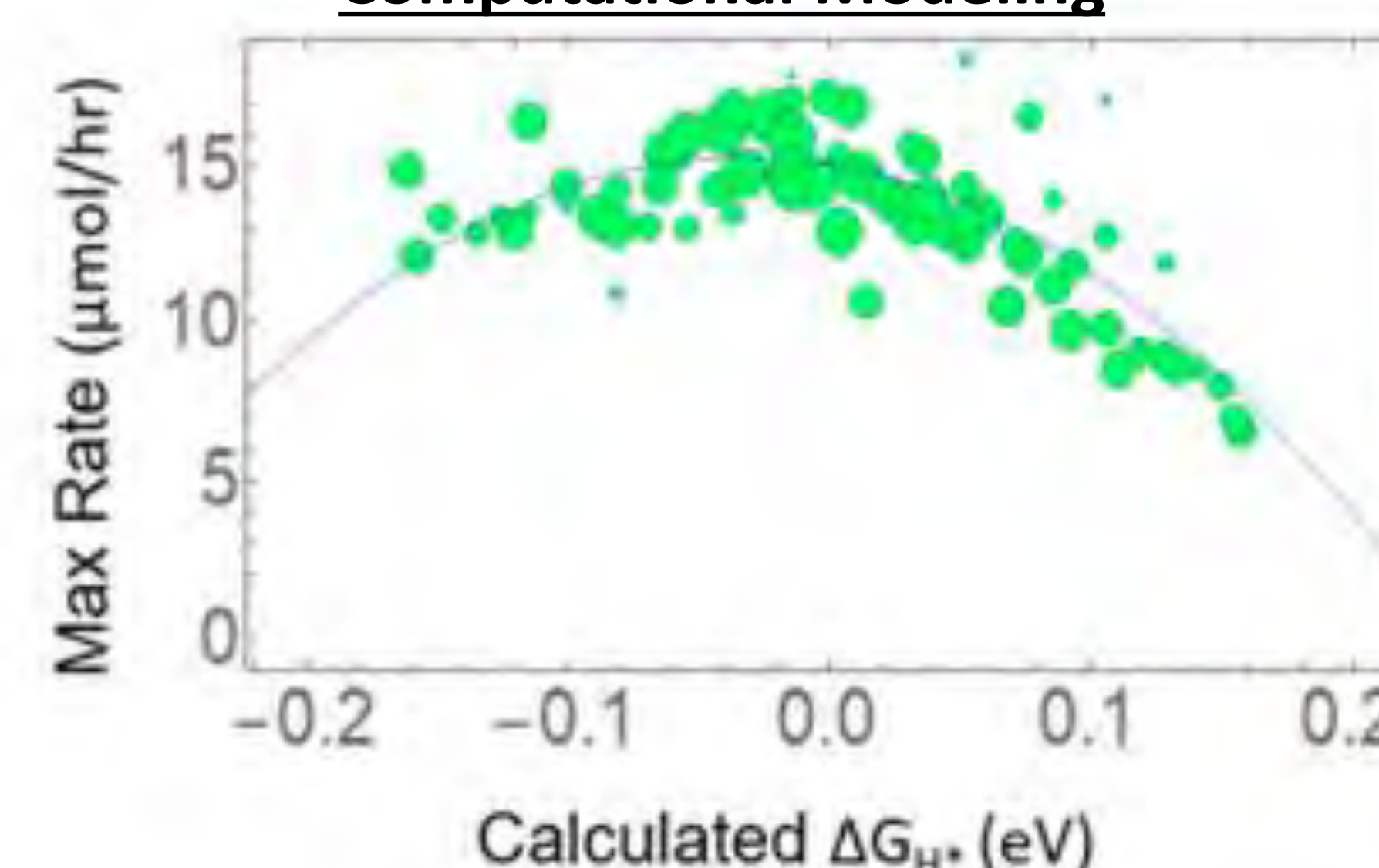


Figure 6. Use of DFT modeled free energy of hydrogen adsorption across PdSn compositions resulting in Sabatier Principle defined behavior for photocatalytic cocatalyst surfaces.⁶

5. Future Directions

- Photo-driven alcohol oxidation to replace steam reforming
- Increased understanding of photo-driven nanoparticle synthesis
- CO₂ Reduction and Organic Reactions

References

- McDaniel N.; Bernhard S. *Dalton Trans.* **2010**, 39, 10021-10030
- Snyder, C.S.; Bruilsema, T.W.; Jensen, T.L.; Fixen, P.E.; *Agriculture, Exosystems and Environment* **2009**, 133, 247-266
- Lewis, N. S.; Nocera, D. G. Powering the planet: Chemical challenges in solar energy utilization. *Proc. Natl. Acad. Sci. U. S. A.* **2006**, 103, 15729-15735.
- Staykov, A.; Lyth, S. M.; Watanabe, M. In *Hydrogen Energy Engineering*; Sasaki, K., Li, W.-H., Hayashi, A., Yamabe, J., Ogura, T., Lyth, S. M., Eds.; Springer: Japan, 2016; pp 159-174.
- Curtin, P. N.; Tinker, L. L.; Burgess, C. M.; Cline, E. D.; Bernhard, S. *Inorganic Chemistry* **2009**, 48(22), 10498-10506.
- Lopato, E.M.; Eikey, E.A.; Simon, Z.C.; Back, S.; Tran, K.; Lewis, J.; Kowaleski, J.F.; Yazdi, S.; Kitchin, J.R.; Ulissi, Z.W.; Millstone, J.E.; Bernhard, S.; *ACS Catal.* **2020**, 10(7), 4244-4252.
- Simon, Z.C.; Lopato, E.M.; Bhat, M.; Moncure P.J.; Bernhard, S.M.; Kitchin, J.R.; Bernhard, S.; Millstone, J.E.; *ChemCatChem*, Submitted

Acknowledgments

This work was supported in part by the University of Pittsburgh and Carnegie Mellon University. This research used resources of the National Energy Research Scientific Computing Center (NERSC), a U.S. Department of Energy Office of Science User Facility operated under Contract no. DE-AC02-05CH11231. This research was supported by the U.S. Department of Energy, Office of Science, Office of Basic Energy Sciences, Data Science for Knowledge Discovery for Chemical and Materials Research program, under Award DE-SC0020392. E.M.L. was supported by the Steinbrenner Institute Graduate Fellowship and the ARCS Foundation Pittsburgh Chapter.

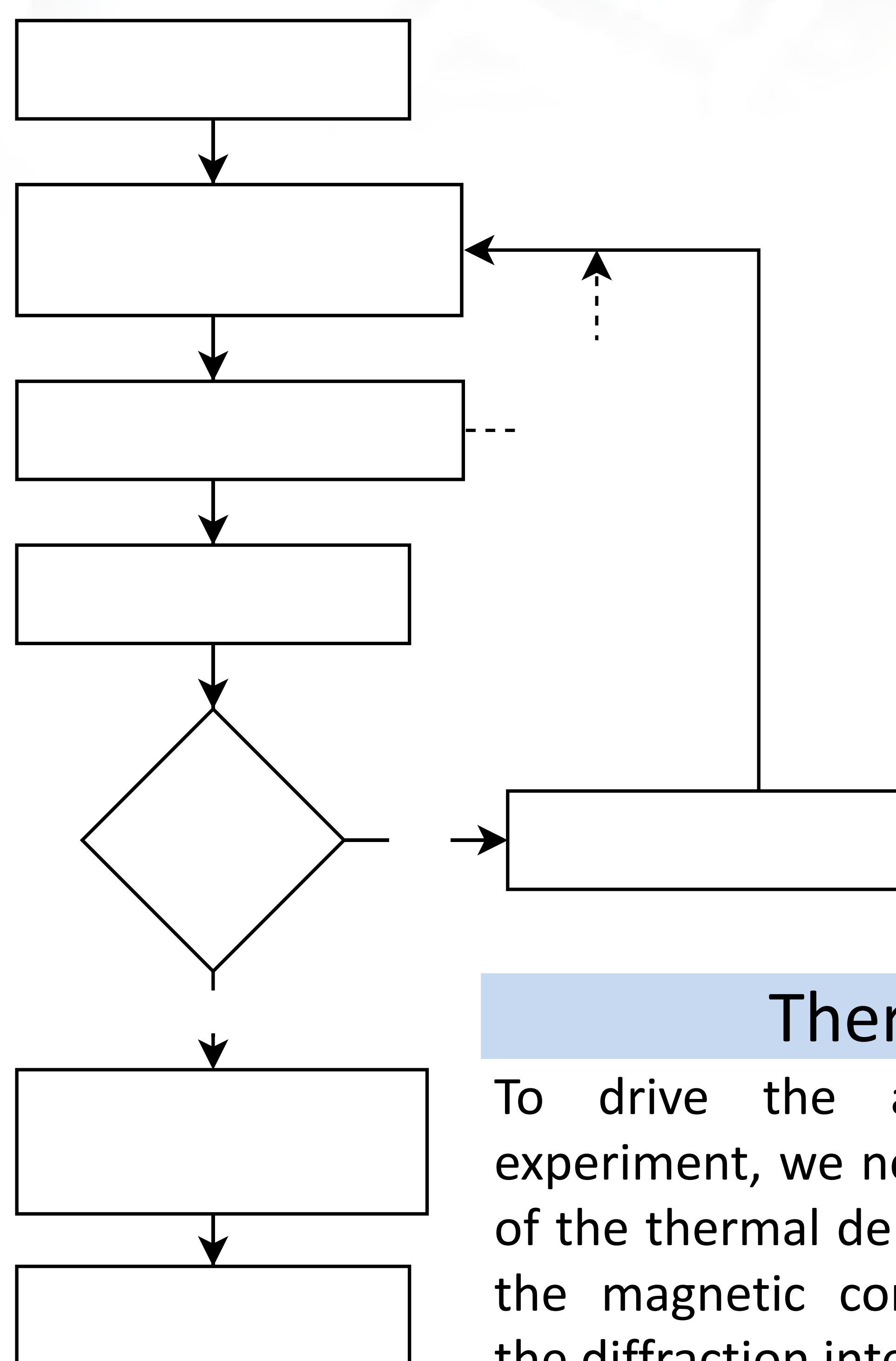
ANDiE: Autonomous Neutron Diffraction Explorer

A. McDannald¹, M. Frontzek², A. T. Savici², M. Doucet², E. E. Rodriguez^{3,4}, K. Meuse⁵, J. Opsahl-Ong⁶, D. Samarov⁷, I. Takeuchi^{4,8}, W. Ratcliff^{8,9}, A. G. Kusne^{1,8}

¹Materials Measurement Laboratory, NIST; ²Neutron Sciences Directorate, ORNL; ³Department of Chemistry and Biochemistry UMD; ⁴Maryland Quantum Materials Center; ⁵Department of Computer Science, Cornell University; ⁶Department of Computer Science, Rice University; ⁷Information Technology Laboratory, NIST; ⁸Department of Materials Science and Engineering, UMD; ⁹NIST Center for Neutron Research, NIST

Algorithm Overview

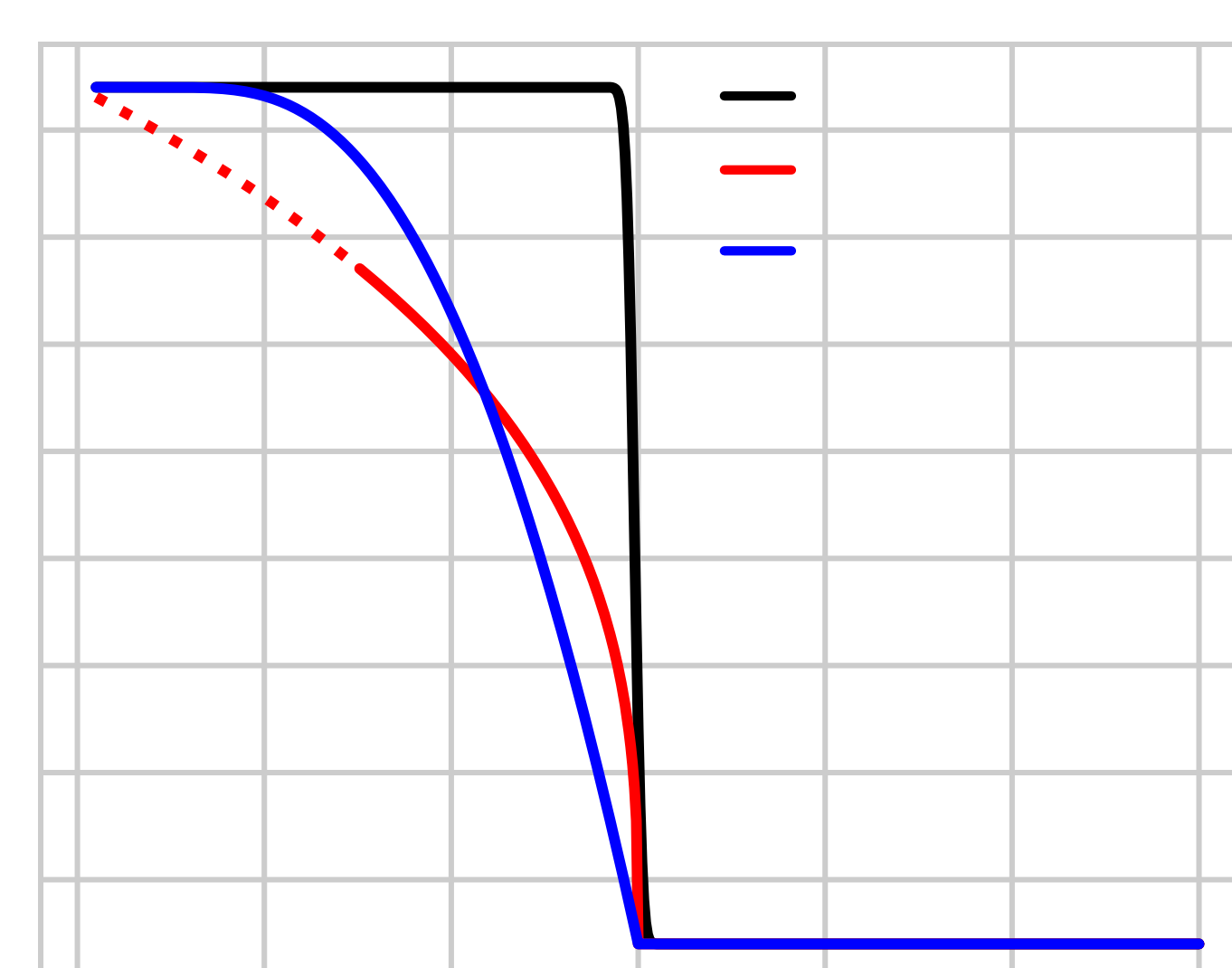
Goal: Autonomously Discover Magnetic Order Parameter of a Material from Neutron Powder Diffraction Measurements



- Autonomous control consists of two nested Bayesian inference loops.
- Isothermal inference identifies the magnetic component of the diffraction and passes that to the thermal inference.
- Thermal inference predicts the temperature dependence of the magnetic component of diffracted intensity.
- Active learning chooses the next temperature based on the uncertainty from the thermal inference.
- Implemented at NCNR and ORNL.
- Autonomously discovered Néel temperature (T_N) of MnO and $\text{Fe}_{1.09}\text{Te}$.

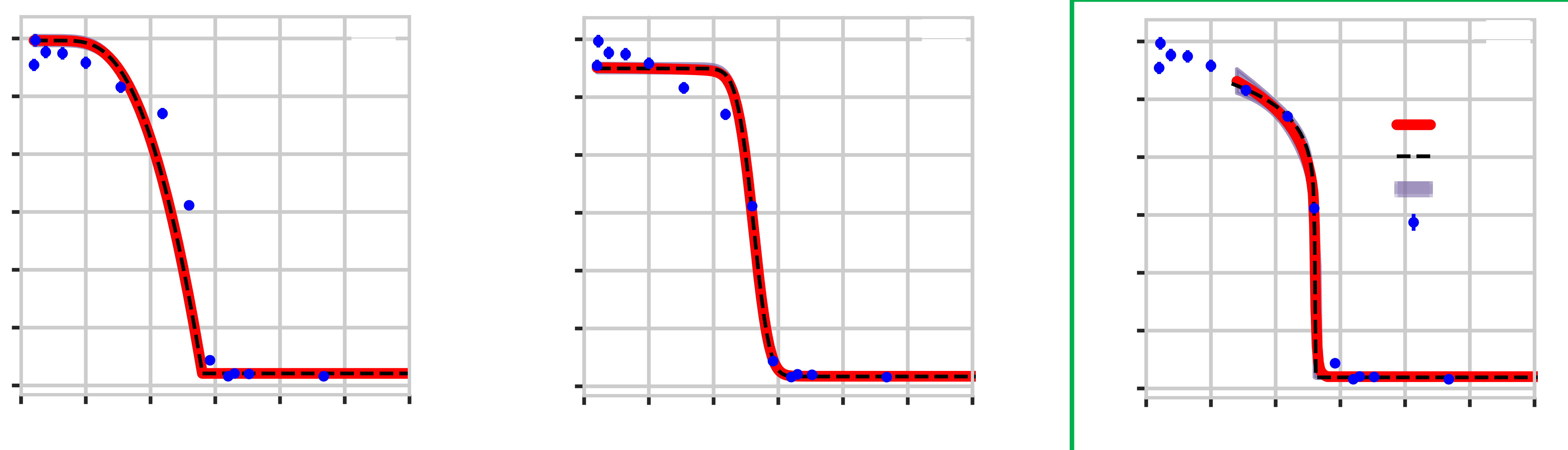
Thermal Dependence Models

To drive the autonomous experiment, we need a model of the thermal dependence of the magnetic component of the diffraction intensity.



A First-Order model gives no indication of the proximity of the experiment temperature to T_N . The Ising model only applies near T_N . For all materials, we drive the selection of the next temperature with the Weiss model.

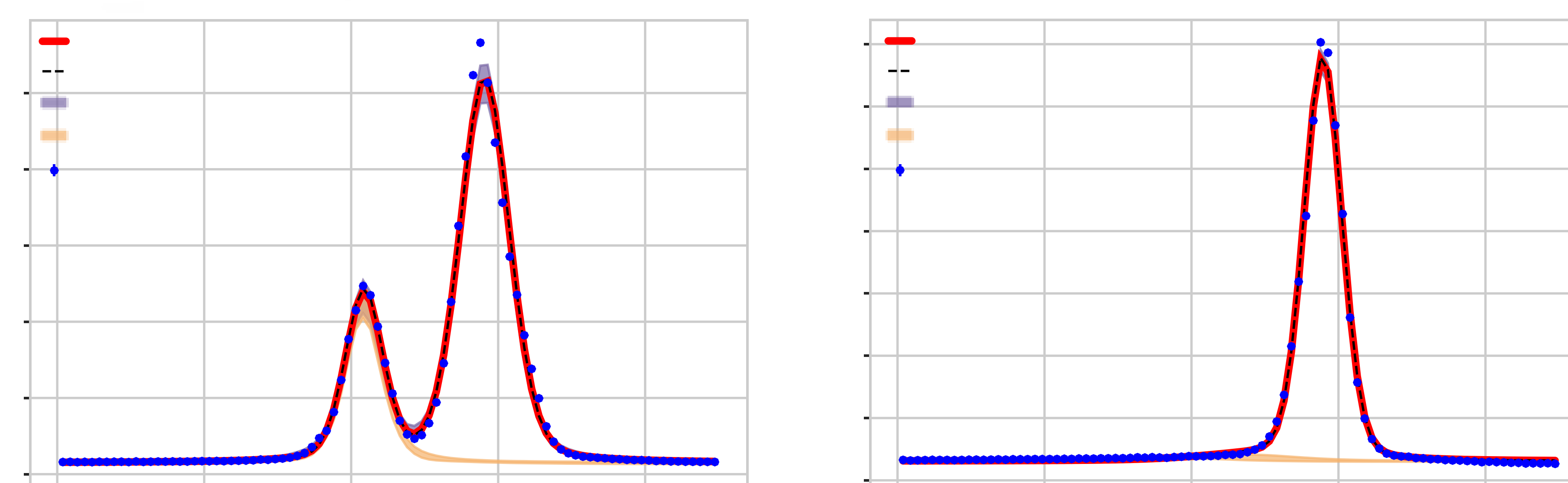
Hypothesis Testing



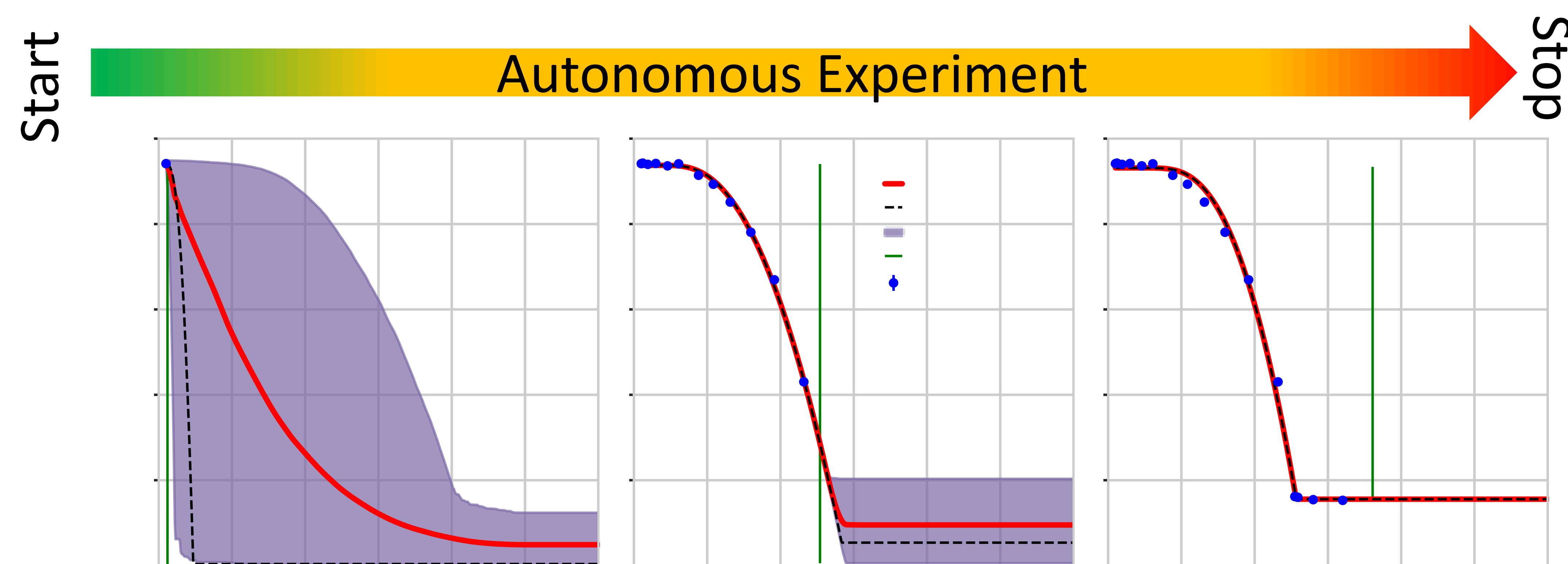
Material	Model	Full Range		$T > 0.5T_N$	
		T_N (K)	Log Likelihood	T_N (K)	Log Likelihood
MnO	First Order	114.49(12)	-2722	119.204(86)	-742
	Weiss	127.948(47)	-427	127.954(52)	-389
	Ising	—	—	120.81(56)	-52
$\text{Fe}_{1.09}\text{Te}$	First Order	68.58(16)	-64	69.09(18)	-21
	Weiss	70.000(15)	-348	70.000(17)	-287
	Ising	—	—	65.05(60)	-49

After the autonomous experiment, ANDiE performs the Bayesian inference on whole data set for the hypothesis testing of which model describes the material best. Since the Ising model is only valid in the range $0.5T_N < T < T_N$ that range is used for direct comparisons to the Ising model. ANDiE concludes that MnO is an Ising type antiferromagnet with a T_N at 120.85(56) K.

Isothermal Diffraction Measurements



At each temperature ANDiE uses Markov Chain Monte Carlo to infer the parameters of the diffraction peaks, shown here for MnO. This inference captures the large changes in the magnetic contribution to the diffraction pattern over the temperature range.



Using the results of the isothermal inference, ANDiE infers the temperature dependence of the magnetic contribution to the diffraction pattern. ANDiE then increases the temperature of the experiment to where the confidence interval exceeds a user-defined

threshold relative to the expected Poissonian-like uncertainty. In this way, ANDiE can choose the most informative measurements, quickly converging on the T_N . ANDiE autonomously discovered the T_N of MnO in 14 measurements and completed the experiment in 16 measurements, whereas a traditional *ad hoc* schedule might take 74 measurements.

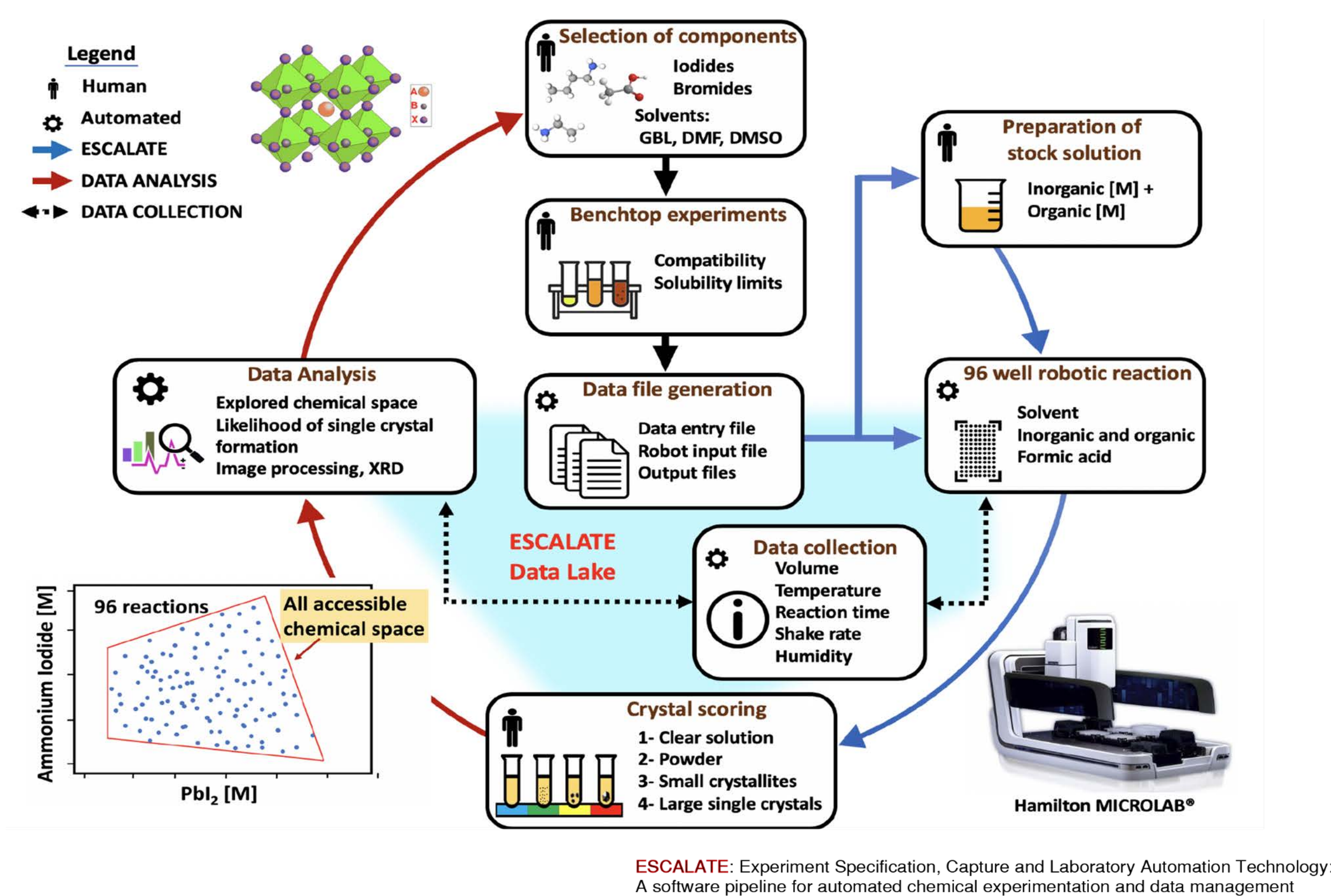
Conclusions

We have developed the autonomous neutron diffraction explorer (ANDiE), a system to control neutron diffraction experiments for the discovery of the magnetic transition temperature of a material. Several relevant physics-based principles (such as the Poissonian counting statistics and models of the temperature dependence of the magnetic contribution to the diffraction) are encoded into ANDiE. The probabilistic Bayesian inference allows ANDiE to choose the most informative measurement to perform next. Despite always driving the experiment with the Weiss model, ANDiE can discover the transition temperature of materials with differing magnetic behavior. At the WAND² HB-2C beamline at HFIR at ORNL, ANDiE autonomously acquired diffraction measurements and correctly discovered an Ising type magnetic transition in MnO. ANDiE reduced the number of measurements compared to traditional experiments by a factor of ~ 5 .

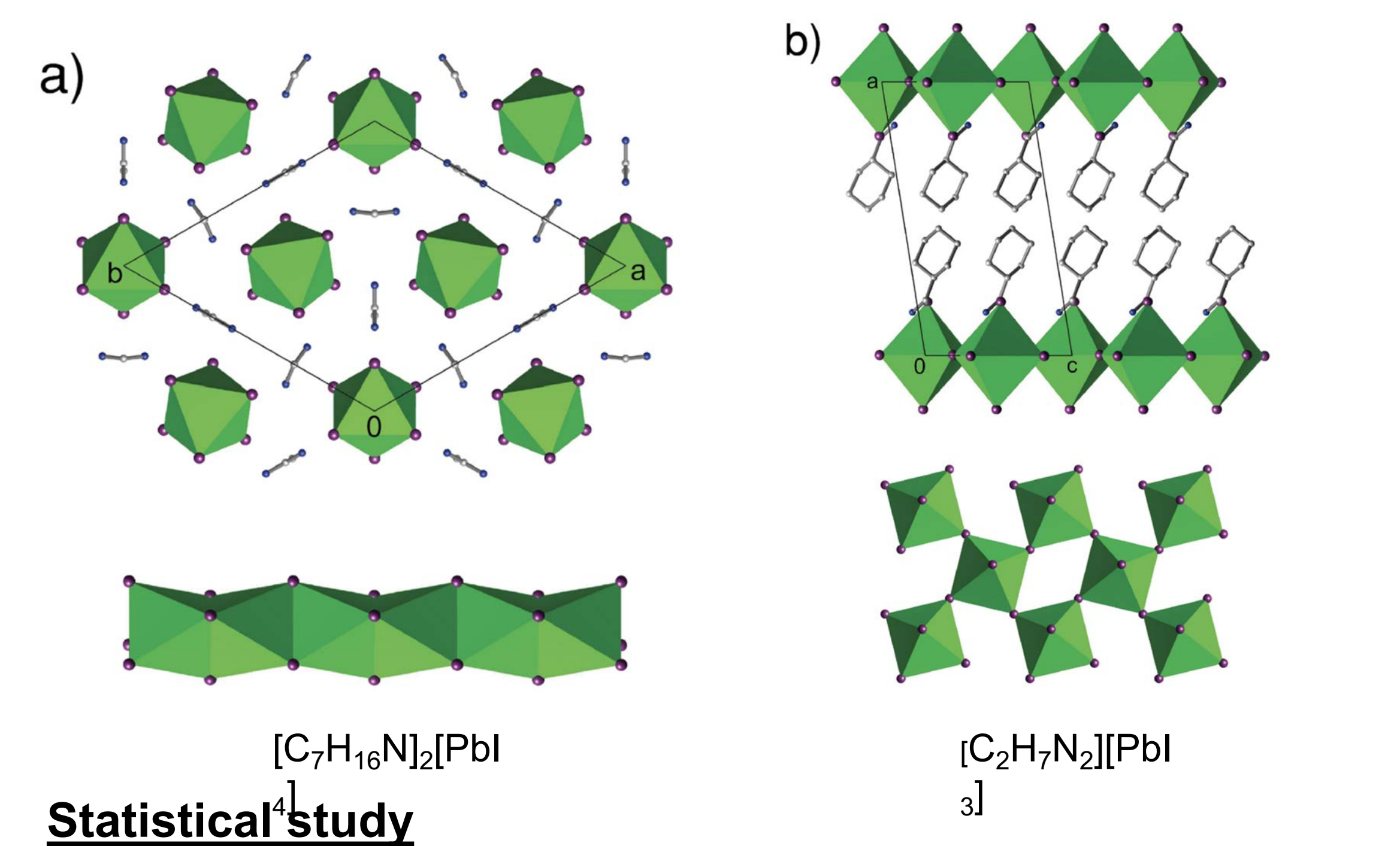
Abstract

Metal halide perovskites are a promising class of materials for next-generation photovoltaic and optoelectronic devices. The discovery and full characterization of new perovskite-derived materials are limited by the difficulty of growing high quality crystals needed for single-crystal X-ray diffraction studies. We present the first automated, high-throughput approach for metal halide perovskite single crystal discovery based on inverse temperature crystallization (ITC) as a means to rapidly identify and optimize synthesis conditions for the formation of high quality single crystals. Using this automated approach, a total of 8172 metal halide perovskite synthesis reactions were conducted using 45 organic ammonium cations. This comprehensive dataset allows for a statistical quantification of the total experimental space and of the likelihood of large single crystal formation. Moreover, this dataset enables the construction and evaluation of machine learning models for predicting crystal formation conditions. This work is a proof-of-concept that combining high throughput experimentation and machine learning accelerates and enhances the study of metal halide perovskite crystallization. This approach is designed to be generalizable to different synthetic routes for the acceleration of materials discovery.

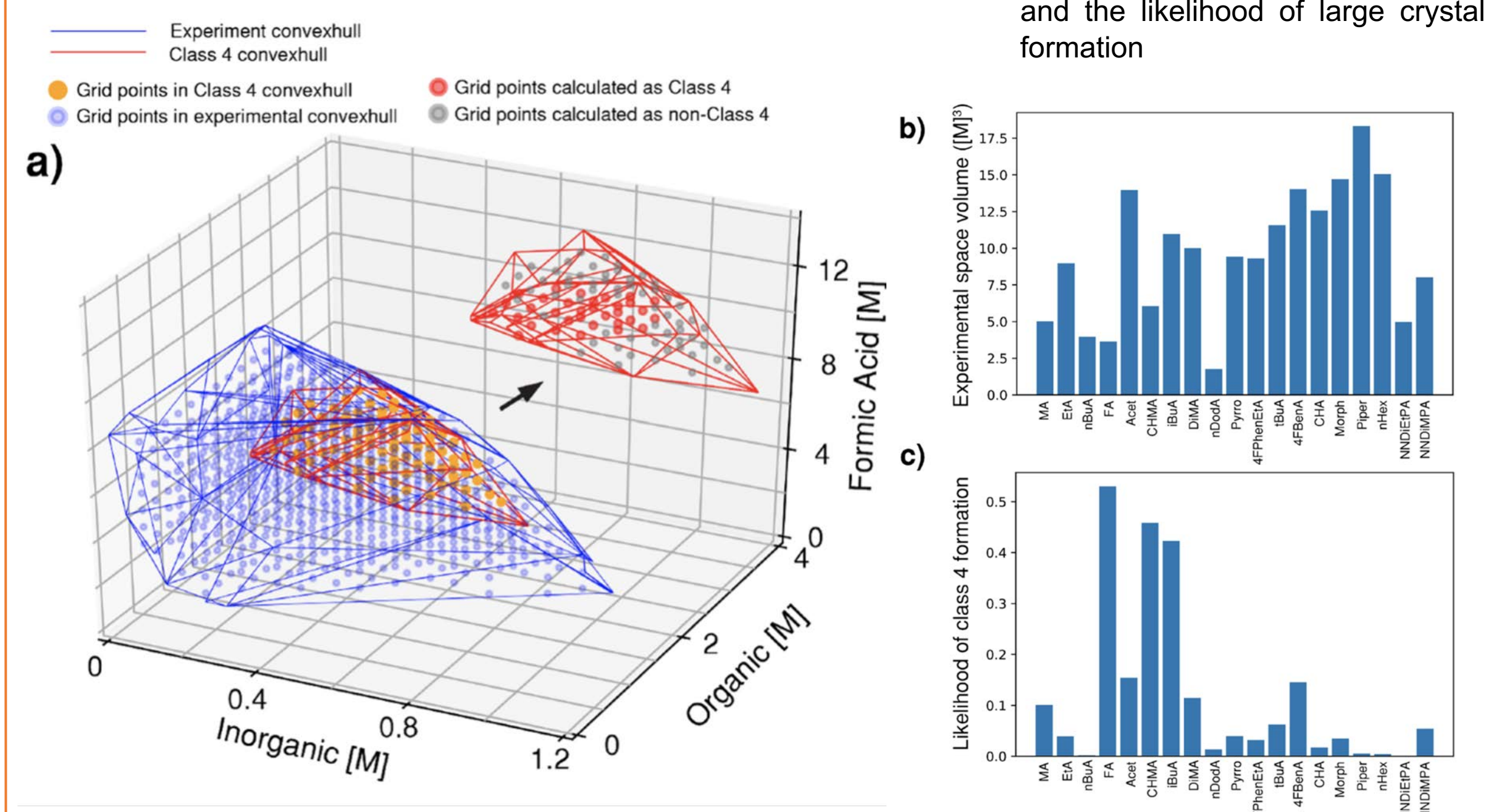
Robot accelerated perovskite workflow



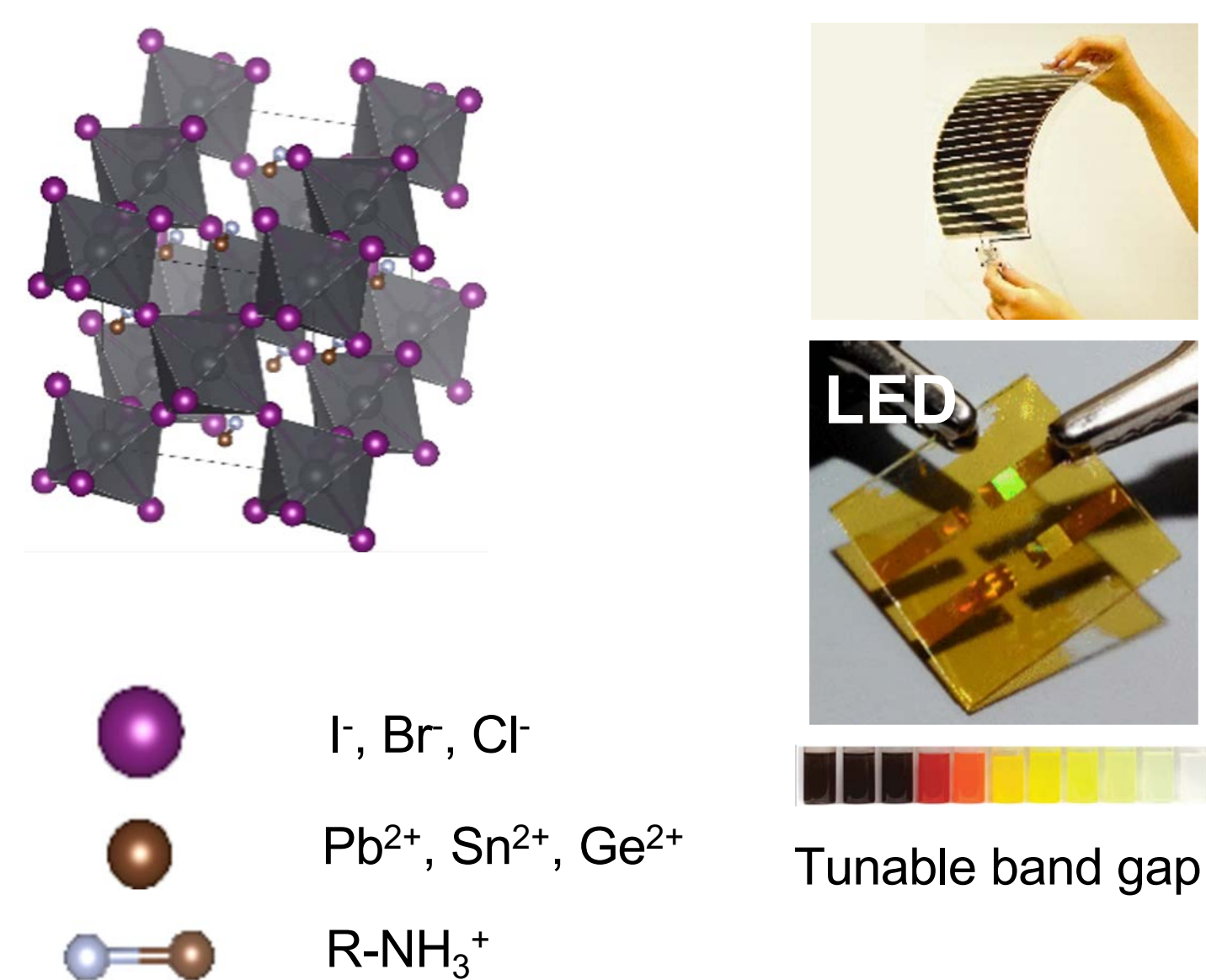
Crystal structure determination



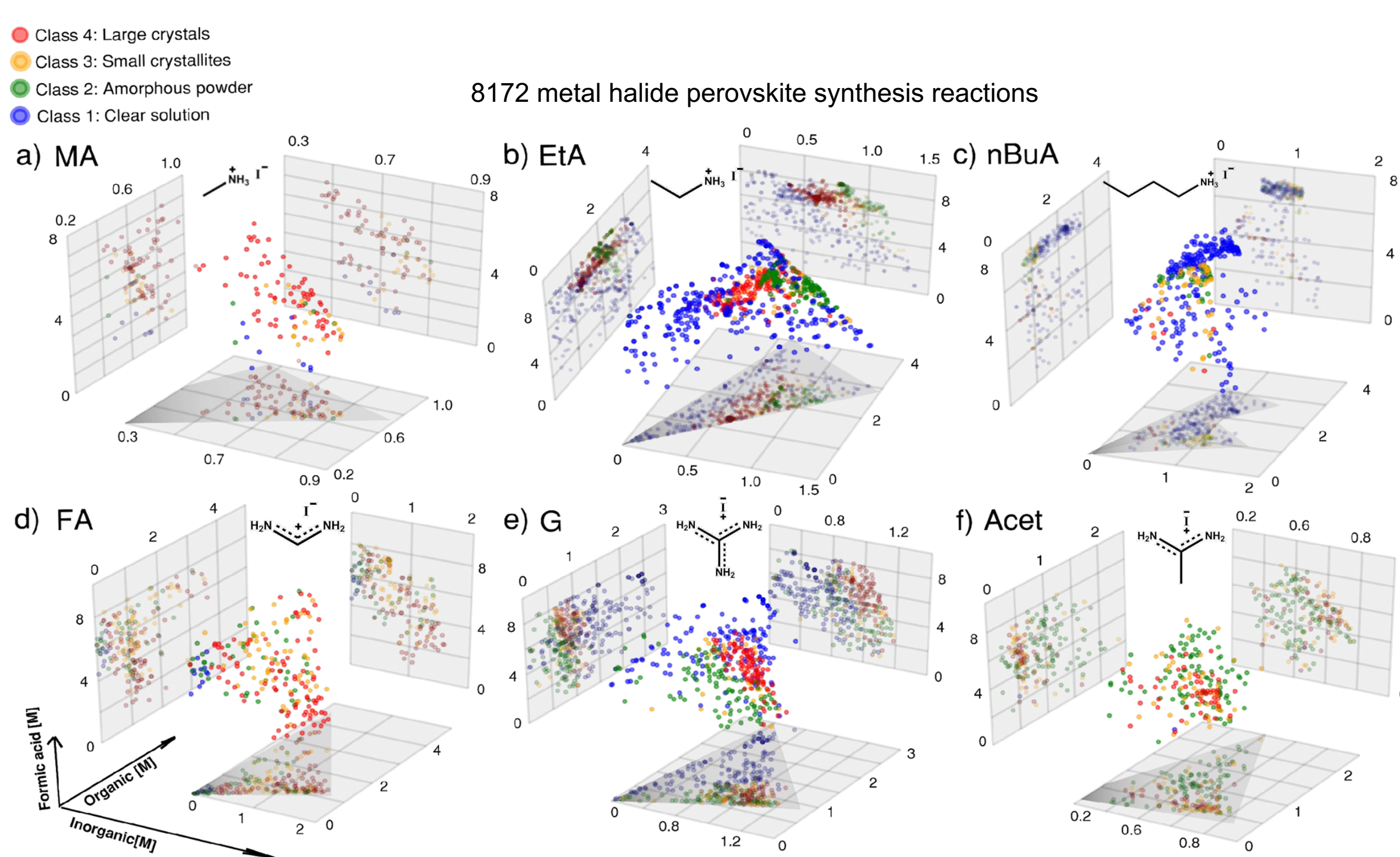
Convexhull of experimental space



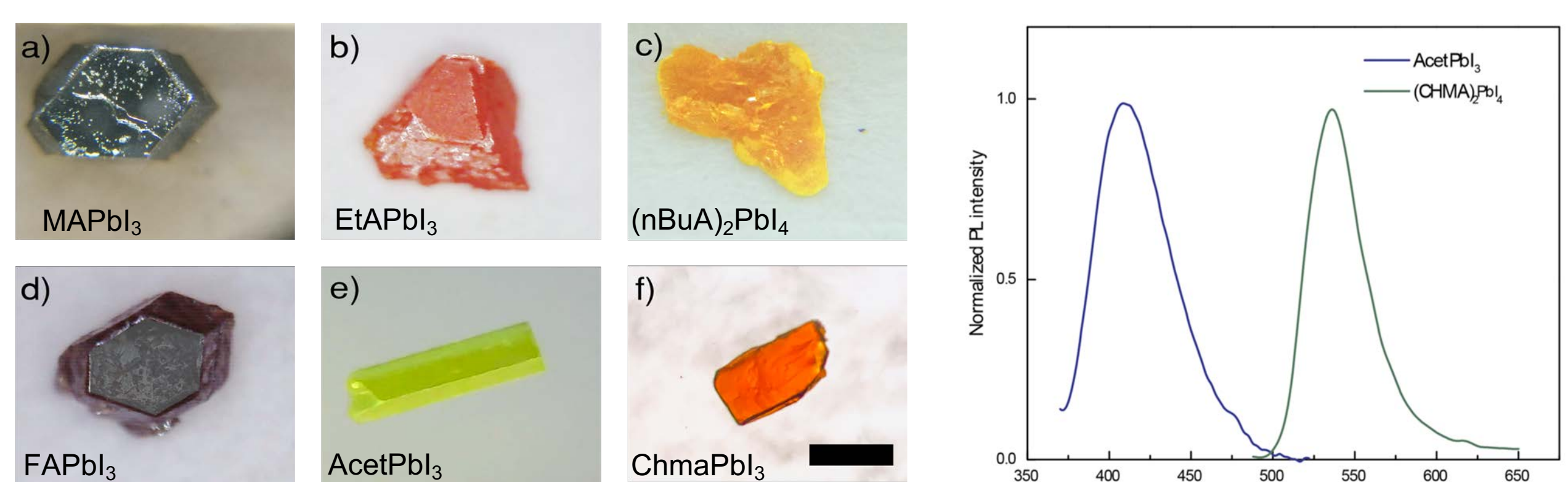
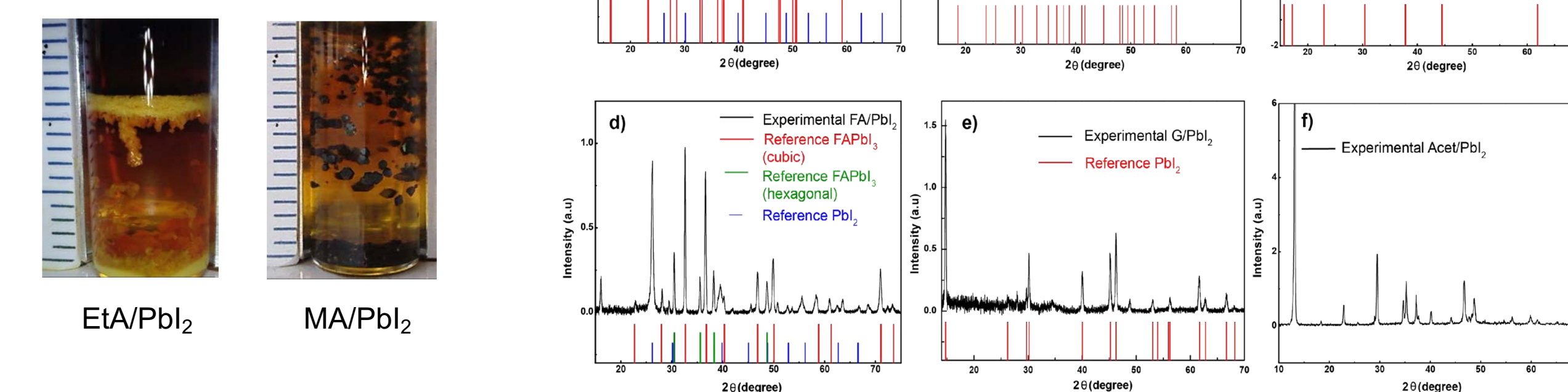
Metal Halide Perovskite



High-throughput screening



Representative samples were collected for powder X-ray diffraction

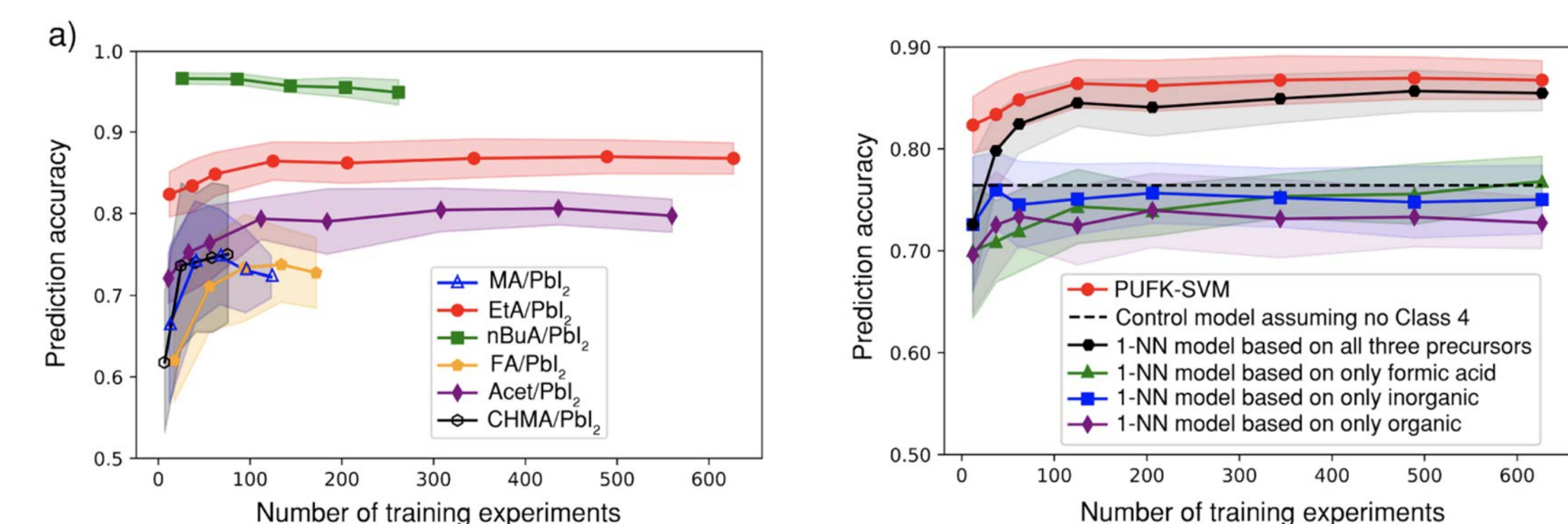


One shot optimization of crystallization conditions

Machine learning

The model for the EtA /PbI₂ system achieves prediction accuracy as high as 83% with only ~100 experiments

PUFK-SVM model trained exclusively on EtA /PbI₂ system data resulted in the highest performance

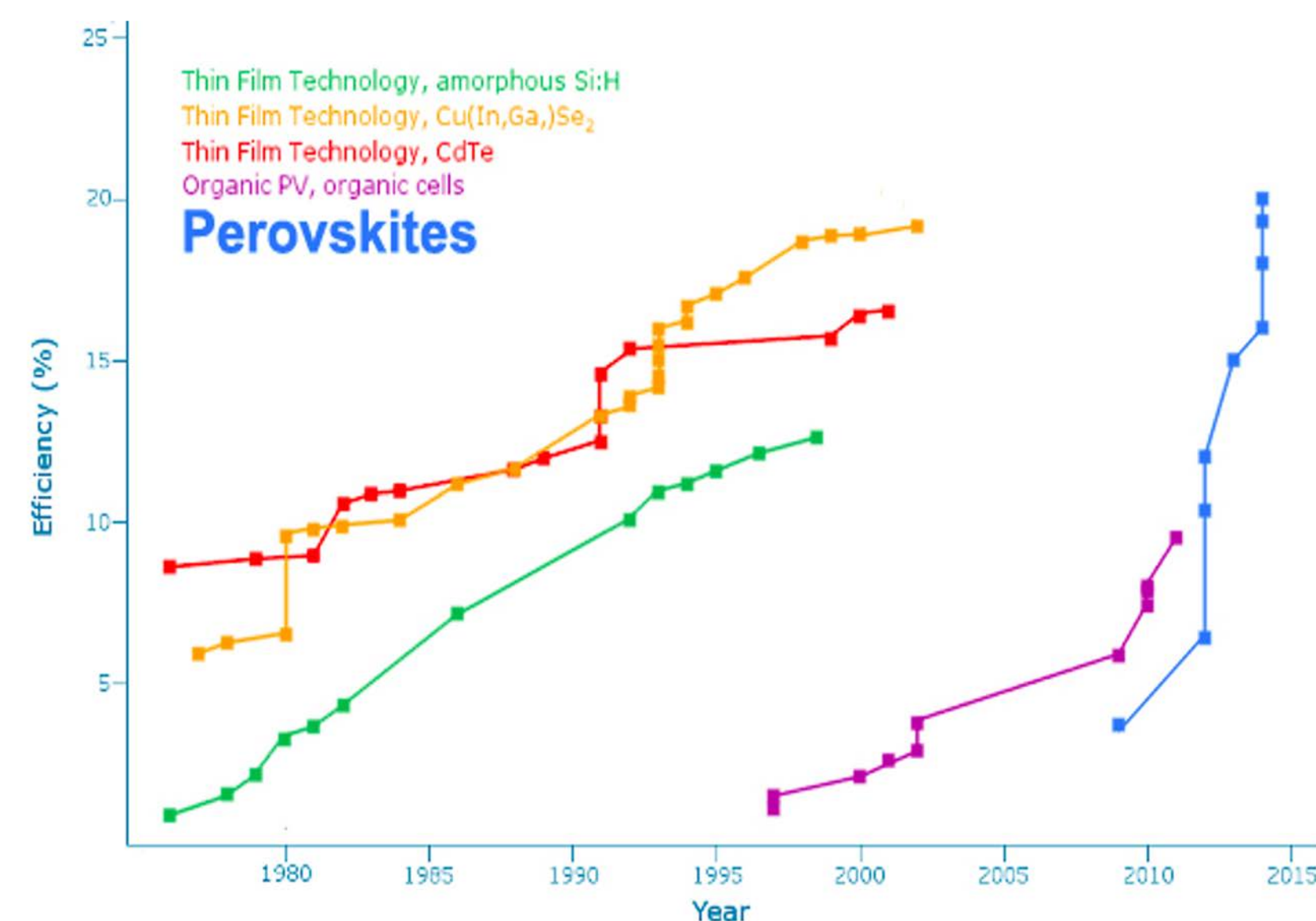


We have developed an automated, high-throughput robotic synthesis platform (Robot-Accelerated Perovskite Investigation and Discovery, or RAPID) for metal halide perovskite single crystal discovery. A total of 8172 reactions were performed using our RAPID workflow. We identified conditions that produce perovskite single crystals for 19 out of 45 target perovskite compositions, adding 17 new materials to the library of metal halide perovskites accessible via ITC (a 400% increase). Among these compounds are two novel perovskite species, AcetPbI₃ and (CHMA)₂PbI₄, for which we reported the crystal structures and performed preliminary characterization. RAPID is a powerful tool for accelerating perovskite discovery and can be readily extended to a broad range of synthetic routes and materials.

Acknowledgement:

Supported by the Defense Advanced Research Projects Agency (DARPA) under Contract No. HR001118C0036 and the Office of Science, Office of Basic Energy Sciences, of the U.S. Department of Energy under Contract No. DE-AC02-05CH11231

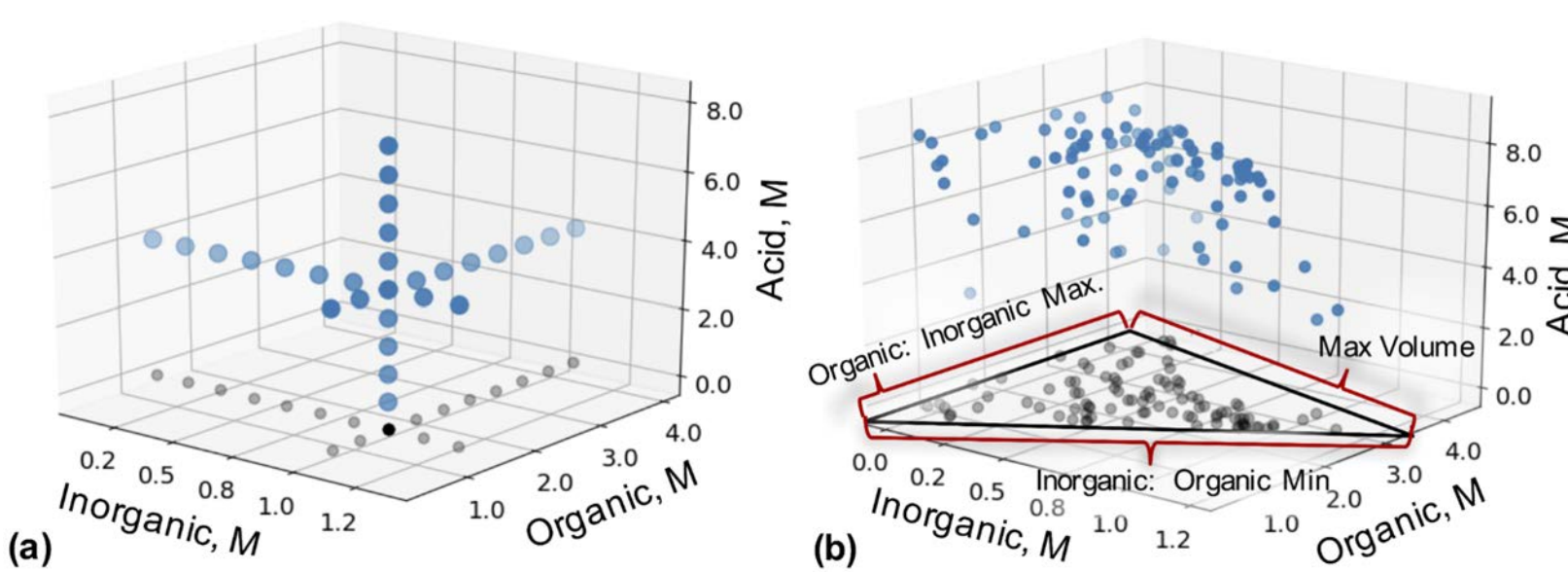
Joshua Schrier (Fordham University), Liana Alves, Alyssa Z. Sherman, Peter Cruz Parrilla, Ian M. Pendleton, Wesley Wang, Venkateswaran Shekar (Haverford College) Matthias Zeller (Purdue University), Phillip W. Nega and Emory Chan (LBNL).



Best Research-Cell Efficiency Chart | Photovoltaic Research | NREL

Human low throughput search

Robot high throughput search



Expanding the Phase-Space of Thick-Layer Metal Halide Perovskites

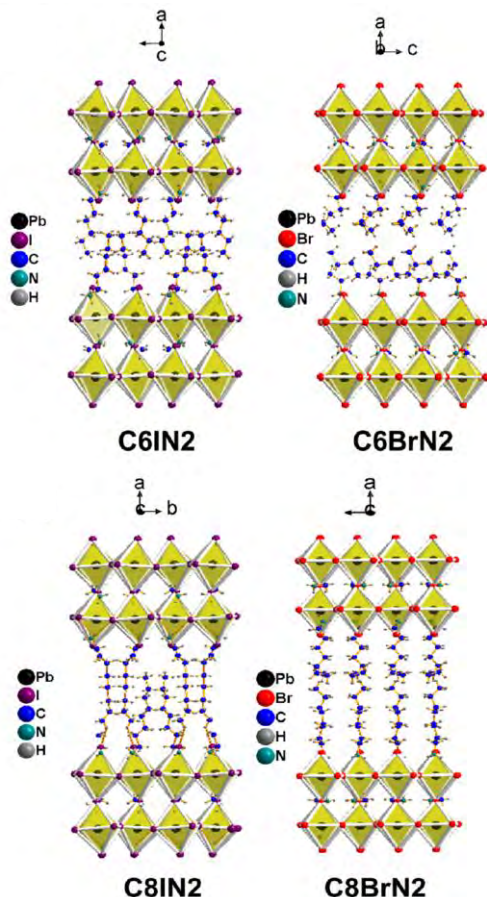
Eugenia S. Vasileiadou, Mercuri G. Kanatzidis;

Department of Chemistry, Northwestern University, Evanston, IL 60208, United States



Recently, the phase-space of thick-layer lead halide perovskites was expanded with our work reporting new member of 2D lead bromide perovskites with the formula: $(C_m H_{2m+1} NH_3)_2 (CH_3 NH_3) Pb_2 Br_7$ ($m = 6-8$).¹ Can machine-learning-accelerated perovskite crystallization be used to create new members of thick-layer metal halide perovskites?²

Methods and Results



2D thick-layer ($n > 1$) lead bromide perovskites remain an unfathomed phase space with the lack of systematic studies reported before our work.¹ We presented a universal solution synthetic methodology for bulk thick-layer lead bromide perovskites based on hydrohalic acid with all structures solved using single crystal X-ray diffraction. Machine learning could help assist in rationally expanding the phase space of these crystalline materials based on *the Input Features for Parameter Exploration* reported in the table below.²

Feature	Constituents/Description
DFT features	the potential, Fermi energy, HOMO, HOMO-1, LUMO, LUMO-1, total energy, and polarizations for each of the A-ligand, A, B, and X sites of the perovskite
Concentrations	one feature each for the A-ligand, A, B, and X sites of the perovskite
Solvent ratios	the DMSO/DMF/GBL ratio
Volume of liquid	the volume of antisolvent in each of the 100- μ L wells and the volume of precursor solution in each of the 1- μ L well
Time	a time for when the crystal is characterized
Crystallization	whether or not there is a crystal present in the well at a given time
Visible photoluminescence	whether or not there is photoluminescence in the visible spectrum at a given time

Conclusion

- Thick-layer metal-halide perovskites consist a vast chemical space that has not been fully explored yet, due to structural geometrical factors governing the synthetic acquisition of these phases.
- Machine learning could guide the synthetic exploration through multiple experimental cycles, as well as contribute to the characterization of these crystalline solids.

References

1. Vasileiadou, E.S.; Kanatzidis, M.G.; et al., *Shedding Light on the Stability and Structure–Property Relationships of Two-Dimensional Hybrid Lead Bromide Perovskites*. *Chem. Mater.* **2021**, *33* (13), 5085-5107.
2. Kirman, J.; Sargent, E. H.; et al., *Machine-Learning-Accelerated Perovskite Crystallization*. *Matter* **2020**, *2* (4), 938-947.